Mechanism of DNA Damage-Induced MDC1 Dimerization

Dissertation

zur

Erlangung der naturwissenschaftlichen Doktorwürde
(Dr. sc. nat.)

vorgelegt der

Mathematisch-naturwissenschaftlichen Fakultät

der

Universität Zürich

von

Stephanie Jungmichel
aus
Deutschland

Promotionskomitee
Prof. Dr. Josef Jiricny (Vorsitz)
PD Dr. Manuel Stucki (Leitung der Dissertation)
Prof. Dr. Ulrich Hübscher
Prof. Dr. Jiri Lukas

Zürich, 2010

TABLE OF CONTENTS

1 SUMMARY

Every cell needs to ensure the maintenance and faithful propagation of genetic information in order to prevent the development of life-threatening diseases such as cancer. However, cells are constantly exposed to various types of genotoxic agents e.g. free oxygen radicals or UV radiation. To counteract these threats, cells have developed specialized mechanisms to detect and repair DNA damage, and to initiate signaling cascades that delay or arrest cell cycle progression, induce certain transcriptional programs or trigger apoptosis. This complex signaling network is collectively denoted as the DNA damage response (DDR).

Double strand breaks (DSBs) are one of the most hazardous forms of DNA damage because they can cause chromosomal instability or cell death if not repaired correctly. This type of DNA lesion can arise from the exposure to ionizing radiation or radiomimetic drugs, both frequently used in cancer treatment. DSBs lead to the activation of the ATM kinase and to the phosphorylation of the histone variant H2AX. Phosphorylated H2AX (γH2AX) is directly recognized by mediator of DNA damage checkpoint protein 1 (MDC1), a large mediator/adaptor protein that regulates the accumulation of DDR factors in chromatin regions flanking DSBs. MDC1 contains a forkhead associated (FHA) domain at its N-terminus. Even though it is known that FHA domains act as phosphopeptide recognition motifs, the function of the MDC1 FHA domain has remained enigmatic.

In this study, we identified a novel phosphorylation-specific binding partner of the MDC1 FHA domain, namely MDC1 itself. We show that ATM phosphorylates MDC1 at the conserved N-terminal Thr4 residue in a DNA damage-dependent manner and that this induces the interaction with the FHA domain of other MDC1 molecules. Biochemical, biophysical and X-ray structural analysis revealed that the presence of a Thr4-phosphopeptide stabilizes the formation of a tight FHA dimer in a head-to-tail-oriented manner. We furthermore demonstrate that the isolated FHA domain is capable of localizing to sites of DNA damage in a phosphorylation-induced and dimerization-dependent manner. The elucidation of this mechanism contributes to our understanding of how MDC1 functions in the mammalian DDR and supports the notion that dimerization/oligomerization is a common theme of DDR mediator proteins.

2 ZUSAMMENFASSUNG

Der Erhalt und die getreue Weitergabe der genetischen Information ist wichtig für jede Zelle, um der Entwicklung von Krankheiten wie Krebs vorzubeugen. Zellen sind jedoch ständig verschiedenen Substanzen ausgesetzt, welche die DNA beschädigen (z.B. freie Sauerstoffradikale und UV-Strahlung). Um diese Gefahren abzuwenden, besitzen Zellen spezialisierte Mechanismen zur Erkennung und Reparatur von DNA Schäden sowie zur Aktivierung von Signalkaskaden, die das Fortschreiten des Zellzyklus hemmen, bestimmte Transkriptionsprogramme einleiten oder programmierten Zelltod (Apoptose) auslösen.

Doppelstrangbrüche (DSBs) stellen dabei eine der gefährlichsten Formen von DNA Schäden dar, da sie bei nicht ausreichender Reparatur chromosomale Instabilität oder Zelltod zu verursachen vermögen. DSBs können durch die Einwirkung ionisierender Strahlung oder ähnlich wirkender Zytostatika, die beide häufig in der Krebstherapie ihre Anwendung finden, entstehen. DSBs führen zur Aktivierung der ATM-Kinase und Phosphorylierung der Histon-Variante H2AX. Phosphoryliertes H2AX wird direkt von MDC1, einem grossen Adapter-Protein, gebunden, das die Ansammlung von weiteren Proteinen in den Doppelstrangbruch umgebenden Chromatinregionen reguliert. MDC1 besitzt eine N-terminale FHA Domäne. Obwohl bekannt ist, dass FHA Domänen als Phosphopeptid-Erkennungsmotive fungieren, konnte die Funktion der MDC1 FHA Domäne bisher noch nicht entschlüsselt werden.

In dieser Arbeit haben wir MDC1 selbst als einen neuen phosphospezifischen Interaktionspartner der MDC1 FHA Domäne identifiziert. Wir zeigen, dass MDC1 an der konservierten Aminosäure Thr4 infolge von DNA Schäden von der Kinase ATM phosphoryliert wird und dass dies für die Interaktion mit der FHA Domäne eines anderen MDC1 Moleküls verantwortlich ist. Biochemische, biophysikalische und Röntgenstruktur-Analysen legen offen, dass das T4-Phosphopeptid die Ausbildung eines FHA-Dimers in umgekehrter Orientierung stabilisiert. Des Weiteren kann die isolierte FHA Domäne an DNA geschädigte Regionen in Abhängigkeit vom Phosphorylierungs- und Dimerisierungsstatus binden. Die Aufklärung dieses Mechanismus trägt zu unserem Verständnis der Funktion von MDC1 in der Antwort auf DNA Schäden in Säugetierzellen bei und unterstützt die Auffassung von Dimerisierung (Oligomerisierung) als allgemeines Leitmotiv in Adapterproteinen.

3 ABBREVIATIONS

ATM	Ataxia telangiectasia mutated
ATR	Ataxia telangiectasia and Rad3 related
BRCA1	Breast cancer 1
BRCT	BRCA1 C-terminal
CHK1/2	Checkpoint protein 1/2
DDR	DNA damage response
DNA-PKcs	DNA-dependent protein kinase catalytic subunit
DSB	Double strand break
EYFP	Enhanced yellow fluorescent protein
FHA	Forkhead-associated
GFP	Green fluorescent protein
HNE	HeLa nuclear extract
HR	Homologous recombination
IR	Ionizing radiation
IRIF	Ionizing radiation induced foci
LOH	Loss of heterozygosity
MDC1	Mediator of DNA damage checkpoint 1
MEF	Mouse embryonic fibroblast
MRN	MRE11-RAD50-NBS1
MS	Mass spectrometry
NBS	Nijmegen breakage syndrome
NHEJ	Non homologous end joining
NMR	Nuclear magnetic resonance
PIKK	Phosphoinositide-3-kinase-related protein kinase
PNK	Polynucleotide kinase
PST	Pro-Ser-Thr
RDS	Radioresistant DNA synthesis
RNF8	Ring finger protein 8
SCD	SQ-TQ cluster domain
SDT	Ser-Asp-Thr

4 INTRODUCTION

4.1 General introduction

4.1.1 The importance of genome maintenance

Preservation of genomic integrity is an essential condition for all living organisms in order to faithfully propagate the genetic information. However, cells are constantly threatened by genotoxic stress arising from various endogenous or exogenous sources. In particular, DNA double-strand breaks (DSBs) display one of the most deleterious forms of DNA damage in mammalian cells. This type of lesion can occur as product of collapsed or stalled replication forks that originate from single strand breaks (SSB) or base damages. DSBs are further generated as programmed events during antigen-receptor rearrangement in lymphocytes or during meiotic recombination and the cells also recognize dysfunctional telomeres as DSBs. Moreover, DSBs can arise from exposure to ionizing radiation (IR) or radiomimetic drugs, which are widely used for clinical treatment of cancer diseases. Improper functioning of mechanisms that deal with DSBs can lead to chromosomal rearrangements that on a broader scale cause chromosomal instability, which is a prominent feature of most human malignant cancer types. Correspondingly, various genetic diseases such as Ataxia-telangiectasia (A-T) or Fanconi Anemia (FA) that are caused by a defective protein in the DNA damage response machinery often show a cancer-prone phenotype. A deeper understanding of the mechanisms that are involved in the recognition of DSBs and regulation of DNA repair processes may therefore form the basis for a rational design of new therapies for treatment of genetic diseases or to selectively kill cancer cells. Since defects in these pathways are often specific to cancer cells and do not occur in normal cells, they can be therapeutically exploited with only very limited side effects, which makes them a much more attractive target compared to conventional cancer targeting strategies that are usually accompanied by high toxicity for normal cells.

Chromosomal instability has recently been classified as an early event during tumorigenesis forming a prerequisite for the accumulation of mutations required for transition of precancerous lesions into cancer cells (Beckman & Loeb, 2006). Mechanisms that have been suggested to contribute to chromosomal instability

include defects in the regulation of genome caretakers, including DNA repair and cell cycle checkpoint genes. Genome caretaker genes are main players in the DNA damage response and mutations of some of them have been shown to be involved in tumorigenesis by enhancing chromosomal instability (Cahill et al, 1998; Wang et al, 2004). However, up to now, only few mutations in classical caretaker genes have been reported in sporadic cancers (Greenman et al, 2007; Sjoblom et al, 2006; Wood et al, 2007). Telomere shortening is also widely accepted to contribute to genomic instability, although it is not yet completely clear whether it constitutes a mechanism that can specifically initiate chromosomal instability during tumorigenesis (Feldser et al, 2003). A relatively new concept as underlying mechanism of chromosomal instability in human precancerous lesions is oncogene-induced replication stress that includes stalling and collapse of replication forks resulting in the formation of DSBs. Common fragile sites turned out to be at particularly high risk for breakage during replication stress (Bartkova et al, 2005; Gorgoulis et al, 2005; Halazonetis et al, 2008). These events have been shown to activate the DDR machinery, thus resulting in either apoptosis or senescence and thereby forming a barrier to tumorigenesis and cancer invasiveness (Bartkova et al, 2006; Di Micco et al, 2006). However, the suppressive effect of active DDR signaling is released upon mutation and inactivation of the p53 gene, which strongly correlates with cancer progression (Gorgoulis et al, 2005). In addition, inhibition of another checkpoint protein, the ATM kinase, was shown to inhibit senescence and to increase tumor invasiveness in tumor mouse models. However, p53 inactivation seems to be the major cause of compromised checkpoint signaling (Bartkova et al, 2006).

4.1.2 The DNA damage response

Mammalian cells have evolved sophisticated mechanisms to sense DNA damage and to activate signal transduction cascades that result in different cellular responses involving delay of cell cycle progression and activation of DNA repair in order to ensure the faithful propagation of the genetic information. Cells can also reach a senescent state or even enter apoptosis if the damage is too severe and difficult to repair. Moreover, a certain subset of genes can be subjected to transcriptional activation or repression. This interactive signaling network is usually referred to as

the DNA damage response (DDR) (Figure 4.1) (reviewed in (Harper & Elledge, 2007; Zhou & Elledge, 2000)).

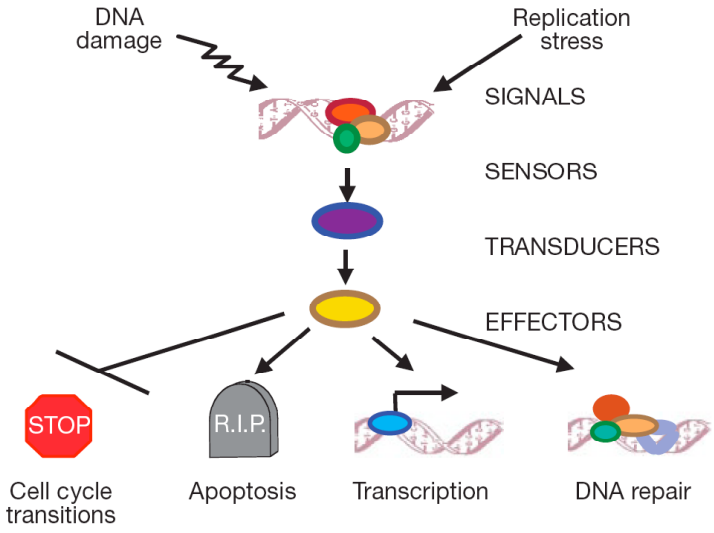

Figure 4.1

The DNA damage response. An interactive signaling network, depicted here as linear pathway, converts the signal of damaged DNA into specific cellular responses mediated by the action of sensors, transducers and effectors. (Zhou & Elledge, 2000)

Proteins that participate in the DDR have initially been categorized as sensors, transducers and effectors, although in some cases, multiple functions can be assigned to the same protein. Sensors monitor the genomic integrity by recognizing damaged DNA either directly or indirectly as part of a protein complex and initiate a signaling cascade by recruiting transducers to sites of DNA damage. Transducers are typically protein kinases that propagate and amplify the signal to downstream effectors. Finally, effector proteins, which are mainly regulated through posttranslational modification such as phosphorylation and ubiquitylation, convert the signal of transducers into a specific cellular response such as transient or permanent cell cycle arrest, DNA repair or transcriptional regulation (Nyberg et al, 2002). Recently, a fourth class of proteins has been introduced to the concept of the DDR. These so-called mediators or adaptors often do not possess any enzymatic activity. However, they generally act as a recruiting platform for other proteins and thus might bring transducers' activities in close proximity to their substrates and facilitate protein complex formation, thereby providing signal transduction specificity and amplification (Sancar et al, 2004).

4.2 Responses to DNA Double Strand Breaks

4.2.1 Double Strand Break Signaling

The response to DSBs is coordinated in space and time and involves numerous proteins that become recruited and activated at sites of DNA damage in a hierarchical order. In mammalian cells, DSBs are directly sensed by the MRN complex, which consists of the proteins MRE11, RAD50 and NBS1. The MRN complex has been described to tether and process broken DNA ends. Moreover, it is required to recruit the ATM kinase via an interaction with NBS1 (Falck et al, 2005). MRN is also involved in ATM activation by as yet poorly understood mechanisms. ATM is the major kinase responsible for signaling from DSBs that are not associated with replication forks. It belongs to the conserved family of phosphoinositide 3-kinase-like kinases (PIKKs), which mainly possesses Ser/Thr kinase activity and further includes the members ATR and DNA-PKc. Activation of ATM in human cells is mediated by autophosphorylation on Ser1981, which results in dissociation of the inactive dimer into active monomers (Bakkenist & Kastan, 2003). Several other proteins have been suggested to contribute to regulation of ATM activity including the MRN complex, 53BP1, histone acetyltransferase Tip60 and protein phosphatases PP2A and PP5 (reviewed in (Lee & Paull, 2007)). However, how these cofactors specifically regulate ATM activity remains largely unclear, but mechanisms likely involve modulation of ATM substrate-specificity, or response to different cell stimuli. Activated ATM phosphorylates a large number of proteins that participate in cell cycle checkpoint regulation, DNA repair, senescence, apoptosis and other cellular processes (Figure 4.2) (Matsuoka et al, 2007).

One key target of the ATM kinase is the histone variant H2AX that becomes phosphorylated at a conserved Ser residue (Ser139) in DSB-flanking chromatin regions (Rogakou et al, 1998), indicating that modification of chromatin components plays an important role in the DNA damage response. Phosphorylated H2AX (γH2AX) forms a direct recognition motif for binding to MDC1 (mediator of DNA damage checkpoint protein 1), which initiates a whole cascade of events that have an impact on checkpoint activation, DNA repair and survival (reviewed in detail below: Jungmichel and Stucki, 2010).

ATR and DNA-PKc have also been shown to become activated in response to DSBs and to target H2AX, although ATR signaling is effectively initiated by the presence of single stranded lesions that occur in response to UV and lead to stalling of replication forks. However, following DSB induction, ATR activity is triggered in an ATM-dependent manner in S and G2 phase of the cell cycle (Jazayeri et al, 2006; Myers & Cortez, 2006).

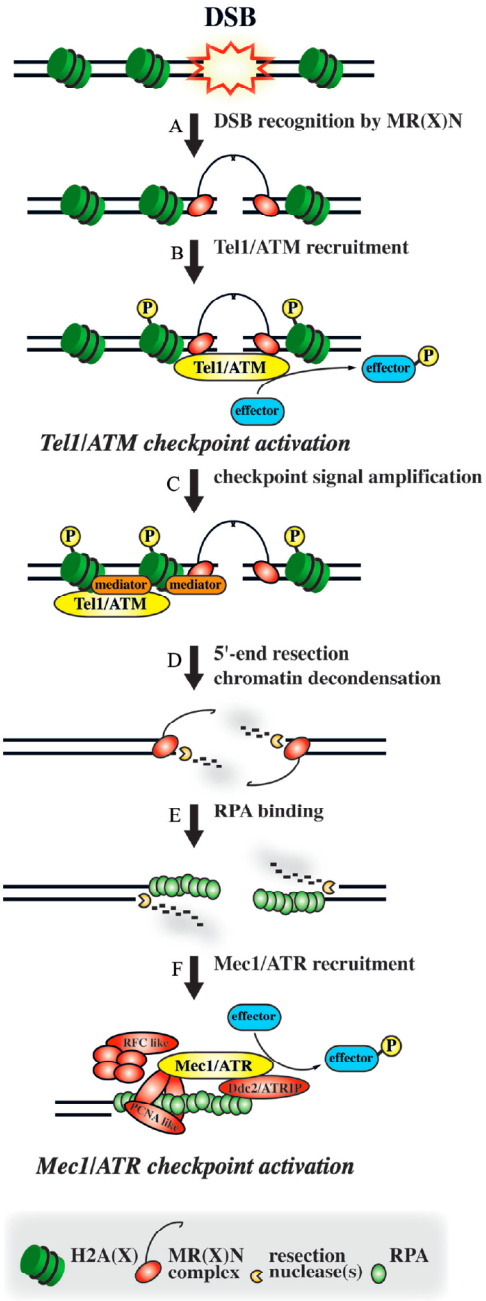

Figure 4.2

Early DNA damage signaling. A DSB is directly recognized by sensor complex MRN, which recruits and activates ATM (yeast homologue Tel1). ATM kinase in turn phosphorylates various downstream effectors, among them the histone variant H2AX in order to elicit a checkpoint response and to promote DNArepair. Broken DNA ends can become resected by nucleases and the generated ssDNA is subsequently bound by RPA, which recruits a complex containing ATR kinase (yeast homologue Mec1), which further contributes to cell cycle arrest (Pardo et al, 2009).

Recently, Shiotani and Zou demonstrated that this ATM-dependent ATR activation is dependent on resection of DSBs. In this process, ATM becomes first activated at blunt ends or short single stranded overhangs in an MRN-dependent manner. Ongoing resection then leads to formation of single stranded tails that can be coated by RPA and subsequently recruits ATR through its binding partner ATRIP to sites of DNA damage resulting in ATR activation followed by ATM inactivation (Shiotani & Zou, 2009) (Figure 4.2). DNA-PKc with its major function during DSB repair via NHEJ seems to act redundantly with ATM, as it can, for instance, take over IR-induced H2AX phosphorylation in ATM-deficient cells (Stiff et al, 2004). The lack of embryonic lethality of ATM null cells, but synthetic lethality between mutations of both ATM and DNA-PKc during murine embryogenesis, further points to DNA-PKc acting as a backup kinase for ATM (Gurley & Kemp, 2001).

The prevalent function of ATM/ATR signaling is initiation of cell-cycle arrest at G1/S, intra-S-phase and G2/M checkpoints. Among the various protein substrates, the checkpoint kinases CHK2/CHK1 are major targets of ATM/ATR. They transduce the signal to further downstream effectors including the key targets CDC25 phosphatases and transcription factor p53, which can also become directly phosphorylated by ATM at Ser15, eventually resulting in inhibition of cyclin-dependent kinases (CDKs) at various stages of the cell cycle. The elicited cell cycle arrest is generally thought to leave time for repair before replication or meiosis can occur.

The critical role of the aforementioned players within the DDR is underlined by congenital deficiencies that give rise to a genomic instability syndrome. Mutations in ATM are associated with Ataxia telangiectasia (AT) and mutations in MRE11 with Ataxia telangiectasia-like disorder (ATLD). The Nijmegen breakage syndrome (NBS) is caused by mutations in NBS1, whereas the Seckel syndrome results from hypomorphic mutations in ATR. In contrast to ATM, ATR is an essential gene since ATR knockout in mice leads to early embryonic lethality, which might be explained by the essential role of ATR signaling required in the stabilization and recovery of stalled replication forks (Kerzendorfer & O'Driscoll, 2009).

4.2.2 DSB Repair

DSB repair occurs primarily by two mechanisms in eukaryotic cells: non-homologous end-joining (NHEJ) and homologous recombination (HR), whose preferential choice seems to be dependent on cell cycle regulations at the level of DSB-end resection and protein protein interactions (reviewed in (Hartlerode & Scully, 2009; Pardo et al, 2009)).

4.2.2.1 Non-homologous end-joining

The underlying principle of NHEJ involves efficient re-ligation of broken DNA ends without the requirement of a homologous sequence as a template. Since this may cause loss or gain of DNA bases it is referred to as an error-prone mechanism. It occurs throughout the cell cycle but is mainly active during G_0, G_1 and early S-phase. The pathway is initiated by direct binding of the KU70/KU80 heterodimer to free double-stranded DNA ends, which recruits and activates the catalytic subunit of DNA-PK (Gottlieb & Jackson, 1993; Walker et al, 2001; Yaneva et al, 1997) (Figure 4.3).

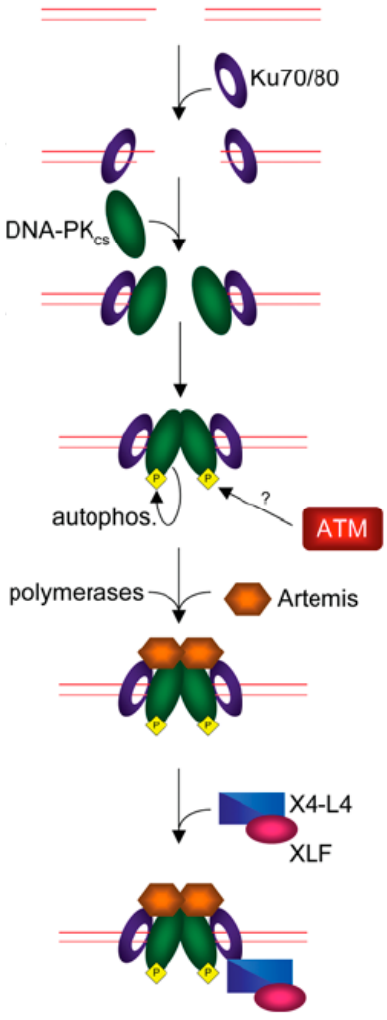

Figure 4.3

NHEJ in mammalian cells. The KU70/80 heterodimer directly binds and tethers DNA ends through the recruitment of DNA-PKcs, which becomes activated and autophosphorylated. Activated DNA-PKcs facilitates recruitment of end-processing factors Artemis and DNA polymerases of the X family that generate ligatable DNA ends. Finally, the Ligase IV/XRCC4/XLF complex completes repair by ligating the DNA ends. (adapted from (Hartlerode & Scully, 2009))

The various phosphorylation targets of DNA-PKcs include XRCC4, Artemis and DNA-PK itself. This autophosphorylation reaction seems to cause a conformational change in DNA-PKcs thereby regulating the accessibility of further factors to DNA ends (Weterings et al, 2003). However, prior to ligation, IR-induced DSB might require some DNA end processing in order to generate ligatable 5'-phosphorylated and 3'-dephosphorylated ends. Polynucleotide kinase (PNK) and the nuclease Artemis together with the activity of DNA-PKcs were shown to stimulate processing of DNA for efficient NHEJ (Chappell et al, 2002; Ma et al, 2002). Remaining single-stranded gaps after pairing of partially complementary strands are filled by DNA polymerases, which might also randomly add nucleotides to DNA ends to generate regions of microhomology for base pairing. The X family DNA polymerases Polλ, Polμ and terminal deoxynucleotidyl transferase (TdT) have been implicated in these processes (Nick McElhinny & Ramsden, 2004). Finally, DNA ends are ligated by the NHEJ ligase complex essentially comprising DNA ligase IV, XRCC4 and XLF (Ahnesorg et al, 2006; Grawunder et al, 1997). Core members of the NHEJ pathway have also function during V(D)J recombination to generate B- and T-cell receptor diversity in vertebrate immune cells, explaining, for example, the radiosensitive severe combined immunodeficiency (RS-SCID) phenotype of patients with defective Artemis (Moshous et al, 2001).

4.2.2.2 Homologous recombination

Homologous recombination requires the presence of identical or highly similar DNA sequences as a template and is considered to be an error-free mechanism of DSB repair in contrast to NHEJ. Due to the availability of a homologous sister chromatid HR is the main DSB repair pathway during late S and G_2 phase of the cell cycle. An important component of the HR machinery is the MRN complex that binds to broken ends and is involved in the initiation of resection (Figure 4.4). Nucleolytic degradation of the 5'-stranded end of DSBs has been shown to be a prerequisite for HR. Much of the information on the resection process has been derived from studies in yeast (Huertas). However, it is unlikely that the MRE11 nuclease carries out the 5' to 3' resection directly because MRE11 is a 3' to 5' exonuclease, at least *in vitro*. Therefore, ExoI and another, yet undefined, exonuclease were suggested to provide

the activity for resection of 5'-stranded DNA. In vertebrate cells, MRE11, RAD50 and CtIP (Sae2 homologue) were sufficient for resection even though it is believed that efficient HR *in vivo* requires additional factors such as the tumor suppressor BRCA1 (Sartori et al, 2007; Yun & Hiom, 2009). The arising single stranded 3'-overhang is then rapidly coated by RPA to avoid formation of secondary structures. Further accumulation of multimers of the RAD51 recombinase in dependency of BRCA1/BARD1 and BRCA2 entails formation of a nucleoprotein filament that is able to perform homology search in duplex DNA (Hartlerode & Scully, 2009). Following strand invasion into a homologous DNA template, which involves pairing with the complementary strand and displacement of the other, a so-called D-loop (displacement loop) structure is formed. After that, several pathways can complete HR with different outcomes, whose detailed mechanisms, regulations and participating factors remain to be elucidated. In principle, SDSA (synthesis-dependent strand annealing) or DSBR (double strand break repair) have been described to occur in case of two-ended DSBs. During SDSA the elongated invading strand pairs again with the second DSB end (Figure 4.4A). Since this process does only produce non-crossovers, SDSA is the preferred recombination-mediated DSB repair in somatic cells in order to prevent loss of heterozygosity (LOH) or other genetic rearrangements. Alternatively, during DSBR, the extended D-loop captures the second DSB end and creates a double Holliday junction (HJ) between the four strands that can undergo branch migration catalyzed by members of the RecQ helicase family (Bohr, 2008). Resolution of these recombination structure intermediates finally occurs in different ways resulting either in non-crossovers or crossovers, which predominantly occur during meiotic recombination (Figure 4.4B). The enzyme complexes BLM/TopoIIIa, MUS81/EME and GEN1 have been suggested to contribute to separation of the two repaired strands (Chen et al, 2001; Ip et al, 2008; Wu & Hickson, 2003). The resulting nicks are finally sealed by DNA ligases. In the absence of homology, SSA (single-strand annealing) might be initiated. This involves resection of both 5'-strands until repetitive sequences are uncovered that can be annealed (Figure 4.4C). Non-homologous terminal DNA is then removed by nucleases followed by DNA synthesis and ligation of the nicks. Due to deletion of the intervening sequences, SSA is considered a mutagenic repair pathway. One-ended DSBs, which can arise through uncapping telomeres or collapse of the replication fork upon encountering a single stranded break (SSB), are repaired by BIR (break-induced

repair) (Figure 4.4D). In this event invasion of the 3'-stranded end into homologous duplex DNA generates a replication fork that replicates the template to the chromosome end. This process is potentially leading to LOH.

Mutation or deletion of HR components often results in cancer development, thus reflecting the critical role of HR in suppressing genome instability. For example, inherited mutations in BRCA1 and BRCA2 are frequently associated with development of breast and ovarian cancer. The genomic instability disorders Werner, Bloom and Rothmund-Thomson syndrome have been linked to mutations in the RecQ helicases WRN, BLM and RECQL4, respectively (Bohr, 2008). Strikingly, deletion of the RAD51, BRCA1 or BRCA2 gene causes early embryonic lethality in mice, thus underlining the essential nature of this repair pathway.

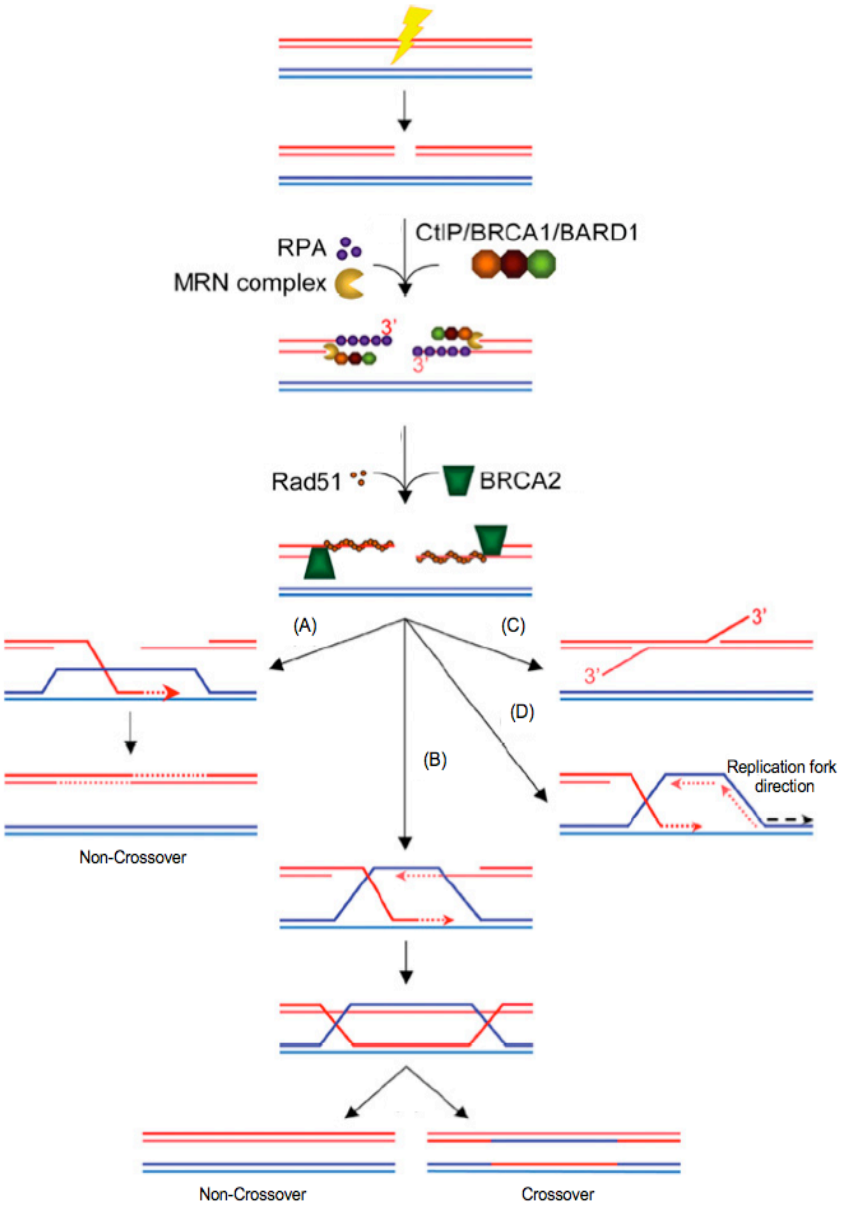

Figure 4.4

Homologous Recombination. The DSB is directly recognized by the MRN complex, which tethers the DNA ends and participates in end processing. The CtIP/BRCA1/BARD1 complex co-operates with MRN to assist in end resection. RPA binds the resulting ssDNA to prevent formation of secondary structures. BRCA1/BARD1 promote accumulation of BRCA2, which catalyses the assembly of Rad51 nucleoprotein filaments. The Rad51 filament is assembled captures duplex DNA and searches for homology. Different repair pathways can be initiated: (A) During SDSA the extended invading strand is displaced and anneals to the resected second DNA end. (B) In the DSB repair pathway both DNA ends are captured by annealing to the extended D loop, forming a double HJ, which is resolved to yield either crossover or non-crossover products. (C) SSA occurs when direct repeat sequences are revealed by resection on complementary strands that can be annealed whereby intervening sequences are deleted. (D) During BIR the 3'-end of the invading strand leads to formation of a replication fork that copies long tracts of the donor DNA strand. (adapted from (Hartlerode & Scully, 2009))

4.3 Mediators

Mediator/adaptor proteins form a distinct category of DDR components and have functionally been placed directly downstream of ATM and ATR. They often do not possess any enzymatic activity, but rather act as recruiting factors and as scaffold for the efficient assembly of protein complexes (reviewed in (Harper & Elledge, 2007)). This way, mediators can relay and amplify the DNA damage signal. Recent years of research have revealed their regulatory functions within the DDR, although detailed mechanisms are not yet completely understood. Mediators that have so far been described in mammalian cells include MDC1, 53BP1, MRN, TopBP1, Claspin, Mcph1/Brit1, PTIP and BRCA1. A typical feature of mediator proteins is the presence of protein-protein interaction motifs in their sequence that are often regulated by the phosphorylation activity of cellular kinases. The best-characterized phosphopeptide-binding motifs constitute the BRCT (BRCA1 C-terminus) and the FHA (Forkhead-associated) domains that recognize short amino acid sequences surrounding a phosphorylated serine or threonine. BRCT- and FHA domain containing proteins mainly regulate the formation of so-called ionizing radiation-induced DNA damage foci (IRIF), distinct nuclear structures that can be microscopically visualized upon treatment with DSB-inducing agents. Early events during the DDR involve activation of ATM kinase, which mediates phosphorylation of H2AX (γH2AX) and the subsequent recruitment of MDC1 to the DSB-flanking chromatin (Stucki et al, 2005). MDC1 is a key player in the process of foci formation since recruitment and retention of MRN, RNF8, 53BP1, BRCA1 and other downstream factors depend on MDC1 and its ability to bind to γH2AX. However, even though H2AX or MDC1 deletion abrogates relocalization of most DDR proteins into nuclear foci, these cells exert comparatively mild defects in radiation sensitivity and checkpoint activation. Hence, the role of mediators and IRIF formation in the DNA damage response remains to be established. However, foci formation can denote the presence of DNA damage in pre-cancerous lesions and therefore may have the potential to be used as markers to visualize genomic instability in early neoplastic lesions (Bartkova et al, 2005; Gorgoulis et al, 2005).

4.3.1 Phosphopeptide interaction motifs

4.3.1.1 BRCT domains

BRCT repeats were first identified in the breast-cancer associated protein BRCA1 and since then have been shown to exist in a large number of proteins involved in the response to DNA damage (Bork et al, 1997). The BRCT domain encompasses 90-100 amino acids in length and can fold independently, despite its frequent appearance as tandem pairs, which are separated by regions of different size. BRCA1, MDC1, NBS1, 53BP1, DNA ligase IV and MCPH1 were shown to contain tandem BRCT repeats. MCPH1 carries a third BRCT domain at its N-terminus, PTIP was characterized with 6 BRCT domains and TopBP1 contains even 8 BRCT domains, while some proteins such as XRCC1, PARP1 and Polλ were shown to contain only a single domain (Mohammad & Yaffe, 2009).

The perception of BRCT domains as phosphopeptide-binding modules emerged only in 2003 and provided a basis for its molecular function during the DDR (Manke et al, 2003; Yu et al, 2003). The phosphopeptide-binding activity of BRCT domains is limited to tandem BRCT repeats and is generally much stronger for phosphoserine than for phosphothreonine. Furthermore, several BRCT domains were shown to strongly select for an aromatic residue in the pSer+3 position. In case of the interaction between BRCA1 and a phosphopeptide derived from BACH1, the phosphoserine binds to a pocket in the N-terminal BRCT domain, whereas the Phe at the pSer+3 position is bound to a deep groove at the interface between the two domains explaining the structural requirement of this BRCT tandem fold (Clapperton et al, 2004; Shiozaki et al, 2004). Similarly, a γH2AX peptide was shown to bind to a groove at the interface between the two BRCT domains of MDC1 with a strong preference for a C-terminal Tyr in the pSer+3 position (Stucki et al, 2005). However, not all BRCT domains act as phosphopeptide binding modules. Phospho-independent interactions have been described between 53BP1 and p53 as well as DNA ligase IV and XRCC4 (Derbyshire et al, 2002; Joo et al, 2002; Sibanda et al, 2001).

The critical role of BRCT domains in the DDR is corroborated by the observation that truncation and missense mutations of the essential BRCA1 BRCT repeats are frequently associated with human breast and ovarian cancers (Williams et al, 2003).

4.3.1.2 FHA domains

The FHA domain was first described for forkhead family transcription factors (Hofmann & Bucher, 1995). Since then, more than 2000 FHA-containing proteins have been identified in prokaryotes and eukaryotes (http://pfam.sanger.ac.uk/family/PF00498). The FHA domain can be found in many regulatory proteins, kinases, phosphatases and transcription factors and it is involved in various biological processes such as cell cycle control, cell growth, signal transduction and transcription and in the DNA damage signaling (reviewed in (Mahajan et al, 2008)). All characterized FHA domains differ greatly from BRCT domains or other phosphopeptide interaction motifs such as 14-3-3 proteins or WW-domains in that they specifically recognize phosphothreonine and not phosphoserine residues.

Up to now, the structures of 19 FHA domains, either free or in complex with their phosphopeptide ligands, have been solved by NMR or X-ray crystallography. Although the known FHA domains share rather low sequence homology, they all adapt a similar fold. The domain spans approximately 80-120 amino acid residues consisting of 11 β-strands. These strands form two large twisted anti-parallel β-sheets, which are folded into a β-sandwich structure. The specificity in binding to phosphopeptides is determined by the loops and turns that connect the β-strands and can vary in length and α-helical insertions between the different FHA domains (Figure 4.5).

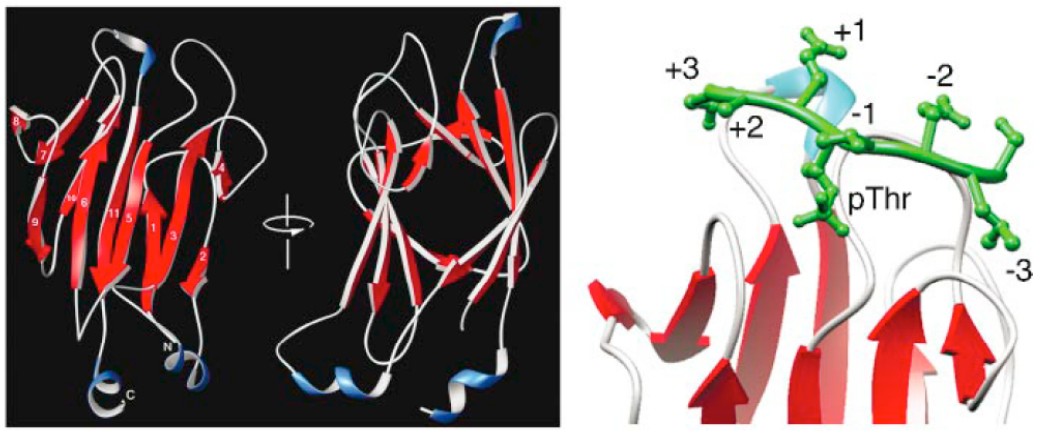

Figure 4.5

Structure of the Rad53 FHA1 domain. Left: The 11 β-strands of the FHA1 domain associate to form a β-sandwich fold. Right: Binding of *in vitro* selected phosphothreonine-containing peptides to the FHA1 domain mediated by interactions with loops and turns in between the β-strands. (Yaffe & Smerdon, 2004)

Combinatorial peptide library screening recently helped to identify ligand specificities for the different FHA domains (Durocher et al, 2000). In this approach peptides with a central phospho-threonine flanked by up to four random amino acid residues on either side were tested. The key finding of this analysis was that the highly conserved pThr and the following pThr+3 residue form the primary and secondary recognition site for binding to FHA domains. On the basis of their pThr+3 specificity, the FHA domains can be categorized into two major groups selecting for either Asp or Ile/Leu at the +3 position. For example, the Cds1-FHA and the Rad53-FHA1 domain showed a particular peptide binding preference for Asp in the pThr+3 position, whereas the Rad53-FHA2 domain selected for Ile or Leu. Some exceptions have also been identified including the proteins KAPP (kinase-associated protein phosphatase) with a preference for Ser or Ala and RNF8 with a preference for Tyr or Phe in the pThr+3 position (Durocher et al, 2000; Huen et al, 2007). Although most of the predicted ligand specificities could be confirmed by biological approaches, some FHA domains showed differences to the results obtained by the chemical library approach. For example, in an *in vivo* approach for Rad9p, which contains 5 potential TXXD motifs, $pThr^{192}$ instead of the predicted $pThr^{390}$ was determined as binding site for Rad53-FHA1 (Schwartz et al, 2002; Yuan et al, 2001).

In addition to the typical binding specificities of FHA domains for pTXXD or pTXX(I/L/V) sequences, three different types of recognition specificities were identified (reviewed in (Mahajan et al, 2008)). One group of FHA domains can additionally recognize residues N-terminal to pThr, as it was shown for murine PNK-FHA (Polynucleotide kinase) in complex with a peptide derived from XRCC4 (Bernstein et al, 2005). Another unique FHA domain is formed by Dun1, which specifically binds to the SQ-TQ cluster domain (SCD1) of Rad53 only when it is dually phosphorylated at Thr^5 and Thr^8. This finding could be confirmed *in vivo*, showing that dual phosphorylation of Rad53 is essential for full activation of Dun1 (Lee et al, 2008). The FHA domain of Ki67 constitutes another exception, as it rather recognizes an extended binding surface of a long peptide (43 amino acids) derived from hNIFK instead of a short phosphopeptide. In addition to pThr, this interaction requires the stacking of the β-strand of the peptide with the β-sheet of the Ki67 FHA domain (Byeon et al, 2005; Li et al, 2004; Mahajan et al, 2008).

Interestingly, in many cases FHA domains have been shown to be involved in kinase activation and oligomerization processes in response to DNA damage. A well-

studied example is the CHK2 kinase, which plays an important role in cell cycle regulation and apoptosis (Bartek et al, 2001). Following DNA damage, ATM phosphorylates CHK2 on Thr68 within an N-terminal SQ/TQ-rich cluster, which promotes the binding of this region to the FHA domain of another CHK2 molecule, resulting in dimerization or oligomerization. Eventually, dimerization triggers trans-autophosphorylation of CHK2 in the kinase activation loop, necessary for full CHK2 activation (Ahn et al, 2002; Xu et al, 2002). It has further been demonstrated that dimerization is a rather transient process since autophosphorylation, in particular of Ser140, destabilizes the dimer leading to its dissociation (Ahn et al, 2002; Li et al, 2008). Recently, the group of Pavletich succeeded in resolving the crystal structure of dimeric CHK2 involving the FHA and kinase-inactive domain but lacking the SCD domain (Cai et al, 2009). The dimer forms through mutual FHA-KD (kinase domain) and FHA-FHA interactions, whereby the FHA-KD interaction involves Ile157, a residue whose mutation gives rise to the cancer-predisposition Li-Fraumeni syndrome. However, the observation of an SCD-independent dimerization seems to be rather weak and is thought that the phospho-Thr68-FHA interaction might further stabilize the dimer *in vivo*. This hypothesis is supported by an approach that uses expressed protein ligation to generate the N-terminal regulatory region of CHK2 (Li et al, 2008). In this case phosphorylation at Thr68 stabilized the weak FHA-FHA interactions that occur in the non-phosphorylated form. It is proposed that thereby the dimerization not only activates CHK2, but also modulates potential phospho-dependent interactions with effector proteins and their substrates.

Similar FHA-dependent dimerization and autophosphorylation mechanisms have been described for the CHK2 homologues Cds1 in *S. pombe* and Rad53 in *S. cerevisae*, albeit the FHA domain structures are not identical and molecular mechanism may vary (Mahajan et al, 2008). The transactivation mechanism of Rad53 is complicated by the presence of two sets of SCD-FHA domains and molecular details of this process have not yet been completely understood.

4.4 MDC1: The art of keeping things in focus

Authors: Stephanie Jungmichel & Manuel Stucki

Journal: Chromosoma (manuscript accepted)

Contribution: Literature Research; preparation of the manuscript draft; preparation and drawing of the figures; proofreading of the manuscript

Chromosoma
DOI 10.1007/s00412-010-0266-9

REVIEW

MDC1: The art of keeping things in focus

Stephanie Jungmichel · Manuel Stucki

Received: 6 January 2010 / Revised: 5 February 2010 / Accepted: 14 February 2010

Abstract The chromatin structure is important for recognition and repair of DNA damage. Many DNA damage response proteins accumulate in large chromatin domains flanking sites of DNA double-strand breaks. The assembly of these structures—usually termed DNA damage foci—is primarily regulated by MDC1, a large nuclear mediator/adaptor protein that is composed of several distinct structural and functional domains. Here, we are summarizing the latest discoveries about the mechanisms by which MDC1 mediates DNA damage foci formation, and we are reviewing the considerable efforts taken to understand the functional implication of these structures.

Introduction

The DNA, the genetic material of our cells, is constantly exposed to DNA-damaging agents such as the sun's radiation or free oxygen radicals that arise as a consequence of natural cellular metabolism. Alternatively, cells may become transiently exposed to external sources of DNA damage such as cigarette smoke or various toxic chemical compounds. DNA double-strand breaks (DSBs), which are a particularly deleterious form of DNA damage, are formed upon treatment of the cells with ionizing radiation (IR) or chemical clastogens. They are also formed in a programmed manner during meiosis and development of the immune system. Since DSBs are highly toxic lesions that can lead to genomic rearrangements if they are not efficiently and accurately repaired, it is not surprising that cells have evolved highly sophisticated mechanisms to counteract those threats. Based on a seminal Nature review article by Zhou and Elledge in 2000, these mechanisms are often referred to as the DNA damage response (DDR; Zhou and Elledge 2000).

The DDR is a conglomerate of signaling transduction pathways consisting of sensors, transducers, and effectors. Although it is often delineated as a linear pathway, it is more accurately described as a network of interacting pathways that together execute the cellular response. Components of the DDR in mammalian cells include the phospho-inositide-like kinases (PIKKs) ATM, ATR, and DNA-PKcs, the transducer kinases CHK1 and CHK2, and the various effector proteins that are either targeted directly by the PIKKs or by one or both of the transducer kinases. Additional proteins have emerged as essential components of the DDR eukaryotes. For example, there is a group of proteins that contain phosphorylation-specific protein–protein interaction modules such as BRCA1 carboxy-terminal (BRCT) domains and/or forkhead-associated (FHA) domains. This protein family is usually referred to as mediators/adaptors of the DDR because most of these proteins lack enzymatic activity but may predominantly act as "molecular matchmakers" through their ability to mediate the efficient interaction of proteins that would otherwise not bind to each other.

A major hallmark of the mammalian DDR is the rapid deploying of a host of proteins to the sites of DNA damage within the nuclei of affected cells. Some of these proteins engage in the repair of the lesions, while others trigger kinase-dependent signaling cascades that induce events not only confined to the region where the damage has occurred,

Communicated by E. Nigg

S. Jungmichel · M. Stucki (✉)
Institute of Veterinary Biochemistry and Molecular Biology,
University of Zürich,
Winterthurerstrasse 190,
8057 Zürich, Switzerland
e-mail: m.stucki@vetbio.uzh.ch

Published online: 12 March 2010

but involving the entire cellular system. Some of the DDR factors that are rapidly recruited to sites of DNA damage have intrinsic affinity to aberrant DNA structures. For example, the MRE11/RAD50/NBS1 (MRN) complex, a conserved DDR sensor and repair factor, has been shown to bind preferentially to free DNA ends that arise at the sites of DSBs (de Jager et al. 2001). Other factors do not just bind to the DNA lesions per se, but accumulate in large nuclear aggregates surrounding the lesion site. These structures, which can be visualized by standard immunofluorescence microscopy, are usually referred to as nuclear foci, DNA damage foci, or ionizing radiation-induced foci (IRIF). The key regulators of IRIF formation are histone proteins that form the core of the nucleosome, the organizational unit of eukaryotic genomes. In mammalian cells, the histone H2A variant H2AX, a component of the nucleosome core structure that comprises 10–15% of total cellular H2A in higher organisms, is rapidly phosphorylated by PIKKs on a conserved Ser residue at its C-terminus in chromatin regions bearing DSBs. Phosphorylation of the H2AX C-terminus (termed γH2AX) "spreads" over large chromatin domains but is strictly confined to the damaged chromosome and does not involve neighboring chromosomes that are not affected by DNA damage (Rogakou et al. 1999). We are henceforth referring to these γH2AX modified chromatin regions as γH2AX chromatin domains. The phosphorylated H2AX C-terminus serves as an epigenetic chromatin mark that flags regions in the genome that contain DNA breaks. Mediator of the DNA damage checkpoint 1 (MDC1; sometimes also referred to as NFBD1), a large protein that belongs to the mediator/adaptor group of DDR factors, specifically binds to the phosphorylated H2AX C-terminus and appears to be the predominant γH2AX recognition factor in mammalian cells. MDC1 knockout mice display a very similar phenotype as H2AX knockout mice, thus corroborating the close functional relationship between these two DDR factors (Table 1). Moreover, MDC1 is an emerging tumor suppressor because loss of MDC1 is associated with increased tumor frequency in mice (Minter-Dykhouse et al. 2008), and reduction or lack of MDC1 is observed in a significant proportion of carcinomas (Bartkova et al. 2007). MDC1 is composed of several distinct domains and regions. Each of these domains or regions seems to be tailored to recognize one or several specific protein interaction partners that are recruited to the damaged chromatin regions.

In the past 5 years, we have seen much progress in the exploration of the molecular mechanisms by which MDC1 recognizes the γH2AX chromatin mark and mediates the interaction of several DDR factors with damaged chromatin regions. Phosphorylation-dependent protein–protein interactions that are dependent upon FHA and BRCT domains appear to be the central theme of these processes. In this article, we will review these latest findings. For the sake of clarity, we decided to follow a structural delineation rather than a chronological account by starting from the MDC1 C-terminus and subsequently working our way up to the N-terminus. We will briefly describe each of MDC1's structural and functional domains and regions and specify the proteins that are binding to these domains and regions. Moreover, we will summarize the functional implications of each of these domains and regions, as far as they are known. Finally, we will point out where our current knowledge about MDC1 is still incomplete and we will also highlight some of the major discrepancies in the literature.

The C-terminal tandem BRCT domain: assembly and maintenance of the γH2AX chromatin domain, regulation of mitotic progression, and control of the decatenation checkpoint

The tandem BRCT domain of MDC1 is located at the very C-terminus of the protein, between amino acid 1891 and 2082 (Fig. 1). X-ray structural analysis revealed that this region of MDC1 retains the typical tandem BRCT fold in which each BRCT repeat adopts a compact α/β fold and is connected by a linker region to form an extended structure about 70 Å long and 35 Å in diameter (Lee et al. 2005; Stucki et al. 2005). The first indication that the MDC1 tandem BRCT domain was involved in the regulation of the assembly of the γH2AX chromatin domain came from the observation that a green fluorescent protein (GFP) tagged version of the protein lacking the C-terminal BRCT region did not accumulate in IRIF in response to IR treatment. Moreover, the same study showed that overexpression of the BRCT region abrogated MDC1 and γH2AX IRIF (Shang et al. 2003).

Since BRCT repeats can act as phosphopeptide-binding domains, oriented phosphopeptide library screening was used to define the optimal phosphopeptide binding motif for the MDC1 BRCT tandem domain (Rodriguez et al. 2003; Stucki et al. 2005). These screens revealed that the MDC1 tandem BRCT domain bound selectively to peptides containing a phosphorylated Ser residue, and furthermore, selected for Glu at the +2 position and Tyr at the +3 position after the phosphorylated serine. These binding preferences closely match the sequence of the phosphorylated H2AX C-terminus (pS-Q-E-Y-COOH), suggesting that γH2AX is one of the binding partners of the MDC1 tandem BRCT domain. Indeed, biochemical, X-ray structural, and cell biological approaches clearly demonstrated that MDC1 directly interacts with γH2AX via its C-terminal BRCT region (Lee et al. 2005; Lou et al. 2006;

Table 1 Phenotypes associated with MDC1 loss. MDC1 loss induces a multitude of phenotypes both on the cellular level and also on the level of the whole organism

KO organism (mouse)	KO cellular (mouse)	siRNA cellular (human)
Small size	Radiosensitivity	Radiosensitivity
Male infertility	Intra-S phase checkpoint	Intra-S phase checkpoint
Radiosensitivity	G2/M checkpoint	G2/M checkpoint
Tumor-prone	IRIF	IRIF
	Phosphorylation (CHK1, CHK2, ATM)	Phosphorylation (CHK1, CHK2, ATM, SMC1)
	DSB repair by HR	DSB repair by HR
	NHEJ of dysfunctional telomeres	Random plasmid integration
	Chromosomal instability	Apoptosis
	Reduced proliferation	Slow mitosis
	Class switch recombination	

In this table we summarized the most important phenotypes associated with MDC1 loss

Stucki et al. 2005) (reviewed in Stucki and Jackson 2006). The structural data revealed that the phospho-peptide binding cleft of the MDC1 tandem BRCT domain is exquisitely tailored to recognize the γH2AX motif (Lee et al. 2005; Stucki et al. 2005). Point mutations in the phosphopeptide binding cleft of the MDC1 BRCT tandem domain, as well as in the H2AX C-terminus, abrogated the MDC1–γH2AX interaction in vitro; disrupted IRIF formation by several DDR factors including MDC1 itself, the MRN complex, phosphorylated ATM, 53BP1, and BRCA1; and rendered cells radio-sensitive (Stucki and Jackson 2006). These findings strongly indicate that one of the major biological functions of the MDC1 C-terminal BRCT region is the initial recognition of the γH2AX chromatin mark and the mediation of the recruitment and retention of DDR factors in chromatin regions flanking DSBs.

MDC1 does not only recognize the γH2AX chromatin mark, but it is also involved in its regulation. It was shown that MDC1 loss or experimental disruption of the MDC1–γH2AX interaction leads to reduced H2AX phosphorylation and small γH2AX IRIF (Lou et al. 2006; Stewart et al. 2003; Stucki et al. 2005). This indicates that MDC1 somehow positively regulates H2AX phosphorylation and that this regulation is dependent on the direct interaction between MDC1 and γH2AX. Since H2AX phosphorylation in response to DSBs does not spread in three dimensions throughout the cell nucleus, but is confined to chromatin regions flanking the break site on

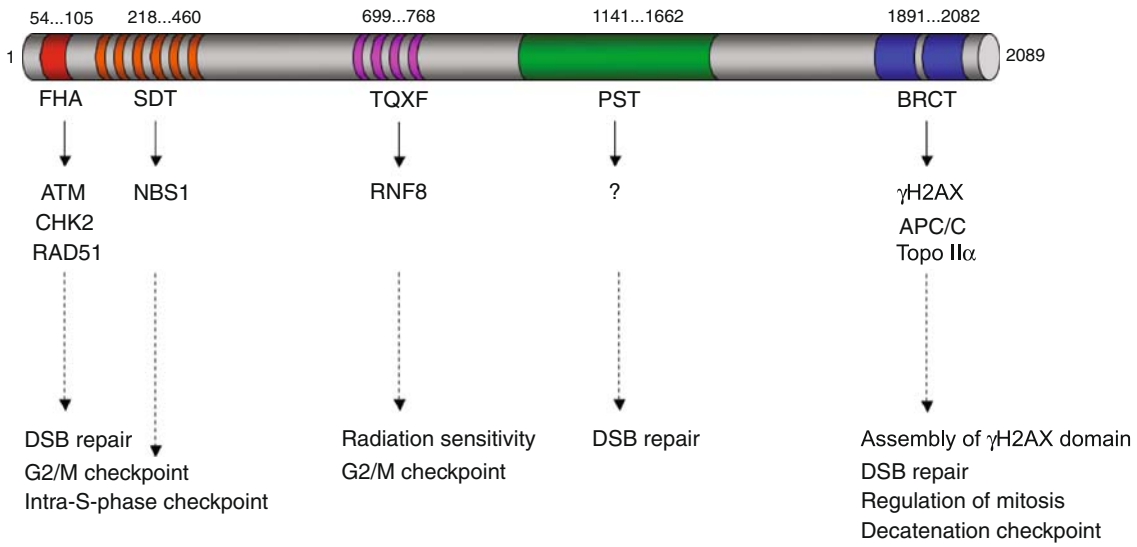

Fig. 1 Schematic representation of the domain architecture of MDC1 and its interaction partners. MDC1 is composed of several distinct domains and regions that either interact with phosphorylated proteins or are themselves phosphorylated and serve as docking sites for other proteins that contain phospho-specific interaction modules such as FHA and BRCT domains. Each of these domains and regions appears to be functionally relevant for the DDR and/or for control of the cell cycle. See text for details

the damaged chromosome (i.e. "spreads" only in two dimensions), it was proposed that MDC1 may be required for γH2AX spreading along the damaged chromatin fiber (Lou et al. 2006; Stucki and Jackson 2006). According to this model, MDC1 is recruited to γH2AX proximal to the lesion and either directly or indirectly mediates the recruitment and retention of activated ATM in the damaged chromatin compartment. ATM could then phosphorylate more H2AX molecules that are located more distal to the initiating lesion. As a consequence, the γH2AX chromatin mark would spread further and further away from the initial break. However, the model of MDC1-fuelled self-reinforcing H2AX phosphorylation cycles to spread the γH2AX chromatin mark along the chromosome axis has recently been challenged. One of the major caveats in assessing the mechanism of γH2AX formation was the lack of "resolution." Up until recently, researchers have relied on microscopic techniques to study the dynamic assembly of the γH2AX chromatin domain. While these microscopic techniques have been very useful to measure the kinetics of protein recruitment to sites of DNA damage and to assess the dynamics of the assembly and disassembly of the γH2AX chromatin domain, they have not been capable of delivering any information about the density of H2AX phosphorylation and the distance of γH2AX spreading along the axis of the damaged chromosome. However, there exists a very powerful technique that can yield this kind of data: chromatin immunoprecipitation (ChIP). While ChIP has been widely and successfully used to study the assembly of protein complexes on chromatin, as well as the dynamic changes of epigenetic states (e.g., in transcriptional control), its successful application in the mammalian DDR field has long been impeded by the challenge to efficiently induce DNA breaks at specific loci in the genome. To circumvent this problem, one group studied the spreading of γH2AX on shortened telomeres in senescent primary cells (Meier et al. 2007). Shortened telomeres in senescent cells have been shown to trigger a DDR similar to the one that is activated by DSBs. In this study, it was shown that the γH2AX chromatin mark spreads up to about 570 kb into the subtelomeric regions. Furthermore, the spreading pattern of MDC1 was very similar to that of γH2AX, confirming the functional and structural link between these two factors. Importantly, this study also revealed that γH2AX density is not uniform along the chromosome axis (Meier et al. 2007). Another study recently used primary mouse lymphocytes to study γH2AX density and spreading during V(D)J recombination in G1 (Savic et al. 2009). The major advantage of this experimental system is the efficiency by which the RAG1/RAG2 (RAG) endonucleases induce DSBs between the variable (V), diversity (D), and joining (J) gene segments and their flanking RAG recognition sequences. Since the genomic locations of the RAG-initiated DSBs are known, γH2AX density and spreading could readily be measured by ChIP at this specific locus. Surprisingly, these data revealed that MDC1 is not required for the spreading of the γH2AX chromatin mark but, instead, for keeping up a high γH2AX density proximal to the break site (Savic et al. 2009). Thus, it is possible that the previously proposed MDC1-dependent γH2AX self-reinforcing mechanism only applies to chromatin regions close to the lesion, while other mechanisms may regulate γH2AX spreading into more distal regions of the damaged chromatin fiber. It remains to be determined whether these observations only apply to RAG-initiated DSBs or if they are a general characteristic of the cellular response to DSBs.

It has been proposed that MDC1 may control H2AX phosphorylation through another mechanism that is not related to its ability to mediate the accumulation of active ATM in damaged chromatin compartments. This model suggests that MDC1 may control the dephosphorylation of H2AX through its direct binding to the phospho-epitope located at C-terminus of H2AX. This interpretation was based on the observation that the purified MDC1 BRCT domains could efficiently shield γH2AX phosphopeptides from phosphatase activity in vitro. Moreover, overexpression of the isolated MDC1 BRCT region in mammalian cells resulted in H2AX hyperphosphorylation (Stucki et al. 2005). It was recently discovered that the phosphatases PP2A and PP4 are involved in the removal of γH2AX from chromatin in mammalian cells (Nakada et al. 2008). Thus, it will be interesting to see if MDC1 can limit the access of these phosphatases to γH2AX in vivo.

The recent discovery of yet another phosphorylation event at the H2AX C-terminus has added an additional layer of complexity to the regulation of the γH2AX chromatin domain. In two recent Nature articles, the Allis and Rosenfeld laboratories described the phosphorylation of Tyr142 (the very C-terminal amino acid of H2AX) by the WICH complex and its dephosphorylation by the EYA1/3 phosphatases (Cook et al. 2009; Xiao et al. 2009). As these findings and their implications for the DDR have recently been reviewed in detail elsewhere (Stucki 2009), we will just briefly summarize the main issues here: while H2AX Ser139 is targeted by DNA damage-activated PIKKs, Tyr142 is phosphorylated by the constitutive kinase WSTF, a subunit of the WICH chromatin remodeling complex. However, upon induction of DNA damage, Tyr142 becomes dephosphorylated by the EYA1/3 phosphatases. How exactly this dephosphorylation is regulated remains elusive, but Tyr142 dephosphorylation is necessary for the assembly of the γH2AX chromatin domain because MDC1 is not capable of efficiently binding to γH2AX as long as Tyr142 is phosphorylated.

But what is the physiological role of H2AX Tyr142 phosphorylation? One attractive possibility is that the

Tyr142 phosphorylation/dephosphorylation equilibrium may determine cell fate in response to genotoxic stress. As mentioned above, Tyr142 phosphorylation attenuates MDC1 recruitment and the establishment of the γH2AX chromatin domain. However, it was proposed that the Tyr142 modification may promote the recruitment of the pro-apoptotic factor JNK1 to sites of DNA damage (Cook et al. 2009). Thus, if repair is possible, Tyr142 is dephosphorylated and the DDR machinery is recruited to sites of DNA damage to promote repair. However, if the damage is too severe to be repaired in time, tyrosine phosphorylation remains and apoptosis is favored through the association of JNK1 with γH2AX. This is still a rather simplified model, and our understanding of the regulation of the γH2AX chromatin domain is still incomplete. Thus, more work is needed to understand this important process in detail.

Recently, two additional phosphorylation-specific interaction partners for the MDC1 BRCT domains have been discovered. CDC27, a subunit of the anaphase promoting complex APC/C was shown to interact directly with MDC1 via its phosphorylated C-terminal region (Coster et al. 2007). The APC/C is a multi-subunit E3 ubiquitin ligase that controls mitotic progression mainly through ubiquitin-dependent destruction of mitotic cyclins and other substrates in a coordinated manner. Interestingly, the sequence of the phosphorylated MDC1 binding site in CDC27 is located at the very C-terminus of the protein and is very similar to the MDC1 binding site in H2AX: the phospho-acceptor Ser residue is also followed by a Glu at the +2 position and a Phe at the +3 position (pS-D-E-F-COOH). Phosphopeptide screening has indicated that the MDC1 BRCT domains strongly select for Glu at +2, and Tyr, but not Phe, at the +3 position (Rodriguez et al. 2003; Stucki et al. 2005). Thus, it appears that CDC27 binding to MDC1 is effectively produced by the strong selection of Glu at +2. Moreover, the relative localization of the C-terminal carboxylate in respect to the phosphorylated Ser residue is identical in CDC27 and γH2AX. The kinase that targets the CDC27 C-terminus is currently unknown, but considering that the MDC1 CDC27 interaction is increased after DNA damage (Coster et al. 2007), CDC27 phosphorylation may be somehow modulated by DNA damage. An interesting possibility would be that MDC1 is involved in the regulation of mitotic progression in response to DNA damage through its interaction with the APC/C. However, no experimental evidence for such a function has yet been produced. Instead, it was recently demonstrated that MDC1 is regulating mitotic progression independently of DNA damage. Grant Stewart and colleagues showed that MDC1-deficient human cells have defects in mitotic progression at the metaphase/anaphase transition (Townsend et al. 2009). Moreover, the activity of the APC/C ubiquitin ligase is compromised in the absence of MDC1. However, mechanistically, MDC1 appears to modulate the APC/C activity rather through its interaction with CDC20 (an activator protein that regulates the substrate specificity of the APC/C ubiquitin ligase) and not through its interaction with the APC/C subunit CDC27 (Townsend et al. 2009). Thus, it remains elusive as to how the phospho-dependent MDC1–CDC27 interaction contributes to the control of mitotic progression.

Another phospho-specific MDC1 BRCT-interacting factor was recently discovered by Lou and colleagues: DNA topoisomerase IIα (Topo IIα; (Luo et al. 2009)). MDC1-Topo IIα interaction seems to regulate the decatenation checkpoint, a checkpoint that controls the entanglement ("catenation") of chromosomes at the end of DNA replication. This checkpoint arrests cells in G2 and delays onset of mitosis until sister chromatids are fully separated. A phosphorylation site close to the C-terminus of Topo IIα appears to mediate the interaction with the MDC1 C-terminal BRCT repeat. Surprisingly though, this phosphorylation site presents only limited sequence similarity to the H2AX and CDC27 C-terminal MDC1-binding epitopes, suggesting a different mode of binding, or perhaps an indirect interaction. Quantitative phosphopeptide-binding studies and/or structural approaches will be required to resolve this issue.

The PST repeat region: regulation of DSB repair and mitotic progression?

The region in human MDC1 between amino acids 1141 and 1662 is generally referred to as the proline–serine–threonine (PST)-rich repeat (Fig. 1). In humans, this region consists of 13 consecutive imperfect repeats of 41 amino acids. The PST repeat is one of the least conserved regions in MDC1 and does not appear to exist at all in MDC1 orthologues of non-vertebrates (e.g., *Drosophila* (Dronamraju and Mason 2009)). However, in most vertebrate species, the PST repeat is present and conserved, even though the number of repeats varies greatly from 13 consecutive repeats in human MDC1 to seven repeats in mouse MDC1. Primary sequence analysis did not reveal any known structural and functional motifs, and sequence comparison and database searches did not retrieve significant homology to any other known protein.

To this day, little is known about the functional implication of the PST repeat region. However, it is clear that the PST repeat is neither required for MDC1 accumulation at sites of DSBs (Shang et al. 2003), nor for MDC1's function to mediate the accumulation of 53BP1, BRCA1, and the MRN complex in damaged chromatin compartments (Lou et al. 2004; Xie et al. 2007) (see also

next sections). In an early study by the Chen laboratory, it was proposed that the PST repeat region constitutes a binding site for DNA-PK. Moreover, in this work, it was shown that deletion of the PST repeat triggers a partial non-homologous end joining (NHEJ) defect (Lou et al. 2004). However, the mechanism by which the MDC1 PST repeat would regulate NHEJ remained elusive because MDC1 is not required for DNA-PK recruitment to sites of DSBs (Gottlieb and Jackson 1993). It was proposed that MDC1 may mediate the accumulation of DNA-PK in chromatin regions flanking DSBs in similar manner as it mediates the accumulation of the MRN complex (Lou et al. 2004). However, DNA-PK does not seem to accumulate in IRIF in response to DSBs (Bekker-Jensen et al. 2006). Thus, a functional implication of the observed interaction between the MDC1 PST region and DNA-PK remains elusive.

Interestingly, the PST repeat region does not only appear to be important for DSB repair by NHEJ, but also for homologous recombination (HR). In a genetic HR reporter system, a mutant MDC1 version lacking the PST repeat region was defective for HR, while this mutant was still proficient in accumulating at sites of DSBs and in mediating the accumulation of other DDR proteins such as 53BP1, BRCA1 at sites of DSBs (Xie et al. 2007). It thus appears that the MDC1 PST repeat region is implicated in DSB repair by both NHEJ and HR, although the mechanism of action of this unusual repeat motif in DSB repair remains to be elucidated.

According to a recent report, the PST repeat region is also implicated in mitotic progression. As outlined in the last section, MDC1 deficient cells have defects in mitotic progression at the metaphase/anaphase transition, which is associated with an increased number of mitotic cells in a population of MDC1 deficient cells as compared to control cells that express normal amounts of MDC1 (Townsend et al. 2009). Expression of a mutant MDC1 version lacking the PST repeat region could not restore this mitotic defect while expression of wild-type MDC1 rescued the phenotype. Interestingly, there seems to be an interaction between several subunits of the APC/C and the MDC1 PST repeat region, which may mechanistically explain the mitotic defect observed in cells expressing a MDC1 version lacking the PST repeat (Townsend et al. 2009).

The TQXF cluster: Regulation of chromatin ubiquitylation

N-terminal of the PST repeat resides a region in MDC1 that is characterized by a noticeable abundance of PIKK consensus phosphorylation Ser/Thr-Gln (S/TQ) sites. Particularly striking is a cluster of four nearby TQ motifs that are all followed by the Phe at the +3 position (located between amino acid 699–768 in human MDC1). We will henceforth refer to this region as the TQXF cluster. Early studies on human MDC1 suggested that the protein is targeted by ATM in response to IR treatment, but the exact location of the phosphorylation sites were not determined (reviewed in Stucki and Jackson 2004). However, at least a subset of the TQXF motifs in MDC1 have recently been identified to represent bona fide ATM targets in response to IR (Kolas et al. 2007; Mailand et al. 2007; Matsuoka et al. 2007). Phosphorylation of these sites mediates the recruitment of the E3 ubiquitin ligase RNF8 through direct interaction of its FHA domain with the MDC1 phosphorylated TQXF region (Huen et al. 2007; Kolas et al. 2007; Mailand et al. 2007) (see Fig. 2). FHA domains, like BRCT tandem domains, recognize amino acid sequences around a central phosphorylation site. However, while BRCT tandem domains recognize both pSer and pThr-containing sequences, FHA domains appear to only recognize pThr-containing motifs (Durocher and Jackson 2002). Intriguingly, the RNF8 FHA domain showed strong selection for Phe and Tyr at the +3 position (Huen et al. 2007). Such a selection for aromatic amino acids at the +3 position closely resembles the optimal phosphopeptide motifs recognized by the tandem BRCT domains of MDC1 and BRCA1 (reviewed in Mohammad and Yaffe 2009; see also above).

Immunofluorescence microscopy showed that deletion of these TQXF motifs in MDC1 or depletion of RNF8 led to impaired IRIF formation for conjugated ubiquitin, 53BP1 and BRCA1, whereas γH2AX, MDC1, and NBS1 IRIF were not affected. Furthermore, 53BP1 and BRCA1 accumulation was dependent on the E3 ubiquitin ligase domain (a RING domain) of RNF8, indicating that IRIF formation of these proteins is controlled by local ubiquitylation of substrates in chromatin regions flanking DSBs. Although the identity of these substrates has currently not yet been addressed in vivo, several lines of in vitro evidence suggest that the major RNF8 substrates that mediate 53BP1 and BRCA1 accumulation at sites of DSBs may be the histone proteins H2A and H2AX (Huen et al. 2007; Mailand et al. 2007).

What is the physiological role of local chromatin ubiquitylation and how exactly does this posttranslational modification influence the accumulation of DDR proteins such as 53BP1 and BRCA1 in damaged chromatin regions? Downregulation of RNF8 by small interfering RNAs (siRNAs) yields a G2/M checkpoint defect and renders cells radiosensitive, implicating MDC1-dependent local chromatin ubiquitylation in DNA damage signaling and perhaps also DSB repair in mammalian cells. The mechanism, by which MDC1-dependent RNF8 recruitment ensues the chromatin ubiquitylation cascade and mediates IRIF formation by 53BP1 and BRCA1 appears to be rather complicated and has yet to be resolved in detail. However,

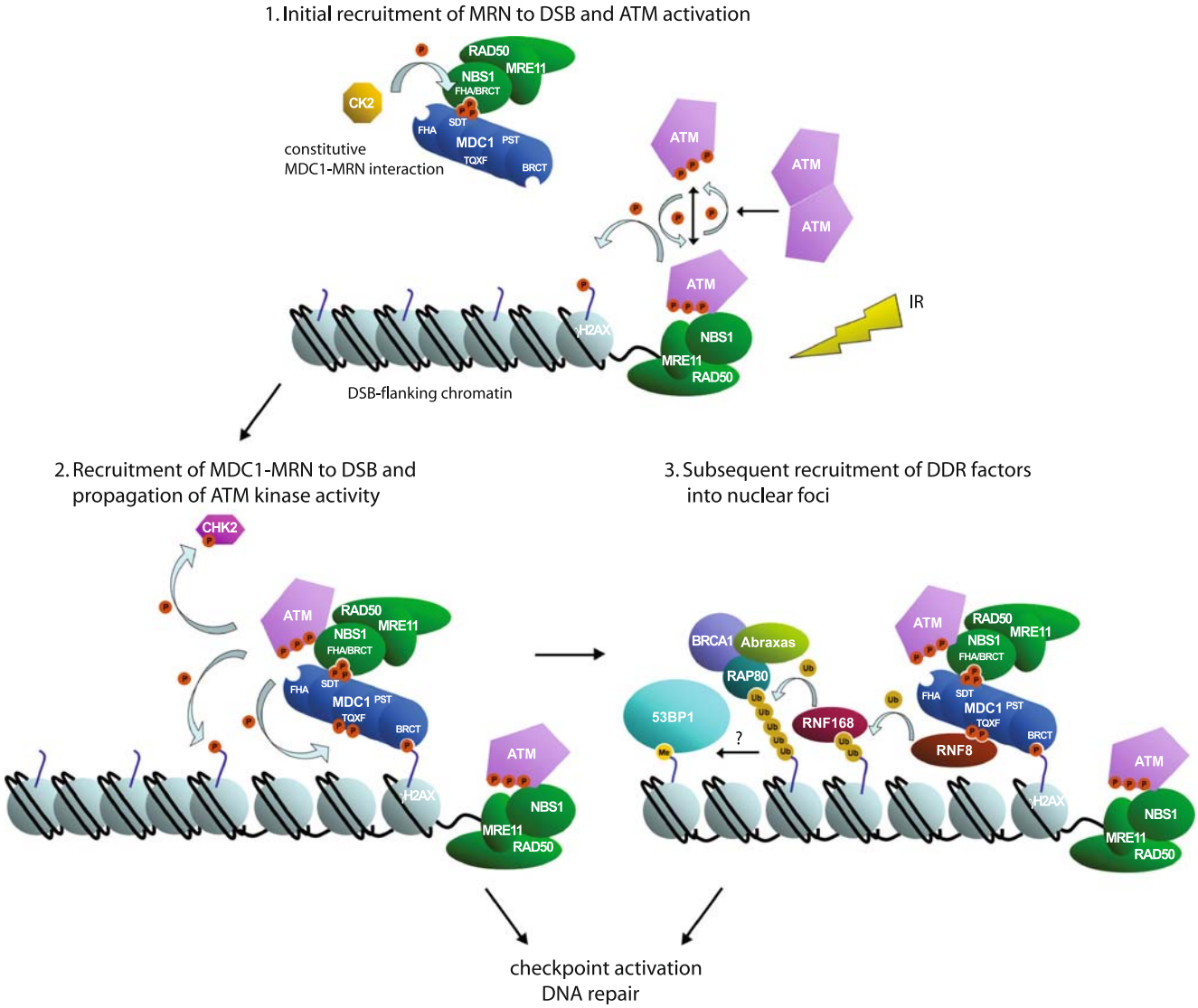

Fig. 2 Model of the assembly of the γH2AX chromatin domain. *1* In response to DSB-causing genotoxic agents MRN directly binds to free DNA ends and facilitates the recruitment and activation of the ATM kinase, which is autophosphorylated and, thus, converted from an inactive dimer into active monomers. ATM phosphorylates H2AX in the nearby DSB-flanking chromatin. *2* MDC1 recognizes the γH2AX chromatin mark and mediates the sustained interaction of the MRN complex with damaged chromatin through direct phosphorylation-dependent interaction. *3* Phosphorylated MDC1 recruits the ubiquitin ligase RNF8 and additional DDR factors, thereby triggering a signaling cascade that is dependent on ubiquitylation of histones and results in checkpoint activation and DNA repair. See text for details

it is clear that at least one additional ubiquitin ligase and ubiquitin-dependent adaptor proteins are involved in these processes. As these downstream events are not directly controlled by MDC1 and have been recently reviewed in detail elsewhere (Panier and Durocher 2009; Van Attikum and Gasser 2009), we will just briefly summarize the most important findings here and outline the current model (see Fig. 2).

While it was shown that the ubiquitin ligase activity of RNF8 is required to trigger DSB-associated ubiquitylation, it is not sufficient to sustain the conjugated ubiquitin in the damaged chromatin regions. Several groups identified RNF168 as a novel chromatin-associated ubiquitin ligase that acts in concert with UBC13 to catalyze formation of K63-linked ubiquitin conjugates and ubiquitylates family members of the H2A family in regions surrounding the DSB as efficiently as RNF8. In addition, RNF168 possesses the ability to bind ubiquitylated H2A in an RNF8-dependent manner (Doil et al. 2009; Stewart et al. 2009). This suggests that, while RNF8 acts as initiating ubiquitin ligase in DSB-flanking chromatin, RNF168 activity stabilizes and/or amplifies the signal in order to reach a threshold level that mediates the recruitment of downstream factors 53BP1 and BRCA1 and thereby allows the completion of the DSB-induced chromatin response. Significantly, RNF168 is mutated in RIDDLE syndrome patients that

suffer from immunodeficiency and radiosensitivity (Stewart et al. 2007, 2009). These phenotypes may arise mainly from defective chromatin ubiquitylation and dysfunctional 53BP1 and BRCA1 retention, a process that may be particularly important for the proper repair of programmed DSBs during the development the immune system in humans (recently reviewed in Stewart 2009).

The ubiquitylated histones likewise form a direct recognition motif for the ubiquitin-interacting motif (UIM)-containing receptor-associated protein 80 (RAP80), leading to its accumulation in IRIF with a preference for K63- and K6-linked ubiquitin polymers (Kim et al. 2007; Sobhian et al. 2007; Wang et al. 2007). RAP80 accumulates in IRIF and facilitates the recruitment of BRCA1, which is mediated by Abraxas that directly interacts with the BRCT domain of BRCA1 in a DNA damage-induced phospho-dependent manner (Wang et al. 2007) (Fig. 2). Taken together, the sequential recruitment of the three ubiquitin ligases RNF8, RNF168, and BRCA1 and the resulting ubiquitylation of chromatin components (perhaps mainly H2A-type histones) imply that this type of posttranslational modification represents a crucial novel regulatory process in the response to genotoxic lesions.

While the MDC1/RNF8-dependent retention of BRCA1 can be mechanistically explained with a model that involves direct protein–protein interactions, the MDC1/RNF8-dependent accumulation of 53BP1 is less well understood. No ubiquitin-binding domains have yet been identified in 53BP1 that could explain its recruitment to DSB-associated ubiquitylated chromatin components. Thus, MDC1 may exert its function also more indirectly, e.g., through initiation of chromatin reorganization events that would eventually increase the accessibility of proteins to newly exposed histone marks that are buried in higher-order chromatin structure. In this regard, the 53BP1 Tudor domain was shown to be required for 53BP1 accumulation at sites of DSBs (Huyen et al. 2004). These domains may bind to methylated histone marks that are masked in unperturbed chromatin, but may become locally exposed in a ubiquitin-dependent manner in response to DNA damage (Botuyan et al. 2006; Huyen et al. 2004). In any case, the vast majority of data presently available promote the idea that MDC1-mediated chromatin modifications and/or higher-order chromatin rearrangements might facilitate the accumulation and sustained retention of 53BP1 at sites of DSBs.

What is the functional implication of MDC1/RNF8-mediated BRCA1 and 53BP1 accumulation at sites of DSBs? While this is still not yet resolved in detail, an interesting clue recently came from the telomere field. It has been known for quite some time that chromosomes that have lost their protective telomeric “cap” undergo chromosome end-to-end fusions in a process that is dependent on the NHEJ machinery. MDC1-deficient cells show a significant reduction in NHEJ of dysfunctional telomeres (Dimitrova and de Lange 2006). This is most likely due to the inefficient accumulation of 53BP1 at dysfunctional telomeres in the absence of MDC1. 53BP1 is thought to promote chromosome end-to-end fusions by altering the dynamic behavior of chromatin at dysfunctional telomeres (Dimitrova and de Lange 2008). However, it is not yet known if this effect is specific for NHEJ of dysfunctional telomeres or if it also applies to NHEJ in general.

The SDT repeat region: constitutive interaction with the MRN complex

Upstream of the TQXF cluster, MDC1 features a second repeat region that is characterized by conserved patches of 8–10 amino acids comprising Ser and Thr residues typically separated by an aspartate and further embedded in an acidic sequence environment. This so called SDT region (in some papers also referred to as SDTD region) interacts with the MRN complex in a phosphorylation-dependent manner (Chapman and Jackson 2008; Melander et al. 2008; Spycher et al. 2008; Wu et al. 2008) (Fig. 2). The MRN complex is an essential component of the DNA damage signaling machinery. Due to its ability to recognize free DNA ends, the MRN complex is capable of acting as a sensor of DSB. It further exhibits DNA-end processing activity, tethers DNA ends, and is required for efficient ATM kinase activation (reviewed in Williams et al. 2007). Accomplishing the aforementioned functions does not seem to require the presence of MDC1. However, similar to 53BP1 and BRCA1 (see above), accumulation and retention of MRN complex in DSB-flanking chromatin regions strictly depends on MDC1 (Bekker-Jensen et al. 2006; Goldberg et al. 2003; Lukas et al. 2004).

In human MDC1, six SDT motifs were identified, and deletion of at least five of them leads to complete abrogation of MRN IRIF formation (Melander et al. 2008; Spycher et al. 2008). Analysis of NBS1 recruitment to sites of DSBs revealed that, upon expression of an MDC1 version lacking the SDT regions, NBS1 only accumulates in micro-IRIF but is not found in the broader chromatin compartments usually covered by γH2AX and MDC1 (Chapman and Jackson 2008). This indicates that the MRN complex is recruited to DSBs in a MDC1-independent manner, but its sustained interaction with the DSB-flanking chromatin requires MDC1.

Interestingly, MDC1 and MRN exist in a complex even in undamaged cells. This interaction is dependent on the activity of the acidophilic caseine kinase 2 (CK2) for which the SDT motifs form consensus phosphorylation sites (Spycher et al. 2008; Wu et al. 2008). Both Ser and Thr residues in each SDT motif are phosphorylated by CK2 in

vivo, and only doubly phosphorylated pSDpT motifs are capable of mediating the interaction with NBS1 (Melander et al. 2008; Spycher et al. 2008).

Two recent X-ray structural studies revealed that NBS1 contains a compact module at its N-terminus formed by an FHA and a tandem BRCT domain (Lloyd et al. 2009; Williams et al. 2009). Phosphopeptide-binding studies revealed that both the FHA domain of NBS1 and its BRCT domains preferentially bind to SDT-like motifs that are phosphorylated on both Ser and Thr residues (Lloyd et al. 2009). These motifs are found in MDC1 (see above), and also in fission yeast Ctp1 (the yeast orthologue of mammalian CtIP that is involved in DSB resection and HR) and budding yeast Lif1 (the yeast orthologue of mammalian XRCC4 that is involved in NHEJ). Both Ctp1 and Lif1 have been shown to interact with the N-terminal region of yeast NBS1 (Lloyd et al. 2009; Matsuzaki et al. 2008; Williams et al. 2009). MDC1 orthologues have so far not been detected in yeast. It is currently also not known if human NBS1 is capable of interacting with the human orthologues of yeast Ctp1 and Lif1 (CtIP and XRCC4, respectively) in a CK2-dependent manner.

Doubly phosphorylated pSDpTD peptides interact with both FHA and BRCT domains of human NBS1 since only mutations in both domains effectively abolished the interaction (Lloyd et al. 2009). Mutation of key residues in the FHA and the tandem BRCT domain similarly reduce the interaction between CK2-phosphorylated MDC1 protein and the MRN complex, thus indicating the requirement of an intact domain structure at the N-terminus of NBS1 for optimal binding (Chapman and Jackson 2008; Lloyd et al. 2009). Moreover, alterations in either FHA or BRCT domains impair relocalization of the MRN complex to IRIF (Cerosaletti and Concannon 2003; Spycher et al. 2008; Wu et al. 2008; Xu et al. 2008). These data point to a dual phospho-dependent interaction mode between MDC1 and the FHA/BRCT region of NBS1.

Functionally, the NBS1 FHA/BRCT region is required for the activation of the intra-S-phase and the G2/M DNA damage checkpoints and is likely also participating in DSB repair. However, the molecular mechanisms underlying these functional implications remain largely elusive. Defective checkpoint activation has been observed in NBS1 FHA and BRCT phospho-binding mutants (Difilippantonio et al. 2007; Wu et al. 2008; Zhao et al. 2002), strongly suggesting that the interaction with MDC1 may be required for ensuing an efficient DNA damage checkpoint response. However, it is not yet clear how exactly MDC1–NBS1 complex formation is implicated in DNA damage signaling. One possibility is that accumulation and retention of the MRN complex in chromatin regions flanking DSBs may help to amplify the checkpoint response in the presence of low numbers of DNA breaks (Spycher et al. 2008; Stucki and Jackson 2006). In addition, MDC1-dependent chromatin retention of NBS1 may also be necessary to efficiently recruit the ATM kinase to the damaged chromatin compartments (Falck et al. 2005), even though this issue is currently still a matter of controversy (see also below).

The N-terminal FHA domain: an enigma at the end

Perhaps with the exception of the PST repeat region, the N-terminal FHA domain of MDC1 is still the most enigmatic element of this large and versatile mediator protein. This is surprising given that FHA domains are well-characterized phospho-specific interaction modules that occur rather frequently in DDR proteins. It has also been clear for a while that the N-terminal FHA domain is important for MDC1's functions in the DDR: deletion of this domain leads to multiple DDR defects, including a defective G2/M DNA damage checkpoint, inefficient DSB repair by sister chromatid recombination, and reduced apoptosis in response to IR (Lou et al. 2003, 2006; Xie et al. 2007; Zhang et al. 2005). Even though several interaction partners for the FHA domain have been identified in the past years, none of them seems to quite "fit in."

As a first candidate, phosphorylated CHK2 was described as putative MDC1–FHA interacting factor (Lou et al. 2003). Immunoprecipitation and peptide-binding studies suggested that CHK2, phosphorlyated on Thr68, could form a stable complex with MDC1 in vitro and in cell extracts. Moreover, the MDC1 FHA domain was required for this interaction. In support of this finding, oriented phosphopeptide library screening revealed that the MDC1 FHA domain bound selectively to peptides containing a phosphorylated Thr residue, and furthermore, selected for Gln at the +1 position and Leu/Ile at the +3 position after the phosphorylated Thr (Durocher et al. 2000). These binding preferences closely match the sequence surrounding the Thr68 of CHK2 (pT-Q-E-L), thus corroborating the interpretation that CHK2 phosphorylated on Thr68 is a bona fide binding partner of the MDC1 FHA domain. However, CHK2 and MDC1 do not co-localize in cells that have been treated by DSB-inducing agents. While MDC1 accumulates in IRIF, CHK2 remains dispersed throughout the nucleus (Lukas et al. 2003). This implies that the interaction between MDC1 and phosphorylated CHK2 is very transient in nature (at least in vivo) and, thus, does not compare, for example, to the stable interaction between the phosphorylated MDC1 TQXF cluster and the RNF8 FHA domain, even though this latter interaction is also based on a phosphorylated TQ motif and an FHA domain. Furthermore, it was recently shown that a tight pThr68-dependent head-to-tail dimerization of CHK2 results in effective occlusion of the phospho-epitope and would prevent

interaction of the phospho-Thr68 motif with the MDC1 FHA domain (Li et al. 2008). However, autophosphorylation of CHK2 releases monomeric CHK2 (Ahn and Prives 2002; Li et al. 2008), which would expose the phospho-Thr68 motif and, potentially, allow binding to the MDC1 FHA domain. This mechanism could cause a very rapid switching of the phosphorylated CHK2 between MDC1-bound state and MDC1-free dimeric state and may account for the observation that, in response to DNA damage, CHK2 remains dispersed throughout the nucleus and does not accumulate in IRIF (Lukas et al. 2003).

MDC1 was also reported to interact with the ATM kinase through its N-terminal FHA domain (Lou et al. 2006). Immunoprecipitation experiments showed that ATM and MDC1 exist in a complex (Stewart et al. 2003). Moreover, ATM seems to weakly associate with the isolated FHA domain of MDC1 in vitro (Lou et al. 2006). Immunofluorescence microscopy revealed that, in the absence of MDC1 (or in the presence of an MDC1 version lacking the N-terminal FHA domain), antibodies raised against the autophosphorylated ATM kinase could not anymore detect phospho-ATM IRIF accumulation, indicating that MDC1 may recruit phosphorylated ATM into damaged chromatin compartments via direct interaction with its FHA domain. However, it should be pointed out that a correct interpretation of these data is difficult because it is currently very difficult to control the specificity of phospho-specific ATM antibodies in indirect immunofluorescence. Phospho-specific antibodies raised against pTQ/pSQ peptides are notoriously promiscuous and usually cross-react with many PIKK target proteins (Matsuoka et al. 2007). It is therefore likely that phospho-specific ATM antibodies are no exception and may be recognizing other proteins besides ATM in immunofluorescence. Thus, it is not yet clear if ATM IRIF formation is really dependent on the MDC1 FHA domain. To complicate matters further, it has also been suggested that ATM accumulation at sites of DSBs is mediated by the C-terminal region of NBS1. ATM IRIF formation was defective in cells expressing a NBS1 version lacking a C-terminal ATM-interacting peptide (Falck et al. 2005). Since NBS1 IRIF formation is also dependent on MDC1, it is possible that ATM accumulation is not mediated by direct interaction with MDC1, but indirectly, through its association with the NBS1 C-terminus. To resolve this matter in an unbiased manner, ATM IRIF formation needs to be analyzed with antibodies raised against the non-phosphorylated protein, whose specificity can be properly controlled in ATM-deficient cells. Alternatively, GFP-tagged recombinant ATM may be used to test if IRIF accumulation is dependent upon the SDT region of MDC1 (that mediates the accumulation of the MRN complex, see above), or upon the FHA domain of MDC1 that may directly interact with ATM.

The MDC1 FHA domain has also been implicated in DSB repair via sister chromatid recombination (Xie et al. 2007; Zhang et al. 2005). It was proposed that this is brought about through a specific interaction between the FHA domain of MDC1 and the recombinase RAD51 (Zhang et al. 2005). However, this is difficult to comprehend because, at early time points after irradiation, RAD51 foci and MDC1 IRIF do not co-localize (Goldberg et al. 2003). Moreover, RAD51 and MDC1 do not occupy the same compartments at sites of DSBs: while RAD51 binds to single-stranded DNA stretches that are the result of DSB resection in S and G2 phases of the cell cycle, MDC1 accumulates in the chromatin compartment flanking sites of DSBs, independently of the cell cycle state (Bekker-Jensen et al. 2006). Thus, whether and how interaction between the MDC1 FHA domain and RAD51 contributes to DSB repair by HR remains elusive.

Concluding remarks

In the past few years, MDC1 has emerged as a prototype mediator, acting mainly as a "molecular matchmaker" in the mammalian response to DNA damage. The entire protein appears to be composed of regions and domains that are involved in protein–protein interactions; most of them occur as phosphorylation-specific interactions.

Recent key findings have also significantly contributed to our understanding as to how MDC1 functions in the DDR. The best-characterized functional role of this protein is that it acts as a bridging element to dynamically tether various DDR factors to damaged chromatin regions that contain phosphorylated H2AX molecules. Mechanistically, this function is based upon a very specific interaction between the MDC1 C-terminal tandem BRCT domain and the phosphorylated H2AX C-terminus. Moreover, several domains and regions within the central and N-terminal sections of MDC1 feature repeated sequence motifs that are shaped by post-translational modifications, mostly phosphorylations. These regions are then recognized by proteins that contain domains capable of specifically binding to the modified amino acid stretches such as FHA and BRCT tandem domains. These factors subsequently accumulate at sites of DSBs and, thus, the γH2AX chromatin domain is efficiently established.

While the mechanism of accumulation of DDR factors in damaged chromatin and the role of MDC1 in this process is now relatively well understood, it is much more difficult to implicate these processes to the physiological roles of MDC1. While we do know that MDC1 is important for the activation of the intra-S phase and G2/M DNA damage checkpoint and for DSB repair, it is not clear yet how exactly these physiological roles are connected to MDC1's

major task to control the assembly of the γH2AX chromatin domain. This is especially true for checkpoint activation. To make this point clear, we touch on just one example: As outlined above, MDC1 is implicated in the G2/M DNA damage checkpoint. Theoretically, this function could be mediated by 53BP1 or BRCA1 accumulation because both 53BP1 and BRCA1 are implicated in the G2/M checkpoint response and mutation of the TQXF cluster of MDC1 that is essential for 53BP1 and BRCA1 accumulation triggers a G2/M checkpoint defect. However, deletion of the MDC1 FHA domain also triggers a G2/M checkpoint defect, which might be related to the ability of the FHA domain to interact with ATM and CHK2, factors that are also critical to induce a proper G2/M checkpoint response. To complicate matters further, MDC1 also mediates the accumulation of the MRN complex via direct interaction of its phosphorylated SDT repeats with the FHA/BRCT region of NBS1. Mutation in the FHA domain of NBS1 also results in a G2/M checkpoint defect, indicating that MDC1-mediated accumulation of NBS1 in damaged chromatin regions may be required for proper G2/M checkpoint activation. The relative contribution of these protein–protein interactions is not yet clear and no firm mechanistic explanation is yet available as to how MDC1-mediated accumulation of DDR factors at sites of DSBs brings about an efficient G2/M checkpoint response.

Thus, while MDC1 has clearly emerged as the major organizer of the assembly and maintenance of the γH2AX chromatin domain, we still need to learn a lot more about how these events translate into a timely and efficient DDR that protects cells from the deleterious and dangerous effects of DNA damage and chromosomal instability.

Acknowledgements We thank Flurina Hari for critical reading of the manuscript. Research in the Stucki laboratory is supported by the Swiss National Foundation and by the Kanton of Zürich.

Conflict of interest The authors declare that they have no conflicts of interest.

References

Ahn J, Prives C (2002) Checkpoint kinase 2 (Chk2) monomers or dimers phosphorylate Cdc25C after DNA damage regardless of threonine 68 phosphorylation. J Biol Chem 277(50):48418–48426

Bartkova J, Hořejsí Z, Sehested M, Nesland JM, Rajpert-De Meyts E, Skakkebæk NE, Stucki M, Jackson S, Lukas J, Bartek J (2007) DNA damage response mediators MDC1 and 53BP1: constitutive activation and aberrant loss in breast and lung cancer, but not in testicular germ cell tumours. Oncogene 26(53):7414–7422

Bekker-Jensen S, Lukas C, Kitagawa R, Melander F, Kastan MB, Bartek J, Lukas J (2006) Spatial organization of the mammalian genome surveillance machinery in response to DNA strand breaks. J Cell Biol 173(2):195–206

Botuyan MV, Lee J, Ward IM, Kim JE, Thompson JR, Chen J, Mer G (2006) Structural basis for the methylation state-specific recognition of histone H4-K20 by 53BP1 and Crb2 in DNA repair. Cell 127(7):1361–1373

Cerosaletti KM, Concannon P (2003) Nibrin forkhead-associated domain and breast cancer C-terminal domain are both required for nuclear focus formation and phosphorylation. J Biol Chem 278(24):21944–21951

Chapman J, Jackson S (2008) Phospho-dependent interactions between NBS1 and MDC1 mediate chromatin retention of the MRN complex at sites of DNA damage. EMBO Rep 9(8):795–801

Cook P, Ju B, Telese F, Wang X, Glass C, Rosenfeld M (2009) Tyrosine dephosphorylation of H2AX modulates apoptosis and survival decisions. Nature 458(7238):591–596

Coster G, Hayouka Z, Argaman L, Strauss C, Friedler A, Brandeis M, Goldberg M (2007) The DNA damage response mediator MDC1 directly interacts with the anaphase-promoting complex/cyclosome. J Biol Chem 282(44):32053–32064

de Jager M, van Noort J, van Gent DC, Dekker C, Kanaar R, Wyman C (2001) Human Rad50/Mre11 is a flexible complex that can tether DNA ends. Mol Cell 8(5):1129–1135

Difilippantonio S, Celeste A, Kruhlak M, Lee Y, Difilippantonio MJ, Feigenbaum L, Jackson SP, McKinnon PJ, Nussenzweig A (2007) Distinct domains in Nbs1 regulate irradiation-induced checkpoints and apoptosis. J Exp Med 204(5):1003–1011

Dimitrova N, de Lange T (2006) MDC1 accelerates nonhomologous end-joining of dysfunctional telomeres. Genes & Development 20(23):3238–3243

Dimitrova N, de Lange T (2008) 53BP1 promotes non-homologous end joining of telomeres by increasing chromatin mobility. Nature 456(7221):524–528

Doil C, Mailand N, Bekker-Jensen S, Menard P, Larsen D, Pepperkok R, Ellenberg J, Panier S, Durocher D, Bartek J (2009) RNF168 binds and amplifies ubiquitin conjugates on damaged chromosomes to allow accumulation of repair proteins. Cell 136(3):435–446

Dronamraju R, Mason JM (2009) Recognition of double strand breaks by a mutator protein (MU2) in Drosophila melanogaster. PLoS Genet 5(5):e1000473

Durocher D, Jackson S (2002) The FHA domain. FEBS Lett 513 (1):58–66

Durocher D, Taylor IA, Sarbassova D, Haire LF, Westcott SL, Jackson SP, Smerdon SJ, Yaffe MB (2000) The molecular basis of FHA domain: phosphopeptide binding specificity and implications for phospho-dependent signaling mechanisms. Mol Cell 6(5):1169–1182

Falck J, Coates J, Jackson S (2005) Conserved modes of recruitment of ATM, ATR and DNA-PKcs to sites of DNA damage. Nature 434(7033):605–611

Goldberg M, Stucki M, Falck J, D'amours D, Rahman D, Pappin D, Bartek J, Jackson S (2003) MDC1 is required for the intra-S-phase DNA damage checkpoint. Nature 421(6926):952–956

Gottlieb TM, Jackson SP (1993) The DNA-dependent protein kinase: requirement for DNA ends and association with Ku antigen. Cell 72(1):131–142

Huen M, Grant R, Manke I, Minn K, Yu X, Yaffe M, Chen J (2007) RNF8 transduces the DNA-damage signal via histone ubiquitylation and checkpoint protein assembly. Cell 131(5):901–914

Huyen Y, Zgheib O, Ditullio RA, Gorgoulis VG, Zacharatos P, Petty TJ, Sheston EA, Mellert HS, Stavridi ES, Halazonetis TD (2004) Methylated lysine 79 of histone H3 targets 53BP1 to DNA double-strand breaks. Nature 432(7015):406–411

Kim H, Chen J, Yu X (2007) Ubiquitin-binding protein RAP80 mediates BRCA1-dependent DNA damage response. Science 316(5828):1202–1205

Kolas N, Chapman J, Nakada S, Ylanko J, Chahwan R, Sweeney F, Panier S, Mendez M, Wildenhain J, Thomson T, Pelletier L, Jackson S, Durocher D (2007) Orchestration of the DNA-damage response by the RNF8 ubiquitin ligase. Science 318(5856):1637–1640

Lee MS, Edwards RA, Thede GL, Glover J (2005) Structure of the BRCT repeat domain of MDC1 and its specificity for the free COOH-terminal end of the gamma-H2AX histone tail. J Biol Chem 280(37):32053–32056

Li J, Taylor IA, Lloyd J, Clapperton JA, Howell S, MacMillan D, Smerdon SJ (2008) Chk2 oligomerization studied by phosphopeptide ligation: implications for regulation and phosphodependent interactions. J Biol Chem 283(51):36019–36030

Lloyd J, Chapman J, Clapperton JA, Haire LF, Hartsuiker E, Li J, Carr AM, Jackson S, Smerdon SJ (2009) A supramodular FHA/BRCT-repeat architecture mediates Nbs1 adaptor function in response to DNA damage. Cell 139(1):100–111

Lou Z, Minter-Dykhouse K, Wu X, Chen J (2003) MDC1 is coupled to activated CHK2 in mammalian DNA damage response pathways. Nature 421(6926):957–961

Lou Z, Chen BP, Asaithamby A, Minter-Dykhouse K, Chen DJ, Chen J (2004) MDC1 regulates DNA-PK autophosphorylation in response to DNA damage. J Biol Chem 279(45):46359–46362

Lou Z, Minter-Dykhouse K, Franco S, Gostissa M, Rivera MA, Celeste A, Manis JP, van Deursen J, Nussenzweig A, Paull TT, Alt FW, Chen J (2006) MDC1 maintains genomic stability by participating in the amplification of ATM-dependent DNA damage signals. Mol Cell 21(2):187–200

Lukas C, Falck J, Bartkova J, Bartek J, Lukas J (2003) Distinct spatiotemporal dynamics of mammalian checkpoint regulators induced by DNA damage. Nat Cell Biol 5(3):255–260

Lukas C, Melander F, Stucki M, Falck J, Bekker-Jensen S, Goldberg M, Lerenthal Y, Jackson S, Bartek J, Lukas J (2004) Mdc1 couples DNA double-strand break recognition by Nbs1 with its H2AX-dependent chromatin retention. EMBO J 23(13):2674–2683

Luo K, Yuan J, Chen J, Lou Z (2009) Topoisomerase IIalpha controls the decatenation checkpoint. Nat Cell Biol 11(2):204–210

Mailand N, Bekkerjensen S, Faustrup H, Melander F, Bartek J, Lukas C, Lukas J (2007) RNF8 ubiquitylates histones at DNA double-strand breaks and promotes assembly of repair proteins. Cell 131(5):887–900

Matsuoka S, Ballif BA, Smogorzewska A, McDonald ER, Hurov KE, Luo J, Bakalarski CE, Zhao Z, Solimini N, Lerenthal Y, Shiloh Y, Gygi SP, Elledge SJ (2007) ATM and ATR substrate analysis reveals extensive protein networks responsive to DNA damage. Science 316(5828):1160–1166

Matsuzaki K, Shinohara A, Shinohara M (2008) Forkhead-associated domain of yeast Xrs2, a homolog of human Nbs1, promotes nonhomologous end joining through interaction with a ligase IV partner protein, Lif1. Genetics 179(1):213–225

Meier A, Fiegler H, Muñoz P, Ellis P, Rigler D, Langford C, Blasco M, Carter N, Jackson S (2007) Spreading of mammalian DNA-damage response factors studied by ChIP-chip at damaged telomeres. EMBO J 26(11):2707–2718

Melander F, Bekker-Jensen S, Falck J, Bartek J, Mailand N, Lukas J (2008) Phosphorylation of SDT repeats in the MDC1 N terminus triggers retention of NBS1 at the DNA damage-modified chromatin. J Cell Biol 181(2):213–226

Minter-Dykhouse K, Ward I, Huen SY, Chen J, Lou Z (2008) Distinct versus overlapping functions of MDC1 and 53BP1 in DNA damage response and tumorigenesis. J Cell Biol 181(5):727–735

Mohammad D, Yaffe MB (2009) 14-3-3 proteins, FHA domains and BRCT domains in the DNA damage response. DNA Repair 8(9):1009–1017

Nakada S, Chen GI, Gingras AC, Durocher D (2008) PP4 is a gamma H2AX phosphatase required for recovery from the DNA damage checkpoint. EMBO Rep 9(10):1019–1026

Panier S, Durocher D (2009) Regulatory ubiquitylation in response to DNA double-strand breaks. DNA Repair 8(4):436–443

Rodriguez M, Yu X, Chen J, Songyang Z (2003) Phosphopeptide binding specificities of BRCA1 COOH-terminal (BRCT) domains. J Biol Chem 278(52):52914–52918

Rogakou EP, Boon C, Redon C, Bonner WM (1999) Megabase chromatin domains involved in DNA double-strand breaks in vivo. J Cell Biol 146(5):905–916

Savic V, Yin B, Maas N, Bredemeyer A, Carpenter A, Helmink B, Yang-Iott K, Sleckman B, Bassing C (2009) Formation of dynamic γ-H2AX domains along broken DNA strands is distinctly regulated by ATM and MDC1 and dependent upon H2AX densities in chromatin. Mol Cell 34(3):298–310

Shang YL, Bodero AJ, Chen PL (2003) NFBD1, a novel nuclear protein with signature motifs of FHA and BRCT, and an internal 41-amino acid repeat sequence, is an early participant in DNA damage response. J Biol Chem 278(8):6323–6329

Sobhian B, Shao G, Lilli DR, Culhane AC, Moreau LA, Xia B, Livingston DM, Greenberg RA (2007) RAP80 targets BRCA1 to specific ubiquitin structures at DNA damage sites. Science 316(5828):1198–1202

Spycher C, Miller ES, Townsend K, Pavic L, Morrice NA, Janscak P, Stewart GS, Stucki M (2008) Constitutive phosphorylation of MDC1 physically links the MRE11-RAD50-NBS1 complex to damaged chromatin. J Cell Biol 181(2):227–240

Stewart GS (2009) Solving the RIDDLE of 53BP1 recruitment to sites of damage. Cell Cycle 8(10):1532–1538

Stewart GS, Wang B, Bignell CR, Taylor AM, Elledge SJ (2003) MDC1 is a mediator of the mammalian DNA damage checkpoint. Nature 421(6926):961–966

Stewart GS, Stankovic T, Byrd PJ, Wechsler T, Miller ES, Huissoon A, Drayson MT, West S, Elledge SJ, Taylor AM (2007) RIDDLE immunodeficiency syndrome is linked to defects in 53BP1-mediated DNA damage signaling. Proc Natl Acad Sci USA 104(43):16910–16915

Stewart G, Panier S, Townsend K, Al-Hakim A, Kolas N, Miller E, Nakada S, Ylanko J, Olivarius S, Mendez M (2009) The RIDDLE syndrome protein mediates a ubiquitin-dependent signaling cascade at sites of DNA damage. Cell 136(3):420–434

Stucki M (2009) Histone H2A.X Tyr142 phosphorylation: a novel sWItCH for apoptosis? DNA Repair 8(7):873–876

Stucki M, Jackson S (2004) MDC1/NFBD1: a key regulator of the DNA damage response in higher eukaryotes. DNA Repair 3(8–9):953–957

Stucki M, Jackson S (2006) γH2AX and MDC1: anchoring the DNA-damage-response machinery to broken chromosomes. DNA Repair 5(5):534–543

Stucki M, Clapperton J, Mohammad D, Yaffe M, Smerdon S, Jackson S (2005) MDC1 directly binds phosphorylated histone H2AX to regulate cellular responses to DNA double-strand breaks. Cell 123(7):1213–1226

Townsend K, Dyson H, Blackford AN, Miller ES, Chapman JR, Sedgwick GG, Barone G, Turnell AS, Stewart GS (2009) Mediator of DNA damage checkpoint 1 (MDC1) regulates mitotic progression. J Biol Chem 284(49):33939–33948

Van Attikum H, Gasser S (2009) Crosstalk between histone modifications during the DNA damage response. Trends Cell Biol 19(5):207–217

Wang B, Matsuoka S, Ballif BA, Zhang D, Smogorzewska A, Gygi SP, Elledge SJ (2007) Abraxas and RAP80 form a BRCA1 protein complex required for the DNA damage response. Science 316(5828):1194–1198

Williams RS, Williams JS, Tainer JA (2007) Mre11-Rad50-Nbs1 is a keystone complex connecting DNA repair machinery, double-strand break signaling, and the chromatin template. Biochem Cell Biol 85(4):509–520

Williams RS, Dodson GE, Limbo O, Yamada Y, Williams JS, Guenther G, Classen S, Glover J, Iwasaki H, Russell P, Tainer JA (2009) Nbs1 flexibly tethers Ctp1 and Mre11-Rad50 to coordinate DNA double-strand break processing and repair. Cell 139(1):87–99

Wu L, Luo K, Lou Z, Chen J (2008) MDC1 regulates intra-S-phase checkpoint by targeting NBS1 to DNA double-strand breaks. Proc Natl Acad Sci USA 105(32):11200–11205

Xiao A, Li H, Shechter D, Ahn S, Fabrizio L, Erdjument-Bromage H, Ishibe-Murakami S, Wang B, Tempst P, Hofmann K, Patel D, Elledge SJ, Allis C (2009) WSTF regulates the H2A.X DNA damage response via a novel tyrosine kinase activity. Nature 457 (7225):57–62

Xie A, Hartlerode A, Stucki M, Odate S, Puget N, Kwok A, Nagaraju G, Yan C, Alt FW, Chen J, Jackson S, Scully R (2007) Distinct roles of chromatin-associated proteins MDC1 and 53BP1 in mammalian double-strand break repair. Mol Cell 28(6):1045–1057

Xu C, Wu L, Cui G, Botuyan M, Chen J, Mer G (2008) Structure of a second BRCT domain identified in the nijmegen breakage syndrome protein Nbs1 and its function in an MDC1-dependent localization of Nbs1 to DNA damage sites. J Mol Biol 381 (2):361–372

Zhang J, Ma Z, Treszezamsky A, Powell SN (2005) MDC1 interacts with Rad51 and facilitates homologous recombination. Nat Struct Mol Biol 12(10):902–909

Zhao S, Renthal W, Lee EY (2002) Functional analysis of FHA and BRCT domains of NBS1 in chromatin association and DNA damage responses. Nucleic Acids Res 30(22):4815–4822

Zhou BB, Elledge SJ (2000) The DNA damage response: putting checkpoints in perspective. Nature 408(6811):433–439

5 RESULTS

5.1 The molecular basis of ATM-dependent dimerization of the MDC1 DNA-damage checkpoint mediator

Authors: Stephanie Jungmichel*, Julie A. Clapperton*, Janette Lloyd, Christoph Spycher, Lucijana Pavic, Jiejin Li, Lesley F. Haire, Mario Bonalli, Claudia Lukas, Jiri Lukas, Manuel Stucki & Stephen J. Smerdon

*equal contribution

Journal: Under revision for Nat Struct Mol Biol

Contribution: Design of experiments (together with M. Stucki);

Generation of reagents and data for Figures 1b-e and Supplementary Figure 2 (*in vitro* ATM kinase assays, evaluation of phospho-specific MDC1 pT4 antibody by Western Blots, inhibitor studies), and Figures 5a-e (cloning of all constructs, co-immunoprecipitation, generation and analysis of stable lines after microirradiation by life cell imaging and immunofluorescence); preparation of figures; proofreading of the manuscript

The molecular basis of ATM-dependent dimerization of the Mdc1 DNA-damage checkpoint mediator

Stephanie Jungmichel[2,*], Julie A. Clapperton[1,*], Janette Lloyd[1], Christoph Spycher[2], Lucijana Pavic[2], Jiejin Li[1], Lesley F. Haire[1], Mario Bonalli[2], Claudia Lukas[4], Jiri Lukas[4], Derek MacMillan[3], Manuel Stucki[2] & Stephen J. Smerdon[1].

[1] *MRC National Institute for Medical Research, Division of Molecular Structure, The Ridgeway, Mill Hill, London NW7 1AA, UK.*

[2] *Institute of Veterinary Biochemistry and Molecular Biology, University of Zürich - Irchel, Winterthurerstrasse 190, CH-8057 Zürich, Switzerland*

[3] *Department of Chemistry, University College, London WC1H 0AJ, UK.*

[4]*Institute of Cancer Biology and Centre for Genotoxic Stress Research, Danish Cancer Society, Strandboulevarden 49, DK-2100, Copenhagen, Denmark*

Correspondence: m.stucki@vetbio.uzh.ch or stephen.smerdon@nimr.mrc.ac.uk (Tel: +44 208 816 2533, FAX: +44 208 816 2580)

[*] These authors contributed equally to this work

Key words: DNA damage / ATM / chromatin / FHA domain / dimerization / mediator / Mdc1 /

Subject Category: DNA replication, repair and recombination

Running title: ATM-dependent Mdc1 dimerization

Main text 3820 words

Abstract

Mdc1 is a large modular phosphoprotein scaffold that maintains signaling and repair complexes at double-stranded DNA break sites. Mdc1 is anchored to damaged chromatin through interaction of its C-terminal BRCT-repeat domain with the tail of γH2AX following DNA damage, but the role of the N-terminal forkhead-associated (FHA) domain remains unclear. We show that a major binding target of the Mdc1 FHA domain is a previously unidentified DNA-damage and ATM–dependent phosphorylation site near the N-terminus of Mdc1 itself. Binding to this motif *in vitro* and in human cells stabilizes a weak self-association of the FHA domain to form a tight dimer. X-ray structures of free and complexed Mdc1 FHA domain reveal a 'head-to-tail' dimerization related to that seen in dimeric forms of the Chk2 DNA-damage kinase. Together, our data highlight dimerization as an unsuspected regulator of Mdc1 activity and show how this may further modulate interactions with other DNA-damage response components.

Introduction

Genomic integrity is constantly challenged by the effects of DNA-damaging agents. Double-stranded DNA breaks (DSBs) are considered to be the most genotoxic lesions since incorrect repair can lead to chromosome breaks and other aberrations that are characteristic of and which may lead to cancer. DSBs initiate a program of cellular responses involving activation of cell-cycle checkpoints and deployment of the repair machinery. Central to DNA-damage response (DDR) regulation is a protein kinase cascade involving ataxia telangiectasia-mutated kinase (ATM) which acts as sensor of DSBs, initiating damage signals that are propogated through phosphorylation of checkpoint kinases and other diverse downstream targets [1]. Many of these phosphorylation events are now known to initiate protein-protein interactions mediated by phosphoserine/threonine-specific binding domains, most commonly forkhead-associated (FHA) and Brca1 C-terminal (BRCT) modules [2], providing for highly regulated, physical links between DDR components.

Mediator of the DNA-damage Checkpoint-1 (Mdc1) is a modular, 2089 amino-acid protein originally identified as an essential factor for establishment of the S-phase checkpoint [3-6]. It functions as an assembly platform for the localization and maintenance of signaling and repair factors at and around DSB sites [7]. As such, Mdc1 is a founding member of a class of large scaffolding/adaptor proteins known as 'mediators' that includes proteins such as human Brca1, 53BP1 and yeast Rad9 and Crb2. While all of these molecules contain two or more copies of BRCT-repeat motifs, Mdc1 also contains an additional FHA domain at its N-terminus.

Functionally, the C-terminal BRCT-repeats tether Mdc1 to regions of DNA-damage by virtue of their specific binding to ATM-phosphorylated H2AX (known as γH2AX), a variant histone H2A which acts as the primary marker of damaged chromatin in all eukaryotic cells [8]. In contrast, the function of the FHA domain is less clear but has been suggested to include interaction with ATM itself [9], Chk2 [3], components of the Mre11/Rad50/Nbs1 (MRN) complex [5,10] and other repair proteins such as Rad51 [11]. In addition, although self-association has been shown to be a functional feature of 53BP1[12], Rad9 [13] and Crb2 [14], the oligomeric status of Mdc1 in DNA-damaged cells has not, to our knowledge, been investigated. We now show that the Mdc1 FHA domain mediates an inter-molecular interaction with a previously uncharacterized,

ATM phosphorylation site located within its own N-terminal region, revealing a role for DNA-damage inducible Mdc1 dimerization in the cellular response to double-stranded DNA breaks.

Results

Mdc1 Thr-4 is a novel site of ATM phosphorylation *in vitro* and *in vivo*.

Mdc1 contains many potential PI3 kinase-like protein kinase (PIKK) target sites (S/TQ-motives) throughout its open reading frame and early studies have shown that upon genotoxic stress, Mdc1 is rapidly phosphorylated in a PIKK-dependent manner [3-5]. However, only few of these potential PIKK target sites are conserved and the extent and physiological relevance of PIKK-dependent Mdc1 phosphorylation are largely unknown. In order to identify *bona fide* PIKK target sites in Mdc1, we generated eight overlapping fragments of the human Mdc1 cDNA and expressed them in *E. coli* as GST-fusion proteins as described previously (**Fig. 1a**; [15]). All but one fragment, M-6 comprising the Mdc1 PST repeat region, expressed well and could be purified (**Fig. 1a**, upper panel). These fragments were then subjected to an *in vitro* kinase assay using immunoprecipitated human ATM [16]. Surprisingly, ATM only phosphorylated fragment M-1 (amino acids 1-124) and fragment M-4 (amino acids 531-770), (**Fig. 1a**, lower panel). Fragment M-4 features a cluster of four conserved 'T-Q-X-F' motifs that constitute binding sites for the FHA domain of the ubiquitin ligase RNF8 following phosphorylation by ATM [17-19]. Fragment M-1 contains two conserved TQ motifs: one at the very N-terminus of Mdc1 (Thr-4/Gln-5) and one within the FHA domain (Thr-98/Gln-99). Thr-4 appears to be the major site of ATM phosphorylation since a deletion mutant of M-1 lacking the first 18 amino acids was not phosphorylated by ATM *in vitro* (**Supplementary Fig. 1**) while a point mutation altering Thr-4 to Ala (T4A) resulted in a protein that could no longer be phosphorylated by ATM *in vitro* (**Fig. 1b**).

In order to investigate Thr-4 phosphorylation *in vivo*, we raised a phosphospecific antibody (pT4) directed against a pThr-4 peptide derived from the Mdc1 N-terminus. The antibody recognized the *in vitro* phosphorylated M-1 fragment and cross-reacted only minimally with the unphosphorylated form of M-1 (**Fig. 1b**, third panel). Moreover, the antibody did not recognize the T4A mutant M-1 fragment, nor did it recognize the repeating TQxF motifs within fragment M-4 (**Supplementary Fig. 2**) either before or after ATM phosphorylation, indicating

clear specificity for the pThr-4 site. We then exposed U2OS cells to various doses of IR and analyzed total cell extracts by immunoblotting with the pT4 antibody. The antibody cross-reacted with several proteins in total cell extracts, but one band (migrating at approximately 250 kDa) only emerged in extracts derived from cells that had been treated with IR. The intensity of this band increased with increasing dose of IR (**Fig. 1c** - left). Stripping and re-probing the blot with an antibody against human Mdc1 revealed that the protein recognized by the pT4 antisera overlapped with at least one of the Mdc1 size variants. Time course analysis showed that 1 h post irradiation, phosphorylation levels were maximal and then slowly decreased to background levels after 21 hours (**Fig. 1c** - right panels).

To exclude the possibility that the pT4 antibody cross-reacted with another protein phosphorylated in response to IR, we subjected $Mdc1^{-/-}$ mouse embryonic fibroblasts and control ($Mdc1^{+/+}$) cells to various doses of IR and analyzed total cell extracts by immunoblotting using the pT4 antibody. In extracts prepared from irradiated $Mdc1^{+/+}$ MEFs, a clear signal appeared on polyacrylamide gels at the position where mouse Mdc1 would be expected. No such signal was detected in extracts derived from irradiated $Mdc1^{-/-}$ cells, indicating that the protein recognized by the pT4 antibody indeed corresponds to Mdc1 (**Fig. 1d**).

Mdc1 phosphorylation in response to IR is ATM-dependent [3-5]. Consistent with this, no Mdc1 signal was detected by the pT4 antibody in extracts from irradiated cells that had been pre-treated with a specific ATM inhibitor or with a combination of ATM and DNA-PKcs inhibitors, while the signal was still present, albeit weaker, when the cells had been pre-treated with the DNA-PKcs inhibitor alone (**Fig. 1e**). Together, these data suggest that Mdc1 contains a conserved PIKK target site at its very N-terminus and that, in response to IR, this is mainly targeted by ATM *in vivo*.

The phosphorylated N-terminus of Mdc1 binds to its own FHA domain.

To understand the functional implication of Mdc1 Thr-4 phosphorylation, we carefully analyzed the amino acid sequence surrounding the PIKK target site. Besides the TQ motif, several additional amino acids are conserved, most notably an isoleucine three residues C-terminal to the phosphoacceptor threonine (**Fig. 1b**). This is intriguing since pT-X-X-I was previously shown to constitute a favoured motif for certain classes of FHA domains [20]. Indeed the

entire N-terminal motif (M-E-D-pT-Q-A-I) resembles that derived for the Mdc1 FHA domain by oriented library screening in these earlier studies (**Fig. 2a**). In order to test whether the phosphorylated N-terminus of Mdc1 could serve as a binding site for an FHA domain-containing protein, we designed a phosphopeptide comprising the first 12 N-terminal residues of human Mdc1 phosphorylated on Thr-4. The phosphopeptide and its unphosphorylated derivative were coupled to magnetic beads and used to pull down proteins from Hela nuclear extracts. Both peptides retrieved several proteins that appeared as clear bands on a SDS polyacrylamide gel (**Supplementary Fig. 3**). At least three proteins were pulled down by the phosphopeptide only, but not by its unphosphorylated counterpart (**Supplementary Fig. 3**). Most prominent were two bands of ~250kDa identified as Mdc1 itself by Western blot analysis with an antibody against human Mdc1 (**Fig. 2b**). The other two bands at ~150 kDa and ~80 kDa were RAD50 and MRE11, respectively. Together with our previous finding that Mdc1 exists in a complex with MRN in Hela nuclear extracts [8,15], these results indicate that Mdc1 may be the predominant interaction partner of its own phosphorylated N-terminus.

Of the two phosphospecific protein binding domains within Mdc1 (**Fig. 1a**), phosphopeptide pull-down experiments with bacterially expressed GST fusion proteins of these regions showed that only the FHA domain bound tightly and specifically to the Mdc1 N-terminal phosphopeptide, with no significant interaction detectable for the C-terminal BRCT-repeat region (**Fig. 2c**). Furthermore, we were able to demonstrate high affinity binding of purified Mdc1 FHA to a synthetic phosphopeptide encompassing the Thr-4 motif by isothermal titration calorimetry (ITC). Interestingly, these data could only be satisfactorily fit using a model incorporating two independent phosphopeptide binding sites (**Fig. 2d**; see below). Thus, these results establish that Mdc1 interacts directly with its own phosphorylated N-terminus via the N-terminal FHA domain and, additionally suggest that it does so in a manner that differs somewhat from pThr-dependent FHA interactions described previously.

The Mdc1 FHA domain forms a dimer

In order to characterize the Mdc1 FHA-pThr 4 interactions further, we determined the structures of both free and phosphopeptide-bound forms at high resolution by X-ray crystallography. The pThr-4 phosphopeptide complex was solved using the single wavelength

anomalous diffraction method with crystals grown from selenomethionine-substituted Mdc1 FHA domain, and a synthetic peptide in which Ala-6 was also replaced by selenomethionine, an approach we have described previously [21]. The refined coordinates of the complex were then used to solve the structure of the peptide-free form by molecular replacement. Data collection and refinement statistics are shown in **Table 1** along with representative electron density for residues at the edge of the FHA dimer interface **(Fig. 3a)**.

As expected, the Mdc1 FHA domain adopts an 11-stranded β-sandwich fold that is characteristic of these signaling modules (**Supplementary Fig. 4**). Strikingly, we observed two FHA domains in the crystallographic asymmetric unit in both peptide-free and bound forms, each similarly arranged around a pseudo 2-fold non-crystallographic symmetry axis (**Fig. 3b**; **Supplementary Fig. 5**). Although other FHA-FHA lattice interactions are observed in the two crystal forms, the non-crystallographic interaction surface is the most extensive burying a total of ~900Å^2/dimer in each case. Of these, ~600Å^2 are contributed by non-polar atoms from the side-chains of Phe 37, Leu 101, Leu 120, Leu 122 and Leu 127 (**Fig 3c**), all highly conserved in available sequences of Mdc1 orthologues (**Fig. 3d**). Together these residues form a hydrophobic cluster on one face of each FHA β-sandwich that is tightly packed with high surface complementarity at the FHA-FHA interface.

In the light of these observations, we examined the solution behaviour of the isolated FHA by size-exclusion chromatography and multi-angle laser light scattering (SEC-MALLS) that is able to conveniently measure shape-independent and accurate molecular weights. This showed significant self-association of the Mdc1 FHA domain with an apparent molecular weight of 18.3 +/- 0.06 kDa, some 40% greater than the calculated monomer mass of 12.8 kDa (**Fig. 3e**). Moreover, a double mutation, L120E/L127E, resulted in a significant reduction in apparent molecular weight (14.3 kDa; **Fig. 3e**) presumably due to juxtaposition of repulsive charges at the interface. Thus, we conclude that the dimeric arrangement observed in the crystal structures is likely to be representative of the dimer we observe in solution.

Thr-4 phosphorylation stabilizes Mdc1 FHA domain dimerization

The structure of the Mdc1 FHA/phosphopeptide complex **(Fig. 4a)** shows a binding mode for the pThr-4 motif resembling that seen in several previously reported FHA domain complexes.

The phosphothreonine is held by a network of hydrogen-bonds with the highly conserved Arg-58 and Ser-72 side-chains along with accessory interactions with the less-well conserved Lys-73 (**Fig. 4b**). Ile-7 occupies the pThr +3 position that has been shown to represent a major determinant of FHA specificity [20] and interacts with the FHA domain through a shallow pocket formed by side-chains of residues 70, 96, 124 and 125. Most interestingly, Trp-9 that is present in all available sequences of Mdc1 orthologues, is the last peptide residue visible in electron density maps and packs into a cleft formed at the edge of the FHA-FHA interface. Here, the Trp-9 indole side-chain packs against Pro-103 and the aliphatic portion of Arg-102 from the second protomer**.** Due to the fact that the local 2-fold symmetry is imperfect, the FHA domain interactions of the Trp-9 side-chain from non-crystallographic symmetry-related peptide are still significant but less extensive, potentially explaining the two binding sites observed in ITC measurements. Regardless, the structural data strongly suggest that pThr motif binding might contribute to the overall stability of the dimeric complex and further SEC-MALLS analysis (**Fig. 4c**) clearly showed that addition of the pThr-4 peptide substantially increases the apparent weight-averaged molecular weight to within ~90% of that calculated for a fully dimeric, peptide-bound complex. Consistent with the structural location of Trp-9 at the FHA-FHA interface, a peptide variant containing a W9A substitution results in no significant dimer stabilization. Thus, accessory interactions mediated by Trp-9 of the bound phosphopeptide seem to directly contribute to Mdc1 FHA domain dimerization.

These structural and hydrodynamic data reveal an unusual dimeric FHA domain architecture that is stabilized through binding of each FHA domain *in trans* to a motif representing the ATM-phosphorylated Mdc1 N-terminal region. Such a head-to-tail model is attractive since we note that the conserved and highly acidic region (residues 10-18) C-terminal to Thr-4 could potentially interact with an equally conserved basic patch adjacent to the pThr-4 binding site but located on the adjacent protomer of the Mdc1 dimer (**Fig. 4d**). Nonetheless, we realized that other arrangements are possible in the normal context where the N-terminal motif is physically attached to the FHA through the intervening linker region (**Fig. 4e**). In particular the peptide-binding data did not eliminate the possibility of polymerization of the intact molecule, nor did they exclude intra-molecular binding of the pThr-4 motif to its own FHA domain, which could potentially disrupt the weakly associated un-phosphorylated dimer. This latter idea is particularly relevant since we have observed just such an intra-molecular regulatory association

in the Rv1827 FHA-domain protein from *M. tuberculosis* [22]. In order to distinguish between these possibilities, we used expressed protein ligation technology to generate a specifically and stoichiometrically Thr-4-phosphorylated sample (**Fig. 4f - left panel**). In doing so we noticed that Cys-26, which could potentially act as an N-terminal nucleophile, is located immediately C-terminal to Arg-25. Thus by limited tryptic cleavage of Mdc1 (residues 1-138), we were able generate a C-terminal FHA-containing fragment with an N-terminal Cys-26 which could be efficiently ligated to a pThr-4 phosphopeptide (residues 1-25) synthesized with a protected C-terminal thioester [23]. SEC-MALLS analysis of this material reported an apparent molecular weight of 31.2 kDa, essentially identical to the formula mass of the fully dimeric phosphorylated fragment (31,110 Da) (**Fig. 4f - right panel**). Thus, we conclude that pThr-4 phosphorylation results in tight Mdc1 dimerization through a head-to-tail mechanism.

Mdc1 self-association occurs in human cells and is pThr-4-dependent

We next asked whether the homodimeric, head-to-tail dimer also occurs in cells. First, we used differentially tagged Mdc1 fragments to detect homotypic interaction by co-immunoprecipitation. As shown in **Fig. 5a**, a Flag-tagged Mdc1 fragment (1-800) efficiently interacted with an identical Myc-tagged fragment. An N-terminal Mdc1 fragment lacking the BRCT domains was used to avoid avid association of Mdc1 with DNA damage-induced chromatin. Surprisingly, interaction between the two fragments was not completely dependent on IR treatment. However, when we probed the membranes with the pT4 antibody, we noticed that transiently expressed Mdc1 (1-800) fragment was constitutively phosphorylated on Thr-4 even without prior irradiation of the transfected cells (data not shown). Since Thr-4 phosphorylation of endogenous Mdc1 is clearly DNA-damage dependent (**Fig. 1**) we assume that this effect is a result of the transfection procedure [24]. Indeed, this effect may have been responsible for earlier observations of pThr-68-dependent oligomerisation of transiently transfected Chk2 in the absence of DNA-damage [25]. Nevertheless, mutation of either the FHA domain (R58A) or the phospho-epitope (T4A) led to a significant reduction of the interaction between Flag-tagged and Myc-tagged Mdc1 (1-800) and concomitant mutation of both the FHA domain and Thr-4 resulted in a complete loss of binding.

On the basis of the foregoing, we reasoned that if DNA damage-induced Mdc1 dimerization occurs via the FHA domain, we should detect partial recruitment of the FHA domain to sites of DSBs through association with endogenous Mdc1. Moreover, this recruitment should be diminished by mutations in either the FHA domain or at the pThr-4 site. To circumvent limitations of the static assessment of IRIF formation in fixed cells, we used an integrated imaging unit that combines microlaser-assisted generation of spatially defined DSB areas in mammalian cells with rapid, continuous and interactive image acquisition [26,27]. Since we and others have previously observed that overexpression of the Mdc1 FHA domain interferes with accumulation of DDR proteins (including Mdc1 and the Mre11/Rad50/Nbs1 complex) at sites of DSBs [5,10,28], we also generated a panel of cell lines derived from checkpoint-proficient U2OS cells carrying stably integrated, tetracycline-regulated expression cassettes directing the expression of the Mdc1 FHA domain fused to enhanced yellow fluorescent protein (EYFP). Significantly, when expressed at low levels, the Mdc1 FHA domain is recruited to microlaser-induced DNA damage (**Fig. 5b**). The real-time measurements revealed a rapid accumulation of the fusion protein around the laser-generated, DSB-containing, subnuclear tracts (**Fig. 5c**), with a detectable increase in fluorescence in the damaged nuclear compartments within 20-30 seconds (**Fig. 5c**, first panel). Subsequently, the fusion protein underwent a rapid accumulation in the DSB regions, and reached a steady-state by 8-10 minutes after laser exposure. Importantly, no increase in fluorescence was observed in DSB-containing laser tracks in Mdc1-depleted cells, indicating that EYFP-FHA domain accumulation is strictly Mdc1-dependent (**Fig. 5d**). Moreover, no accumulation was detectable in cells that express T4A or the R58A and L120/127E mutant derivatives of the FHA domain (**Fig. 5d**). Thus, these data reveal that FHA accumulation to microlaser-induced DNA damage in living human cells mirrors the *in vitro* requirements for Mdc1 dimerization. We therefore conclude that Mdc1 dimerization in response to DNA damage occurs *in vivo* in a manner that is consonant with our structural data.

Discussion

Mediator proteins perform a variety of crucial roles in many, if not all aspects of the response to DNA-damage. Although these molecules are essentially unrelated, oligomerisation now appears to be core feature of their activities and 53BP1, along with budding yeast Rad9 and

fission yeast Crb2 have all been shown to self-associate albeit through different mechanisms. Rad9 oligomerises via BRCT interactions with phosphosites generated by the ATR orthologue, Mec1, in a process that promotes activation of the Rad53 checkpoint kinase [13,29]. In contrast Crb2 and 53BP1 dimerization appear to be independent of any post-translational modification [12,14,30,31]. To date, the oligomeric status of Mdc1 has not been examined. Here, we have presented a molecular description of FHA-mediated Mdc1 dimerization in response to ATM phosphorylation following DNA damage.

Our observation of phospho-independent FHA dimerization is intriguing. Previous sequence comparisons have identified a patch of low-level conservation associated with β-strands 9 and 10 and the connecting loop of a subset of FHA domains, leading to the suggestion that this may act as a self-interaction surface [32]. Our structure now shows that this putative surface substantially overlaps with the Mdc1 dimer-forming region (**Supplementary Fig. 6**) and we also show that mutations within this region disrupt FHA-FHA interactions *in vitro* (**Fig. 3d**) and in living human cells (**Fig. 5e**). Similarly, weak self-association of the isolated FHA domain of the Chk2 kinase [23] has recently been shown to arise from a dimeric FHA domain architecture [33] that appears to be related to but distinct from that of Mdc1 consistent with substantial divergence at the sequence level. Although the structural basis for Chk2 dimer stabilization by ATM phosphorylation remains elusive, these data, together with our recent observation that a similar region of a mycobacterial FHA domain mediates phospho-independent intermolecular interactions with several physiological targets [22], support a more expansive role for the β-sandwich architecture in FHA-mediated interactions than has previously been assumed.

Functionally, our observation that a major binding partner for the Mdc1 FHA domain is Mdc1 itself is of major significance and suggests several ways in which FHA binding activity may be both positively and negatively regulated (**Fig. 6a-c**). Firstly, pThr-4 mediated dimerization would be expected to occlude the canonical FHA domain phospho-binding surface and restrict the availability of pThr-4 itself (**Fig. 6a**). Such a 'bind and release' mechanism could, in principle, operate for any Mdc1 binding partner containing a suitable pThr-containing motif. However, it does potentially resolve the paradoxical observations that Chk2 is highly mobile in DNA-damaged nuclei prior to and following its activation at dsDNA break sites [26] in spite of a direct interaction of Chk2 pThr-68 with the Mdc1 FHA domain [3] that would otherwise retain

monomeric, pThr-68 forms of Chk2 within regions of damage. Similarly, formation of the tight pThr-4 Mdc1 dimer would also occlude the FHA-FHA interfacial region that could function as a phospho-independent binding surface in the weakly self-interacting Mdc1 FHA prior to Thr-4 phosphorylation (**Fig. 6b**). Consistent with this idea, and as mentioned above, we have recently shown that part of this FHA domain surface can function in just such a fashion in other signaling contexts [22]. Finally, we surmise that Mdc1 dimerization might create new composite phospho-independent surfaces spanning both FHA domains (**Fig. 6c**) and note that such an extensive, negatively charged surface is evident in our crystal structures (**Supplementary Fig. 7**). Indeed a role for phospho-independent interactions implied by the latter two models likely may have significance for the previously described *in vitro* interaction of the Mdc1 FHA produced as a GST-fusion with bacterially expressed, and thus un-phosphorylated Rad51 [11].

Finally, from a more macroscopic viewpoint, a major effect of Mdc1 Thr-4 phosphorylation is to stabilize formation of a ~4000 residue dimeric super-scaffold. Although the major means by which broken DNA ends are maintained in proximity for efficient repair is through the bridging function of the MRN complex [34], it may be that Mdc1 dimers play a contributing role in stabilizing more global structure within chromatin loops containing damage sites [35-37]. Such a 'velcro' model may also contribute to an overall modulation of local chromatin compaction, thereby facilitating retention of downstream repair factors in this compartment. This model is particularly attractive since Mdc1 has long been known to occupy large areas of chromatin flanking double-stranded DNA break sites.

In conclusion, the last ten years or so have seen a considerable expansion in our appreciation of the fundamental importance of post-translational modifications, particularly serine/threonine phosphorylation, in pathways of DNA-damage dependent checkpoint establishment and assembly of repair and signaling complexes. Mdc1 has emerged as a focal point for many of these processes, functioning as a scaffold and adaptor in various contexts. We now reveal an additional and unsuspected level of Mdc1 regulation through DNA-damage and phosphorylation-dependent FHA domain dimerization, suggesting a number of ways in which this phenomenon might contribute to Mdc1 activities in these pathways. Thus, our observations not only emphasise and extend the significance of mediator self-association, but also provide the first insights into how this can occur at a structural level.

Methods

Plasmids

Human Mdc1-GST constructs were previously described [15] Human Mdc1 (aa 1-800) was generated by PCR and C-terminally tagged with HA/FLAG and Myc, respectively, and cloned into pcDNA3.1 (+) mammalian expression vector (Invitrogen). The Mdc1 FHA domain-containing fragment (aa 1-154) was amplified by PCR and cloned into a modified pEYFP-nuc vector (Clontech), in which two tetracycline-repressor binding elements were inserted between promotor and coding sequences to generate an inducible expression cassette [8]. Point mutations were introduced by PCR-based methods or using the QuikChange Site-Directed Mutagenesis kit (Stratagene).

Protein expression and purification

DNA fragments encoding human Mdc1 residues 1-138, 19-138 or 27-138 were amplified from a Mdc1 cDNA clone and ligated into BamH1/Xho1 digested pGEX-6P1. GST fusion proteins were affinity purified on glutathione-4B resin (Amersham) and cleaved from the affinity resin with rhinovirus 3C protease overnight at 4°C. Cleaved Mdc1 fragments were further purified by gel-filtration chromatography on Superdex 75.

Crystallisation and X-ray data collection

Crystals of peptide-free Mdc1 (27-138) were grown by microbatch methods under Al's oil at 18°C at a protein concentration of 10 mg/ml mixed with an equal volume of 1.32 M ammonium sulphate, 50 mM sodium acetate pH 4.6 and 5% v/v methyl-pentanediol. Complex crystals were grown from 1:1 complexes of selenomethionine substituted Mdc1 (19-138) with pThr-4 peptide containing a selenomethionine substituent at the pT+2 position, at a concentration of 15 mg/ml, mixed with an equal volume of 25% v/v ethanol, 0.1 M sodium acetate pH 5.5. Crystals were cryo-protected in mother liquor supplemented with 25 % v/v glycerol (peptide-free) or 17.5 % v/v ethylene glycol/10 % v/v ethanol prior to data collection.

Structure solution and refinement

The structure of the selenomethionine peptide complex was solved by the single-wavelength anomalous diffraction (SAD) method using data collected on beamline 10.1 at the SRS Daresbury, UK. Four selenium sites were located and phases refined by SOLVE/RESOLVE [38].

The resulting map was readily interpretable allowing an essentially complete model for the two complexes in the asymmetric unit. The resulting FHA domain structure was then used to solve the non-complexed crystal form by molecular replacement using PHASER [39]. Model-building was carried out with 'Coot' [40] and both structures were refined using REFMAC5 [41].

Cell culture and gene transfer

Mdc1$^{-/-}$ and Mdc1$^{+/+}$ MEFs were gifts from J. Chen (Yale University, New Haven, CT). U2OS, HEK 293T and MEFs were grown in D-MEM (Invitrogen) supplemented with 10% FCS (Gibco) and streptomycin/penicillin (100 U/ml, Gibco). Transfection of plasmids was done using either FuGene 6 (Roche) or calcium phosphate. U2OS-TetOn cells stably expressing the tetracycline repressor were generated by transfection of EYFP-tagged Mdc1-FHA domain following selection in G418-containing medium (Calbiochem). The siRNA oligonucleotides against endogenous human Mdc1 were purchased from Ambion (siRNA ID: 21738) containing the following sequence: sense 5'-GGAUCACACAAAGAUUAGAtt and antisense 5'-UCUAAUCUUUGUGUGAUCCtt. SiRNA transfections were performed using Lipofectamine RNAiMAX (Invitrogen) according the manufacturer's protocol. DNA damage was induced in a Faxitron X-ray cabinet at 5-10 Gy/min. or by means of single-cell laser microirradiation (see below).

Antibodies

The mouse monoclonal γH2AX antibody was obtained from Millipore and the rabbit polyclonal c-Myc antibody (sc-789) from Santa Cruz Biotechnology. The rabbit polyclonal FLAG antibody and the anti-FLAG M2 affinity gel, used for co-immunoprecipitation, were purchased from Sigma. Rabbit polyclonal Mdc1(889) and sheep polyclonal Mdc1(3835) antibodies were raised against Mdc1-FHA–GST as described previously [5]. The phosphospecific antibody Mdc1 'pT4' was raised in rabbit against the phosphopeptide MEDT(P)QAIDWDVC and affinity purified using the phosphorylated and non-phosphorylated peptide (Eurogentec). Rabbit polyclonal ATM antiserum for ATM immunoprecipitation was a kind gift from Graeme Smith (KuDOS Pharmaceuticals, Cambridge, UK).

Biochemical analysis

Hela nuclear extract was purchased from Cilbiotech (Mons, Belgium). Mdc1-GST fragments were affinity purified on glutathione-Sepharose (GE Healthcare Biosciences) as

described previously [15]. For peptide pull down analysis, the C-terminally biotinylated phosphopeptide MED[pT]QAIDWDAE[KBtn] (Sigma) was used. Where indicated, 25 nmol of the peptide were pre-incubated with 100 U λ phosphatase (New England BioLabs) at 30°C for 20 min. Peptide pull down analysis was done as described [8].

For *in vitro* ATM kinase assays, ATM was immunoprecipitated with a rabbit polyclonal ATM antiserum [16] from HeLa nuclear extract (Cilbiotech) in IP buffer (25 mM HEPES pH 7.4, 250 mM KCl, 2 mM $MgCl_2$, 10% glycerol, 0.1% NP-40, 0.5 mM EDTA, 1 mM NaF, 1 mM β-glycerophosphate). The immunocomplex was subsequently bound to Protein A-Sepharose beads (GE Healthcare). The kinase assay was performed by adding 1 μg GST-Mdc1 (aa 1-154) to the beads in ATM-kinase buffer (50 mM HEPES pH 7.4, 150 mM NaCl), 4 mM $MnCl_2$, 6 mM $MgCl_2$, 10% glycerol, 1 mM DTT, 1 mM NaF, 1 mM β-glycerophosphate, 0.5 mM ATP and 10 μCi γ-[^{32}P]ATP) and incubating for 30 min at 30°C. Gels were analyzed by autoradiography and GelCode (Pierce) or Coomassie blue staining. ATM inhibitor KPL0064 and DNA-PK inhibitor NU7026 were a kind gift from Graeme Smith (KuDOS Pharmaceuticals, Cambridge, UK) and were used at 10 μM and 20 μM, respectively.

Expressed protein ligation

Purified Mdc1 1-158 was digested with trypsin (Promega) at a ratio of 1:250 w/w enzyme:substrate to yield a 112 residue fragment (26-138) containing the FHA domain and part of the preceding linker with Cys-26 at its N-terminus. Synthesis of a C-terminally protected pThr-4 peptide (MEDpTQAIDWDVEEEEETEQSSESLR-SBn) and *in vitro* ligation to the Mdc1 26-138 fragment were carried in 200 mM phosphate buffer pH 8.0, 150 mM NaCl, 10mM TCEP, 2% w/v 2-mercaptoethanesulphonic acid overnight at room temperature.

SEC-MALLS

Samples were applied at a concentration of 80-100 M to a Superdex 75 10/300 GL column mounted on a Jasco HPLC and equilibrated in 20 mM Tris-HCl pH 8.3, 150 mM NaCl 3 mM DTT at a flow rate of 0.5 ml/min. Scattered light intensities of the column eluate were recorded at sixteen angles using a DAWN-HELEOS laser photometer (Wyatt Technology Corp., Santa Barbara, CA) and protein concentration of the eluted peak fractions were determined from the refractive index change (dn/dc = 0.186) using an OPTILAB-rEX differential refractometer equipped with a temperature-regulated flow cell at 25°C. The weight-averaged molecular weights

of proteins and complexes within the elution peaks were determined using the ASTRA software version 5.1 (Wyatt Technology Corp., Santa Barbara, CA).

Isothermal titration calorimetry

ITC was carried out using a VP-ITC calorimeter (MicroCal, USA). Protein and peptides were equilibrated with a buffer containing 20 mM Tris-HCl pH 8.3, 150 mM NaCl, 0.5 mM TCEP. Typically, 10 l aliquots of peptide at a syringe concentration of 0.5 mM were titrated over 30 injections into Mdc1 FHA domain samples at a concentration in the ITC cell of 50 M. Data were corrected for heats of dilution and analysed using the Origin 5.0 software. Phosphopeptides were synthesized by Dr. W. Mawby (University of Bristol, UK).

Co-immunoprecipitation

HEK 293T cells were transiently co-transfected with pcDNA3.1-Mdc1(800)-FLAG and pcDNA3.1-Mdc1(800)-Myc or the T4A, R58A, T4A/R58A mutants respectively using calcium phosphate. 48 h later, cells were mock- or IR-treated with 10 Gy. After 45 min, cells were lysed in NP-40 buffer (50 mM HEPES-KOH pH 7.9, 100 mM NaCl, 1mM EDTA, 1mM DTT, 0.5 % NP-40, 20% glycerol, PMSF, Leupeptin, Pepstatin A, Bestatin, 10 mM β-glycerophosphate and 1 mM NaF) for 15 min at 4°C and subsequently centrifuged at 14 000 rpm for 30 min at 4°C. Proteins in the supernatant were immunoprecipitated with anti-FLAG affinity gel (Sigma) in IP-buffer (see NP-40 buffer, but use of 40 mM HEPES-KOH pH 7.4, 0.05 % NP-40, no glycerol, no DTT) for 4h at 4°C. Immunocomplexes were washed three times in IP-buffer, boiled in SDS sample buffer and loaded on an SDS-polyacrylamide gel. Protein analysis was performed with standard immunoblot methods as described above.

Micro-irradiation and single-cell analysis

In order to generate DSBs in defined nuclear volumes laser microirradiation was performed with a MMI CELLCUT system containing a 355 nm UVA laser (55 Hz, Molecular Machines & Industries, Switzerland) coupled to an Olympus IX71 microscope station and focused through an LUCPLFLN 40X objective. The MMICELLTOOLS software with MMIUVCUT plug-in assisted the laser operation using an energy output of 55% (unless stated otherwise). Prior to laser irradiation, cells were grown on coverslips in cell culture dishes in the presence of 10 μM BrdU (Bromodeoxyuridine; Sigma) for 24 h. Expression of EYFP-MDC-FHA constructs in U2OS-TetOn cells was induced for 0.5 – 2 h with 1μg/ml Doxocycline. Coverslips were then transferred

into LabTek chamber slides (Nunc) and mounted on the microscope stage for irradiation. After irradiation, cells were placed back in the incubator for 30-60 min before fixation.

In case of live cell imaging, EYFP-Mdc1-expressing cells were directly grown on LabTek chamber slides in the presence of 10 μM BrdU for 24 h. Laser irradiation was performed with a 337 nm PALM microlaser workstation (30 Hz, Palm MicroBeam, Carl Zeiss Microimaging Inc.) mounted on an Axiovert 200 microscope (Zeiss) and focused through a LD 40x, NA 0.6 Zeiss Achroplan objective. The microlaser procedure was assisted by the PALMRobo-Software. Images were immediately recorded after laser treatment.

For immunofluorescence analysis, cells grown on coverslips were fixed in 4 % paraformaldehyde for 20 min and permeabilized in 0.25 Triton X-100 in PBS for 15 min. After blocking in 10% FCS/PBS, cells were incubated in 5% FCS/PBS with the indicated primary antibodies for 1 h and secondary antibodies Alexa Fluor 568 (Molecular Probes) or Texas Red (Jackson Immuno Research) for 30 min. Finally, the coverslips were mounted with DAPI-containing Vectashield (Vector Laboratories). Confocal image acquisition was performed on a Leica SP2 microscope with a 40 x (NA 1.25) oil immersion objective or on an LSM-510 (Carl Zeiss Imaging) microscope with a 40 x Plan-Apochromat (NA 1.3) oil immersion objective.

Acknowledgements

We thank Graeme Smith and Steve Jackson for providing valuable reagents, Ian Taylor for assistance with MALLS, Katrin Rittinger for advice and assistance with ITC measurements and Philip Walker for help with X-ray data collection. JL and CL were supported by the Danish Cancer Society, Danish National Research Foundation, and Danish Medical research Council. MS acknowledges grants from the Swiss National Foundation (Grant Nr. 3100A0-111818), the UBS AG (Im Auftrag eines Kunden) and the Kanton of Zürich. SJS would like to thank the Medical Research Council, UK for continuing support.

Conflict of interest

The authors state that they have no conflicts of interest

Accession numbers

Coordinates and structure factors for the free and complexed Mdc1 FHA domains structures have been deposited with the Protein Data Bank under accession codes 1XYZ and 2XYZ respectively.

References

1. Riches, L.C., Lynch, A.M. & Gooderham, N.J. Early Events in the Mammalian Response to DNA Double-Strand Breaks. *Mutagenesis* **23,** 331-9 (2008).
2. Mohammad, D.H. & Yaffe, M.B. 14-3-3 proteins, FHA domains and BRCT domains in the DNA damage response. *DNA Repair (Amst)* **8**, 1009-17 (2009).
3. Lou, Z., Minter-Dykhouse, K., Wu, X. & Chen, J. MDC1 is coupled to activated CHK2 in mammalian DNA damage response pathways. *Nature* **421**, 957-61 (2003).
4. Stewart, G.S., Wang, B., Bignell, C.R., Taylor, A.M. & Elledge, S.J. MDC1 is a mediator of the mammalian DNA damage checkpoint. *Nature* **421**, 961-6 (2003).
5. Goldberg, M. et al. MDC1 is required for the intra-S-phase DNA damage checkpoint. *Nature* **421**, 952-6 (2003).
6. Shang, Y.L., Bodero, A.J. & Chen, P.L. NFBD1, a novel nuclear protein with signature motifs of FHA and BRCT, and an internal 41-amino acid repeat sequence, is an early participant in DNA damage response. *J Biol Chem* **278**, 6323-9 (2003).
7. van Attikum, H. & Gasser, S.M. Crosstalk between histone modifications during the DNA damage response. *Trends Cell Biol* **19**, 207-17 (2009).
8. Stucki, M. et al. MDC1 directly binds phosphorylated histone H2AX to regulate cellular responses to DNA double-strand breaks. *Cell* **123**, 1213-26 (2005).
9. Lou, Z. et al. MDC1 maintains genomic stability by participating in the amplification of ATM-dependent DNA damage signals. *Mol Cell* **21**, 187-200 (2006).
10. Xu, X. & Stern, D.F. NFBD1/MDC1 regulates ionizing radiation-induced focus formation by DNA checkpoint signaling and repair factors. *FASEB J* **17**, 1842-8 (2003).
11. Zhang, J., Ma, Z., Treszezamsky, A. & Powell, S.N. MDC1 interacts with Rad51 and facilitates homologous recombination. *Nat Struct Mol Biol* **12**, 902-9 (2005).
12. Adams, M.M. et al. 53BP1 oligomerization is independent of its methylation by PRMT1. *Cell Cycle* **4**, 1854-61 (2005).
13. Soulier, J. & Lowndes, N.F. The BRCT domain of the S. cerevisiae checkpoint protein Rad9 mediates a Rad9-Rad9 interaction after DNA damage. *Curr Biol* **9**, 551-4 (1999).
14. Kilkenny, M.L. et al. Structural and functional analysis of the Crb2-BRCT2 domain reveals distinct roles in checkpoint signaling and DNA damage repair. *Genes Dev* **22**, 2034-47 (2008).
15. Spycher, C. et al. Constitutive phosphorylation of MDC1 physically links the MRE11-RAD50-NBS1 complex to damaged chromatin. *J Cell Biol* **181**, 227-40 (2008).
16. Hickson, I. et al. Identification and characterization of a novel and specific inhibitor of the ataxia-telangiectasia mutated kinase ATM. *Cancer Res* **64**, 9152-9 (2004).
17. Kolas, N.K. et al. Orchestration of the DNA-damage response by the RNF8 ubiquitin ligase. *Science* **318**, 1637-40 (2007).
18. Mailand, N. et al. RNF8 Ubiquitylates Histones at DNA Double-Strand Breaks and Promotes Assembly of Repair Proteins. *Cell* **131**, 887-900 (2007).
19. Huen, M.S. et al. RNF8 Transduces the DNA-Damage Signal via Histone Ubiquitylation and Checkpoint Protein Assembly. *Cell* **131**, 901-14 (2007).
20. Durocher, D. et al. The molecular basis of FHA domain:phosphopeptide binding specificity and implications for phospho-dependent signaling mechanisms. *Mol Cell* **6**, 1169-82 (2000).
21. Li, J. et al. Structural and functional versatility of the FHA domain in DNA-damage signaling by the tumor suppressor kinase Chk2. *Mol Cell* **9**, 1045-54 (2002).
22. Nott, T.J. et al. An intramolecular switch regulates phosphoindependent FHA domain interactions in Mycobacterium tuberculosis. *Science signaling* **2**, ra12 (2009).

23. Li, J. et al. Chk2 Oligomerization Studied by Phosphopeptide Ligation: IMPLICATIONS FOR REGULATION AND PHOSPHODEPENDENT INTERACTIONS. *J Biol Chem* **283**, 36019-30 (2008).
24. Rodriguez, A. & Flemington, E.K. Transfection-mediated cell-cycle signaling: considerations for transient transfection-based cell-cycle studies. *Anal Biochem* **272**, 171-81 (1999).
25. Xu, X., Tsvetkov, L.M. & Stern, D.F. Chk2 activation and phosphorylation-dependent oligomerization. *Mol Cell Biol* **22**, 4419-32 (2002).
26. Lukas, C., Falck, J., Bartkova, J., Bartek, J. & Lukas, J. Distinct spatiotemporal dynamics of mammalian checkpoint regulators induced by DNA damage. *Nat Cell Biol* **5**, 255-60 (2003).
27. Lukas, C. et al. Mdc1 couples DNA double-strand break recognition by Nbs1 with its H2AX-dependent chromatin retention. *EMBO J* **23**, 2674-83 (2004).
28. Dimitrova, N. & de Lange, T. MDC1 accelerates nonhomologous end-joining of dysfunctional telomeres. *Genes Dev* **20**, 3238-43 (2006).
29. Usui, T., Foster, S.S. & Petrini, J.H. Maintenance of the DNA-damage checkpoint requires DNA-damage-induced mediator protein oligomerization. *Mol Cell* **33**, 147-59 (2009).
30. Ward, I. et al. The tandem BRCT domain of 53BP1 is not required for its repair function. *J Biol Chem* **281**, 38472-7 (2006).
31. Zgheib, O., Pataky, K., Brugger, J. & Halazonetis, T.D. An oligomerized 53BP1 tudor domain suffices for recognition of DNA double-strand breaks. *Mol Cell Biol* **29**, 1050-8 (2009).
32. Lee, G.I., Ding, Z., Walker, J.C. & Van Doren, S.R. NMR structure of the forkhead-associated domain from the Arabidopsis receptor kinase-associated protein phosphatase. *Proc Natl Acad Sci USA* **100**, 11261-6 (2003).
33. Cai, Z., Chehab, N.H. & Pavletich, N.P. Structure and activation mechanism of the CHK2 DNA damage checkpoint kinase. *Mol Cell* **35**, 818-29 (2009).
34. Williams, R.S. et al. Mre11 dimers coordinate DNA end bridging and nuclease processing in double-strand-break repair. *Cell* **135**, 97-109 (2008).
35. Bassing, C.H. & Alt, F.W. H2AX may function as an anchor to hold broken chromosomal DNA ends in close proximity. *Cell Cycle* **3**, 149-53 (2004).
36. Franco, S. et al. H2AX prevents DNA breaks from progressing to chromosome breaks and translocations. *Mol Cell* **21**, 201-14 (2006).
37. van Gent, D.C. & van der Burg, M. Non-homologous end-joining, a sticky affair. *Oncogene* **26**, 7731-40 (2007).
38. Terwilliger, T. SOLVE and RESOLVE: automated structure solution, density modification and model building. *Journal of synchrotron radiation* **11**, 49-52 (2004).
39. McCoy, A.J. Solving structures of protein complexes by molecular replacement with Phaser. *Acta Crystallogr D Biol Crystallogr* **63**, 32-41 (2007).
40. Emsley, P. & Cowtan, K. Coot: model-building tools for molecular graphics. *Acta Crystallogr D Biol Crystallogr* **60**, 2126-32 (2004).
41. Murshudov, G.N., Vagin, A.A. & Dodson, E.J. Refinement of macromolecular structures by the maximum-likelihood method. *Acta Crystallogr D Biol Crystallogr* **53**, 240-55 (1997).

Figure Legends

Figure 1 – ATM targets Mdc1 on a conserved threonine residue at its N-terminus.

(a) *In vitro* ATM kinase assay of recombinant Mdc1 fragments. Top: Schematic representation of Mdc1's domain architecture and of the GST-fusion fragments derived from its cDNA. Bottom: Upper panel: Coomassie blue stained polyacrylamide gel of the purified GST-fusion fragments. Bottom panel: Autoradiography of *in vitro* phosphorylated Mdc1 fragments

(b) A conserved motif at the very N-terminus of Mdc1 is phosphorylated by ATM in vitro. Top: Sequence alignment of the Mdc1 N-terminus. The highly conserved Thr residue at position 4 (T4) is highlighted by an arrowhead. Bottom: ATM-phosphorylation of fragment M-1 and the mutant T4A. AR: Autoradiograph; CB: Coomassie blue; IB: immunoblot; PS: Ponceau red

(c) Left panel: Dose titration using the pThr-4 phosphospecific antibody (pT4). Right panel: Kinetics experiment using the pT4 antibody. The band corresponding to Mdc1 is highlighted by an arrowhead.

(d) $Mdc1^{+/+}$, $Mdc1^{-/-}$ MEFs were irradiated with various doses of IR. Extracts were probed with the pT4 antibody.

(e) Mdc1 Thr-4 phosphorylation in response to IR is ATM-dependent. U2OS cells were pre-treated with ATM inhibitor, DNA-PKcs inhibitor or a combination of both inhibitors. Cell extracts were probed with the phosphospecific pT4 antibody.

Figure 2 – The phosphorylated Mdc1 N-terminus constitutes a recognition motif for the Mdc1 FHA domain.

(a) The N-terminal Mdc1 pThr-4 sequence closely resembles the optimal binding motif derived previously [20] by oriented peptide library selection. Circled residues highlight exact matches.

(b) Immunoblot analysis indicates that endogenous Mdc1 is efficiently pulled down by the pThr-4 phosphopeptide.

(c) Coomassie blue-stained PAGE of a pThr-4 phosphopeptide pull-down experiment using purified M-1 GST-fragment (containing the FHA domain) and purified M-8 GST-fragment (containing the BRCT domains).

(d) ITC binding isotherm for interaction of a synthetic pThr-4 peptide with recombinant Mdc1 FHA domain. Data were analysed assuming one or two site binding which consistently favoured the latter model, showing tight, stoichiometric (1:1) binding to similar but non-identical sites.

Figure 3 - Mdc1 FHA domain dimerization

(a) Stereo view of a segment of omit electron density map (1.25σ) at the periphery of the FHA-FHA interface from the 1.8Å resolution peptide complex. Protein residues are shown as stick representation and water molecules are shown as red spheres.
(b) Ribbons representation of the dimeric arrangement observed in the peptide-free Mdc1 FHA crystal structure. The position of the local 2-fold symmetry axis is indicated. All structural representations were generated using PyMOL (http://pymol.sourceforge.net/).

(c) FHA-FHA interactions are predominantly mediated by a conserved cluster of five hydrophobic residues from each protomer.

(d) Interface residues are highly conserved in all available sequences of Mdc1 orthologues. The locations of β-strands observed in the structure are indicated in the lower panel, along with the positions of the four residues most highly conserved in the FHA domain family (circles).

(e) SEC-MALLS analysis of the wild-type Mdc1 FHA (27-138) and a mutant form in which two residues that form the core of the observed dimer interface have been substituted with glutamate. The observed weight-averaged molecular weight of the mutant is substantially less than the wild-type protein. The shorter retention time for the mutant may reflect a more extended shape for monomeric forms, or differential electrostatic effects on interaction with the column matrix.

Figure 4 - Head-to-tail dimerization is stabilised by pThr-4

(a) Structure of the Mdc1/pThr-4 peptide complex is shown as a Cα plot/surface representation with the peptide shown as sticks, viewed along the local 2-fold symmetry axis.

(b) The phosphopeptide interacts with conserved FHA domain residues mainly through pThr-4 and main-chain atoms from pT+1 and +3 residues. The Trp-9 indole nestles in a cleft formed at the interface between the two FHA domains in the dimer.

(c) SEC-MALLS analysis shows that a substantial stabilization of the Mdc1 FHA dimer by the pThr-4 peptide is greatly reduced by substitution of Trp-9 with alanine (W9A).

(d) The sequence C-terminal to the pThr-4 motif (yellow) contains a highly conserved stretch of acidic residues highlighted in blue (top panel). These would be predicted to interact with arginine and lysine residues that are also conserved and form a basic patch adjacent to the binding site for the peptide C-terminus of the bound peptide (bottom).

(e) Cartoon showing the three most likely effects of Thr-4 phosphorylation

(f) Ligation of an extended pThr-4 peptide to trypsin-cleaved Mdc1 FHA (left) produces a stoichiometrically and specifically phosphorylated protein encompassing the entire N-terminal region that forms a tight dimer by SEC-MALLS analysis (right). M_o- observed molecular weight, M_c - calculated molecular weight.

Figure 5 – Dimerization of the Mdc1 N-terminal region *in vivo*

(a) The interaction between differentially tagged Mdc1 N-terminal fragments is dependent upon the intact FHA domain and Thr4 phosphorylation. 293T cells were transiently transfected with Flag-tagged Mdc1(1-800aa) and Myc-tagged Mdc1(1-800aa) wildtype and the indicated mutants, respectively. Protein complexes were immunoprecipitated with monoclonal anti-Flag agarose and immunoblotted with polyclonal anti-Myc and polyclonal anti-Flag antibodies.

(b) The Mdc1 FHA domain is recruited to damaged chromatin regions. U2OS expressing a tetracycline-inducible EYFP-FHA(WT)^{TetOn} fusion protein were treated with doxocyclin for 1 hour and subjected to laser irradiation. Cells were fixed 30 min after irradiation and immunostained for γH2AX.

(c) Kinetics of Mdc1 FHA domain recruitment. U2OS FHA(WT)-EYFP^{TetOn} cells were incubated with doxocycline for 1h and subjected to laser irradiation. Time-lapse live cell microscopy was performed and images were taken at the indicated times. Note that for technical reasons, 0 min time point was taken about 20 sec after micro-irradiation.

(d) Recruitment of Mdc1 FHA domain is dependent on endogenous Mdc1. U2OS FHA(WT)EYFP^{TetOn} cells were either treated with control siRNA or siRNA against endogenous Mdc1. Cells were induced with doxocycline for 1h, subjected to laser irradiation and images were

taken 30 min thereafter. Cells were subsequently fixed and immunostained for γH2AX.

(e) Recruitment of Mdc1 FHA domain is dependent on phospho-specific interaction between Thr4 and the FHA domain as well as on an intact hydrophobic interface between FHA monomers. U2OS FHA-EYFP^{TetOn} cells expressing the wild type and indicated mutants were induced with doxocycline for 1h, subjected to laser irradiation and images were taken 30 min thereafter. Cells were subsequently fixed and immunostained for γH2AX.

Figure 6 – Regulation of Mdc1 interactions through phospho-dependent and phospho-independent FHA domain surfaces by dimerization.

(a) Binding of Thr-phosphorylated partners such as Chk2 (gold) can occur through the canonical phospho-dependent surface on the Mdc1 FHA (green patch) that is subsequently occluded following Thr-4 phosphorylation and tight head-to-tail dimerization.

(b) Interaction of phospho-independent binding partners (red) with some or all of the Mdc1 dimerization interface residues (yellow) competes with weak FHA-FHA interactions in un-phosphorylated Mdc1, but is occluded in the pThr-4 dimer.

(c) Tight Mdc1 dimerization might create a contiguous phospho-independent binding surface (cyan) spanning the two FHA domains.

Table 1 - Crystallographic Statistics

	Mdc1/pThr-4 (Se SAD)	Mdc1
Data Collection		
Space group	$P2_12_12_1$	$P2_12_12_1$
Cell dimensions (Å)		
a, b, c (Å)	58.5, 59.9, 72.1	35.3, 54.7, 98.1
	Peak	
Wavelength (Å)	0.9790	
Resolution (Å)	15.0 – 1.8 (1.86-1.80)	20.0 – 2.3 (2.40-2.30)
R_{merge} (%)	3.7 (31.5)	8.4 (40.4)
$< I/\sigma (I) >$	27.5 (2.1)	11.7 (2.8)
Completeness (%)	93.4 (55.3)	93.7 (90.2)
Redundancy	3.2 (2.1)	3.0 (2.9)
Refinement		
Resolution (Å)	15 – 1.8	15.0 - 2.3
No. reflections	21805	8461
R_{work}/Rf_{ree} (%)[b]	21.3/24.0	23.8/27.1
No. atoms		
Protein	1741	1693
Peptide	134	-
Water	200	106
B-factors ($Å^2$)		
Protein	24.5	48.6
Peptide	38.7	-
Water	36.6	53.4
R.m.s deviations		
Bond lengths (Å)	0.008	0.009
Bond angles (°)	1.2	1.3

*Values in parentheses are for highest-resolution shell

Figure 1

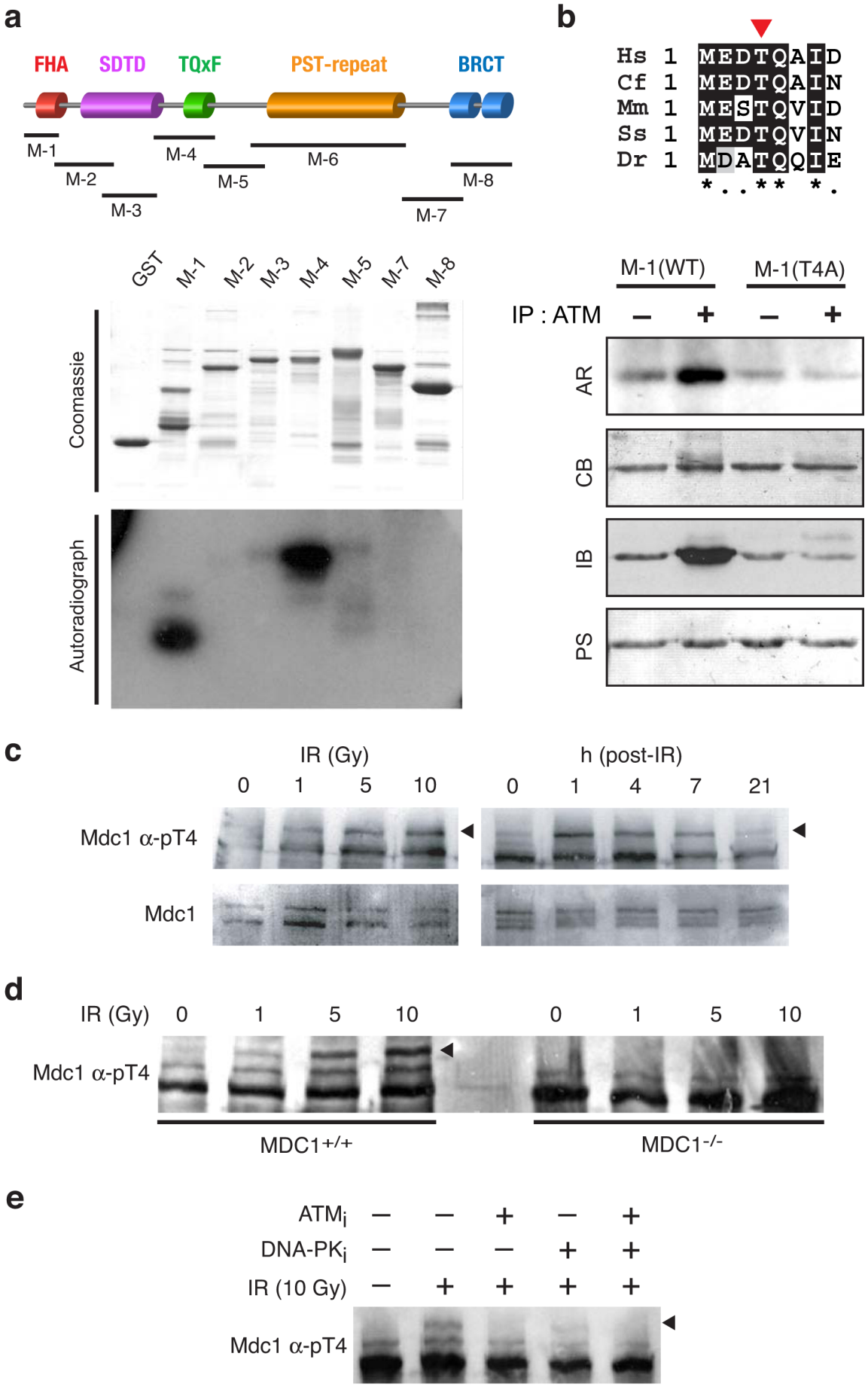
a
FHA
SDTD
TQxF
PST-repeat
BRCT
M-1
M-2
M-3
M-4
M-5
M-6
M-7
M-8
GST
M-1
M-2
M-3
M-4
M-5
M-7
M-8
Coomassie
Autoradiograph
b
Hs 1 MEDTQAID
Cf 1 MEDTQAIN
Mm 1 MESTQVID
Ss 1 MEDTQVIN
Dr 1 MDATQQIE
M-1(WT)
M-1(T4A)
IP : ATM
AR
CB
IB
PS
c
IR (Gy)
0 1 5 10
h (post-IR)
0 1 4 7 21
Mdc1 α-pT4
Mdc1
d
IR (Gy) 0 1 5 10 0 1 5 10
Mdc1 α-pT4
MDC1+/+
MDC1-/-
e
ATMi
DNA-PKi
IR (10 Gy)
Mdc1 α-pT4

Figure 2

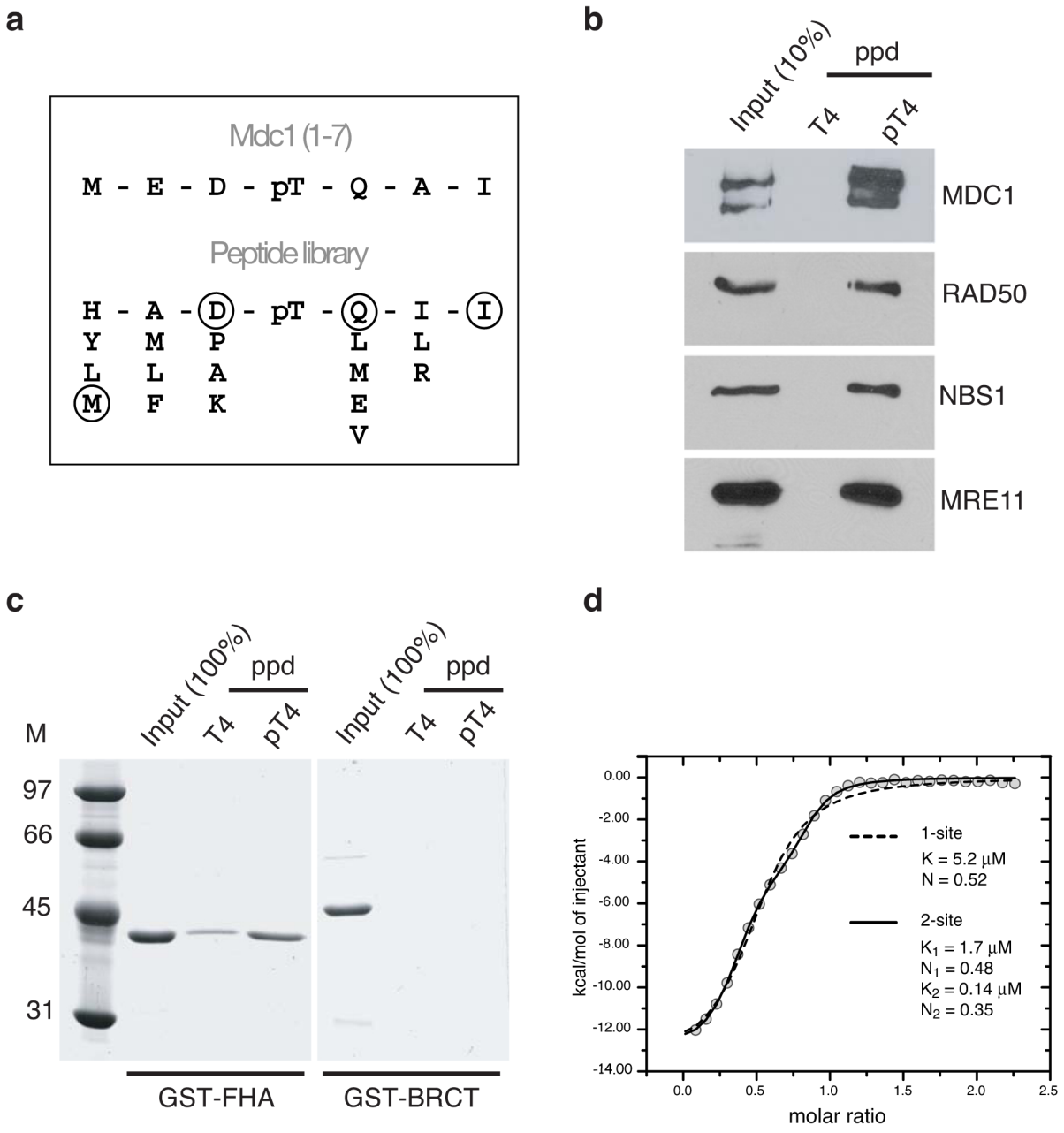
a
Mdc1 (1-7)
M - E - D - pT - Q - A - I
Peptide library
H - A - D - pT - Q - I - I
Y M P L L
L L A M R
M F K E
V
b
Input (10%)
ppd
T4
pT4
MDC1
RAD50
NBS1
MRE11
c
Input (100%)
ppd
T4
pT4
M
97
66
45
31
GST-FHA
GST-BRCT
d
kcal/mol of injectant
molar ratio
1-site
K = 5.2 μM
N = 0.52
2-site
K1 = 1.7 μM
N1 = 0.48
K2 = 0.14 μM
N2 = 0.35

Figure 3

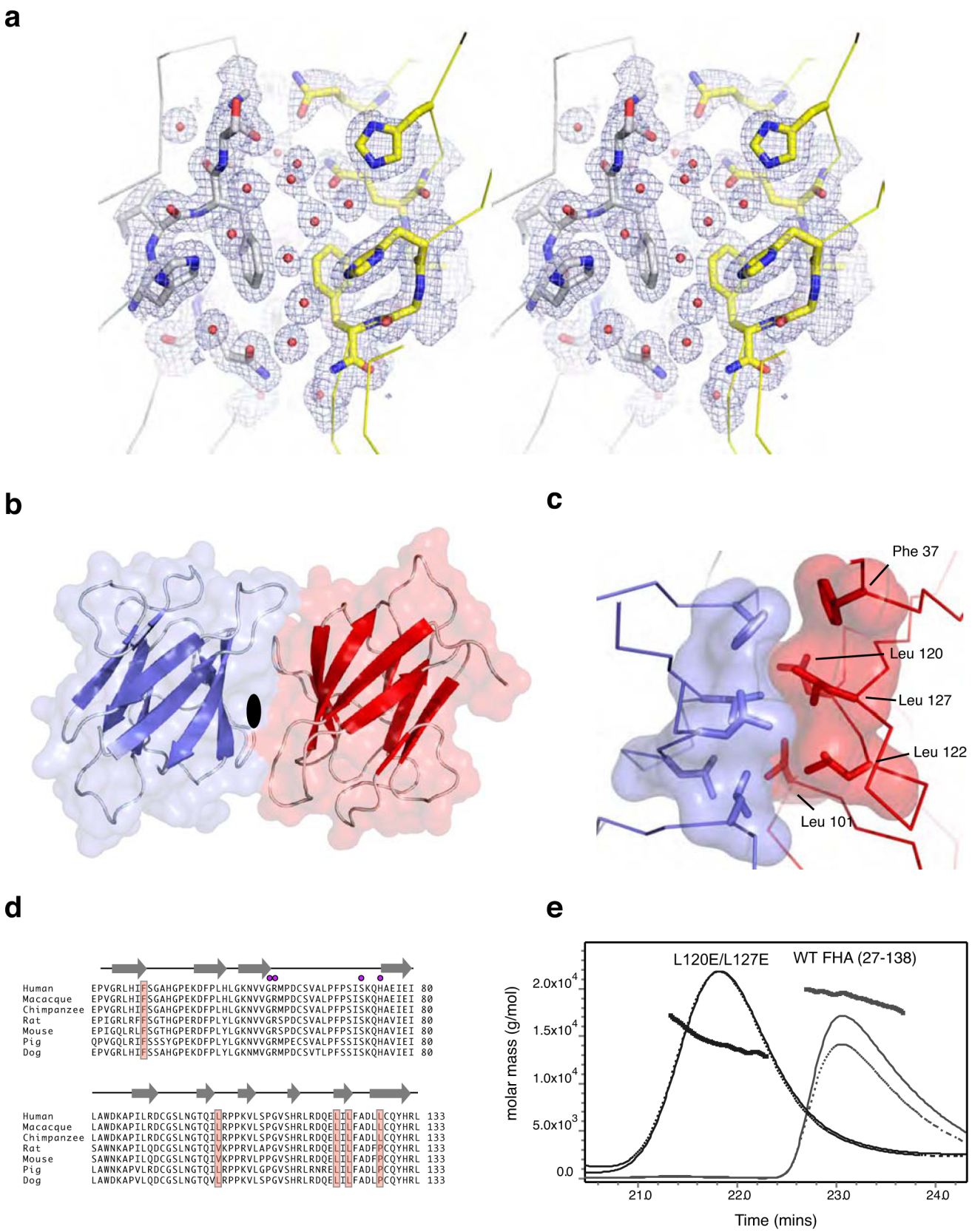
a
b
c
Phe 37
Leu 120
Leu 127
Leu 122
Leu 101
d
Human EPVGRLHIFSGAHGPEKDFPLHLGKNVVGRMPDCSVALPFPSISKQHAEIEI 80
Macacque EPVGRLHIFSGAHGPEKDFPLHLGKNVVGRMPDCSVALPFPSISKQHAEIEI 80
Chimpanzee EPVGRLHIFSGAHGPEKDFPLHLGKNVVGRMPDCSVALPFPSISKQHAEIEI 80
Rat EPIGRLRFFSGTHGPERDFPLYLGKNVVGRSPDCSVALPFPSISKQHAVIEI 80
Mouse EPIGQLRLFSGTHGPERDFPLYLGKNVVGRSPDCSVALPFPSISKQHAVIEI 80
Pig QPVGQLRIFSSSYGPEKDFPLYLGKNVVGRMPECSVALPFSSISKQHAVIEI 80
Dog EPVGRLHIFSSAHGPEKDFPLYLGKNMVGRMPDCSVTLPFSSISKQHAVIEI 80
Human LAWDKAPILRDCGSLNGTQILRPPKVLSPGVSHRLRDQELILFADLLCQYHRL 133
Macacque LAWDKAPILRDCGSLNGTQILRPPKVLSPGVSHRLRDQELILFADLLCQYHRL 133
Chimpanzee LAWDKAPILRDCGSLNGTQILRPPKVLSPGVSHRLRDQELILFADLLCQYHRL 133
Rat SAWNKAPILQDCGSLNGTQIVKPPRVLAPGVSHRLRDQELILFADFPCQYHRL 133
Mouse SAWNKAPILQDCGSLNGTQIVKPPRVLPPGVSHRLRDQELILFADFPCQYHRL 133
Pig LAWNKAPVLRDCGSLNGTQILRPPKVLGPGVSHRLRNRELILFADLPCQYHRL 133
Dog LAWDKAPVLQDCGSLNGTQVLRPPKVLSPGVSHRLRDQELILFADLPCQYHRL 133
e
L120E/L127E
WT FHA (27-138)
molar mass (g/mol)
2.0x10^4
1.5x10^4
1.0x10^4
5.0x10^3
0.0
21.0
22.0
23.0
24.0
Time (mins)

Figure 4

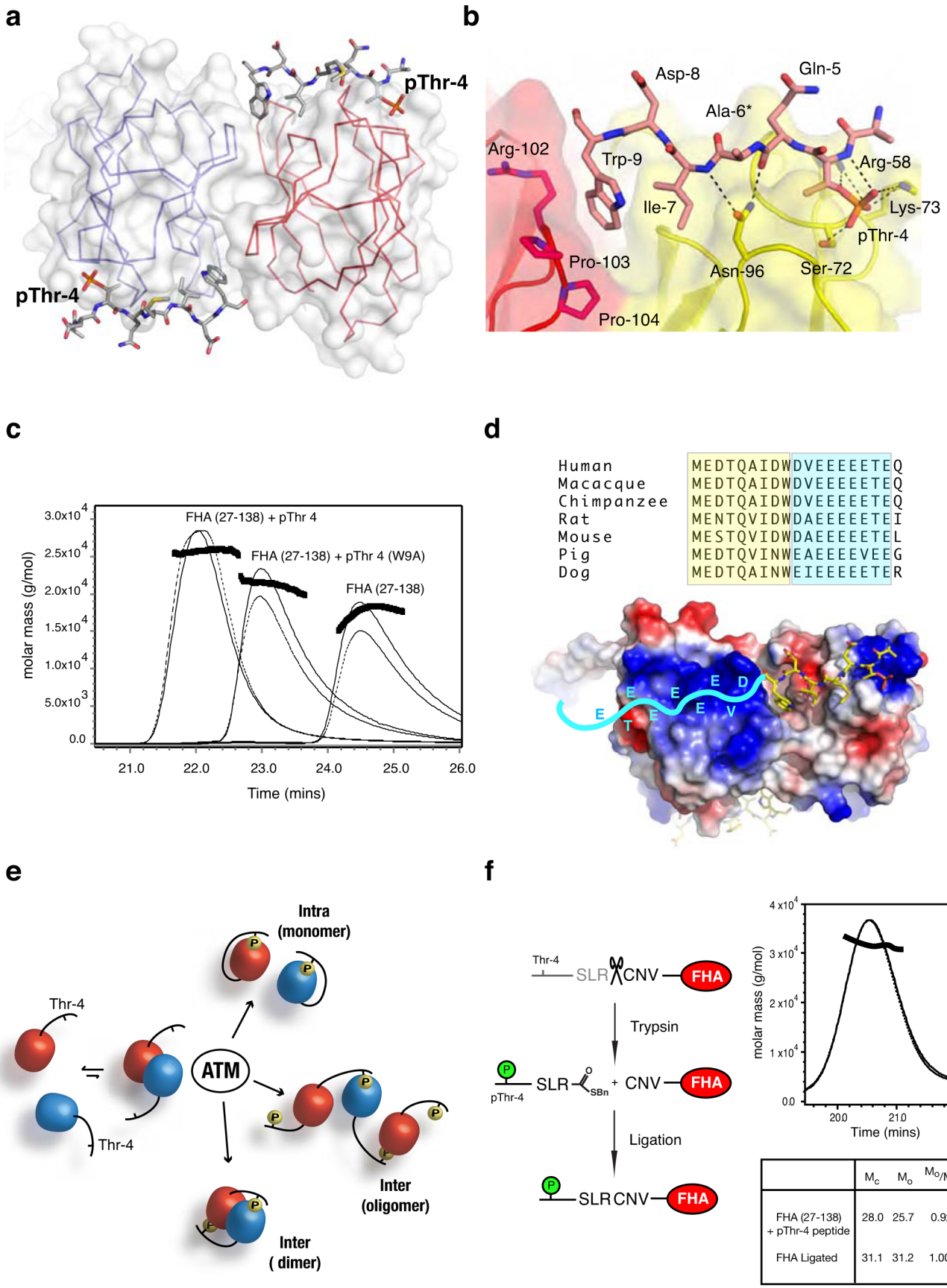

	M_c	M_o	M_o/M_c
FHA (27-138) + pThr-4 peptide	28.0	25.7	0.92
FHA Ligated	31.1	31.2	1.00

Figure 5

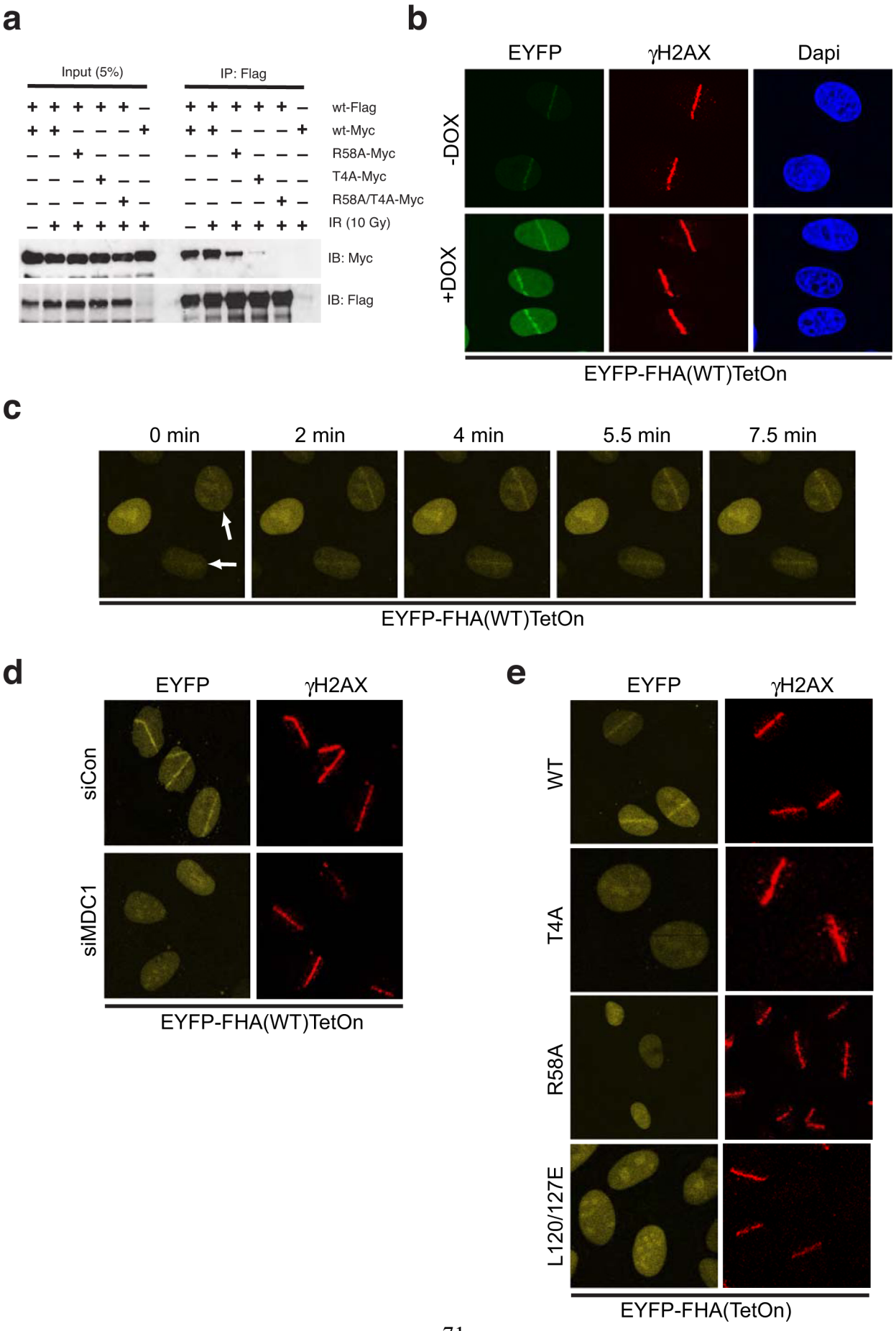
a
Input (5%)
IP: Flag
wt-Flag
wt-Myc
R58A-Myc
T4A-Myc
R58A/T4A-Myc
IR (10 Gy)
IB: Myc
IB: Flag
b
EYFP
γH2AX
Dapi
-DOX
+DOX
EYFP-FHA(WT)TetOn
c
0 min
2 min
4 min
5.5 min
7.5 min
EYFP-FHA(WT)TetOn
d
EYFP
γH2AX
siCon
siMDC1
EYFP-FHA(WT)TetOn
e
EYFP
γH2AX
WT
T4A
R58A
L120/127E
EYFP-FHA(TetOn)

Figure 6

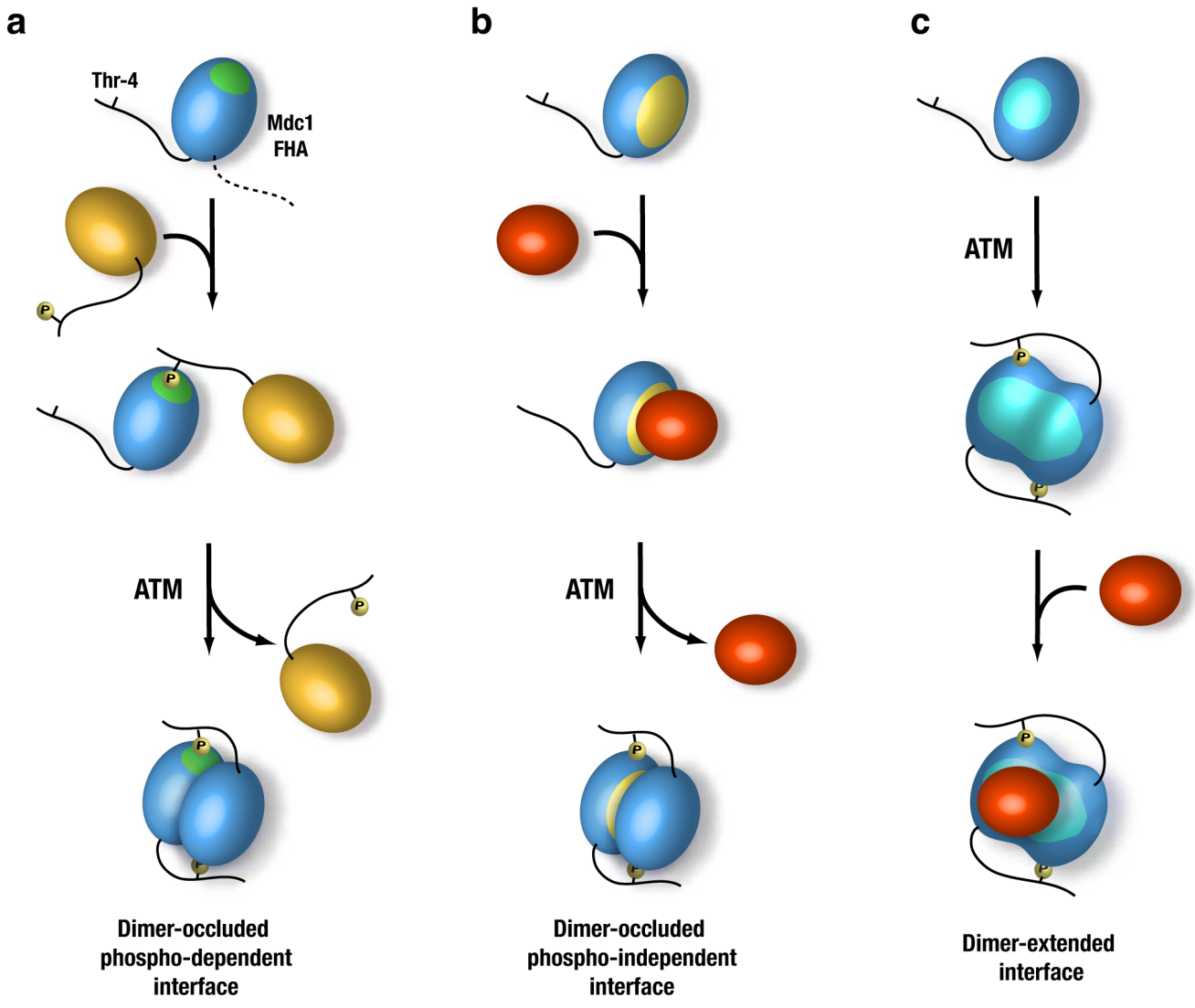
a
Thr-4
Mdc1
FHA
P
ATM
P
Dimer-occluded
phospho-dependent
interface
b
ATM
Dimer-occluded
phospho-independent
interface
c
ATM
Dimer-extended
interface

Supplementary information

The molecular basis of ATM-dependent dimerization of the MDC1 DNA-damage checkpoint mediator

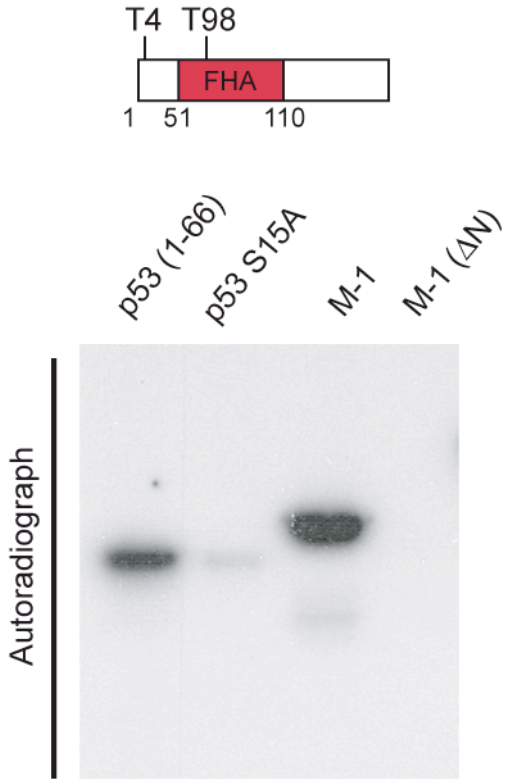

Supplementary Figure 1 – Autoradiography of *in vitro*-phosphorylated N-terminal MDC1 fragment comprising the FHA domain. In this fragment, two ATM/ATR consensus sites (TQ) are present (T4 and T98). However, only T4 is phosphorylated by ATM in vitro since M1 (ΔN) lacking the N-terminal T4 is not phosphorylated.

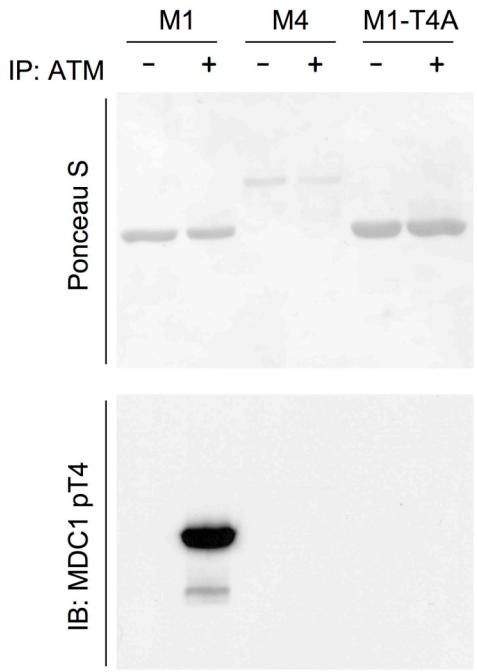

Supplementary Figure 2 – The MDC1 pT4 antibody specifically recognized phosphorylated T4 but not the phosphorylated TQXF cluster. *In vitro* ATM kinase assay of recombinant fragments M1 (containing Thr-4), mutant M1-T4A and M4 (containing the MDC1 TQXF cluster).

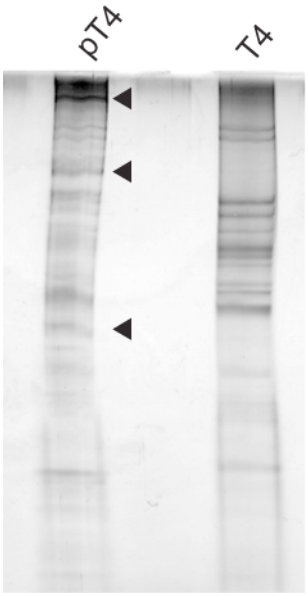

Supplementary Figure 3 - Silver-stained SDS PAGE gel of proteins pulled down by the Thr-4 phosphopeptide and its unphosphorylated derivative. The major bands present only in the phosphopeptide pull-down are highlighted by arrowheads.

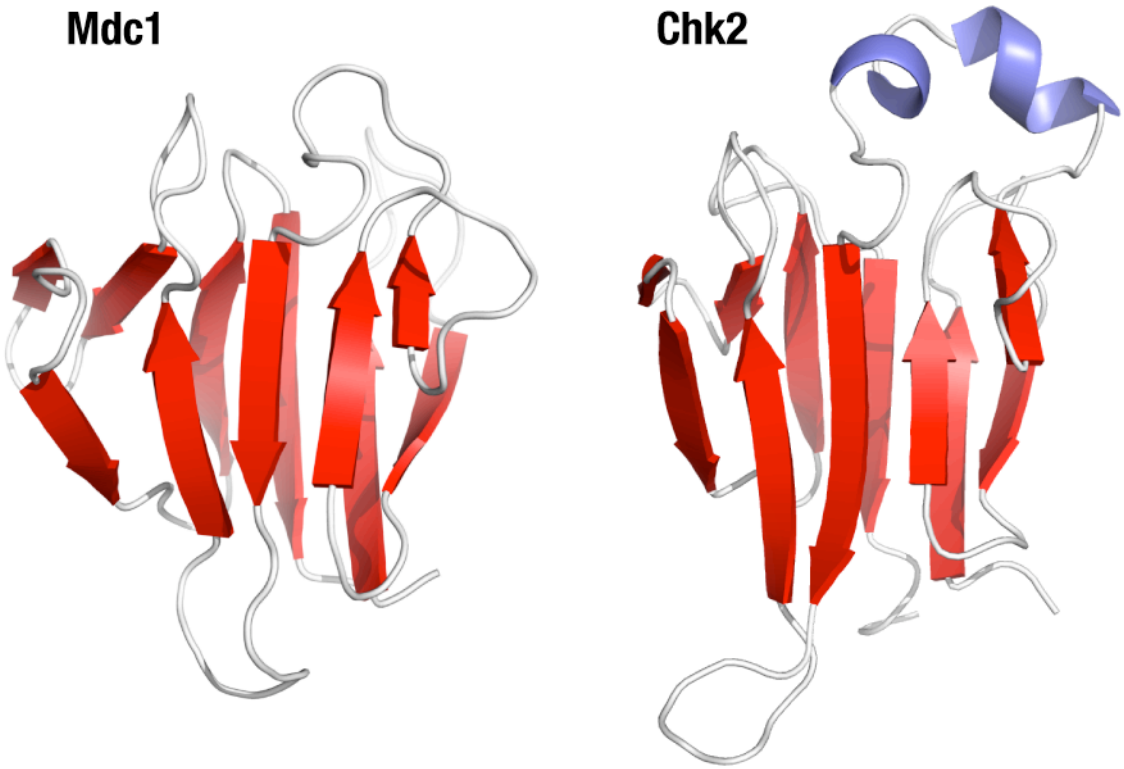

Supplementary Figure 4 - Comparison of the Mdc1 FHA structure with that of human Chk2 (PDB ID: 1GXC) reveals a similar, characteristic core FHA domain β-sandwich architecture.

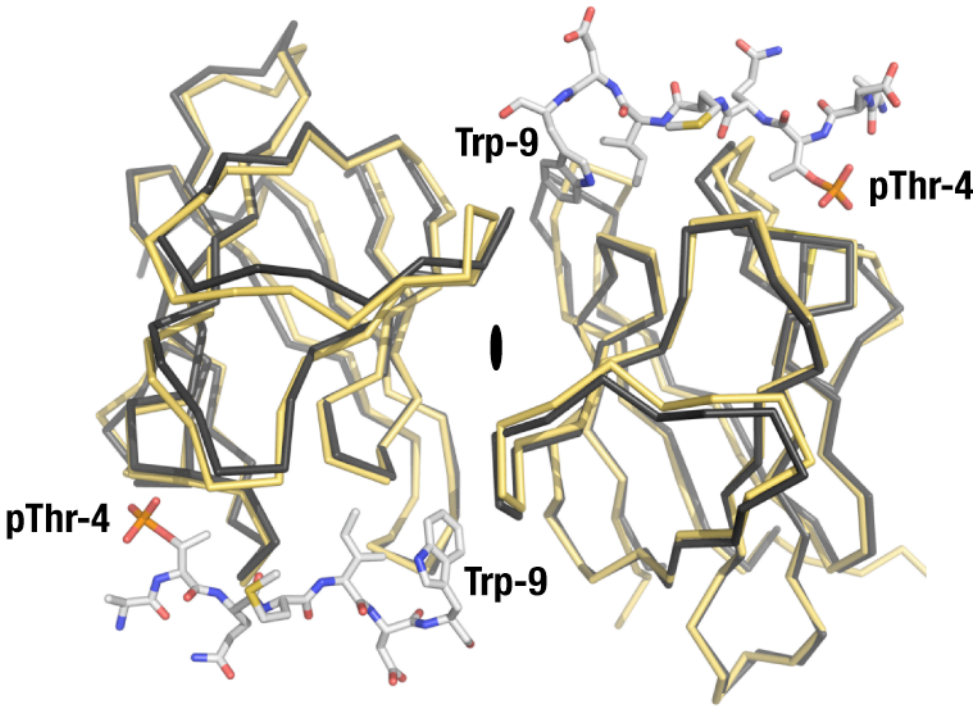

Supplementary Figure 5 - Least-squares superposition of the Mdc1 FHA domain dimer in the peptide-free (black) and pThr-4 peptide-bound (gold) structures, shown as Cα plots. The bound phosphopeptide is shown in stick representation.

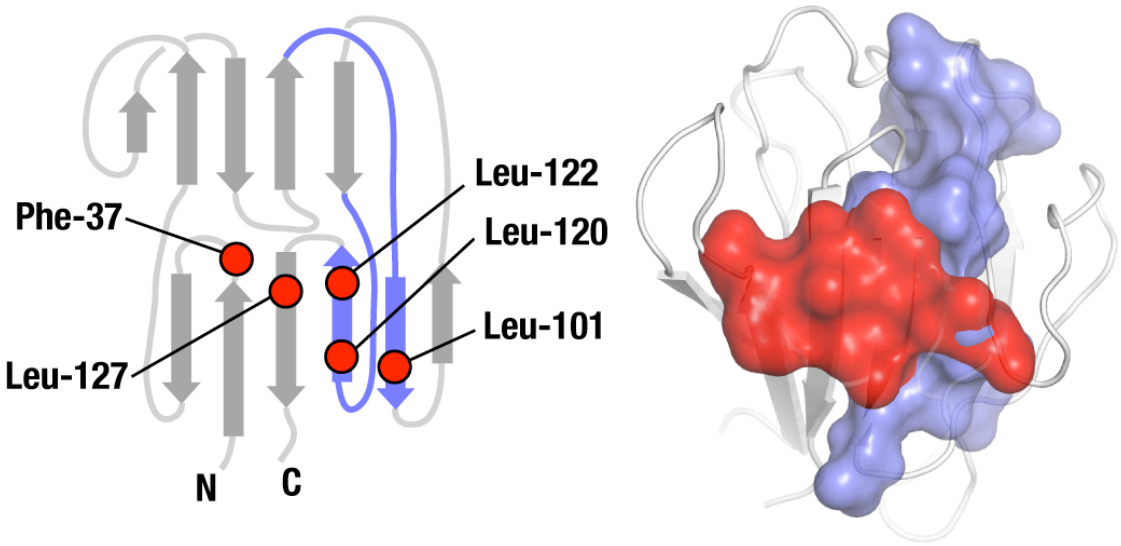

Supplementary Figure 6 - Topology diagram (left panel) and surface representation (right panel) show that hydrophobic residues that form the conserved Mdc1 FHA-FHA interface (red circles) overlap with a putative self-interacting surface (blue) previously identified by sequence analysis (Lee et. al 2003).

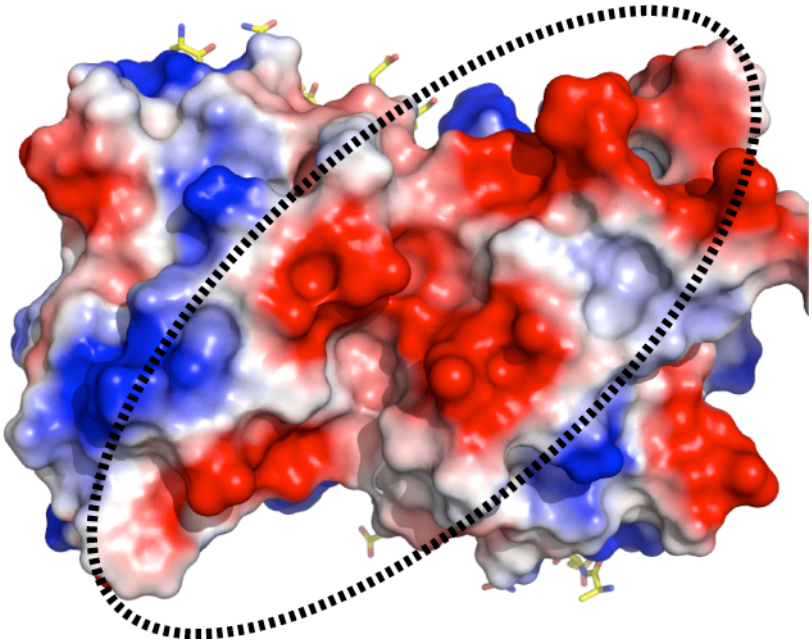

Supplementary Figure 7 - Electrostatic surface representation of the Mdc1 FHA dimer viewed along the non-crystallographic 2-fold axis. Regions of positive potential are shown in blue and acidic regions in red. Association of the two FHA domains produces a continuous region of negative charge that extends across the dimer.

References

Lee, G.I., Ding, Z., Walker, J.C. and Van Doren, S.R. (2003) NMR structure of the forkhead associated domain from the Arabidopsis receptor kinase-associated protein phosphatase. *Proc Natl Acad Sci USA*, 100, 11261-11266.

5.2 A divalent FHA/BRCT-binding mechanism couples the MRE11/RAD50/NBS1 complex to damaged chromatin

Authors: Flurina J. Hari*, Christoph Spycher*, Stephanie Jungmichel, Lucijana Pavic & Manuel Stucki

*equal contribution

Journal: EMBO Reports (manuscript accepted)

Contribution: Generation of data for Fig. 4C and Supplementary Fig. 1 (G2/M checkpoint assay, expression analysis of stable NBS1 cell lines by Western Blot); preparation of figures; proofreading of the manuscript

EMBO
reports

scientific report

A divalent FHA/BRCT-binding mechanism couples the MRE11–RAD50–NBS1 complex to damaged chromatin

Flurina J. Hari, Christoph Spycher*, Stephanie Jungmichel, Lucijana Pavic & Manuel Stucki+*
Institute of Veterinary Biochemistry and Molecular Biology, University of Zurich, Zurich, Switzerland

The MRE11–RAD50–NBS1 (MRN) complex accumulates at sites of DNA double-strand breaks in large chromatin domains flanking the lesion site. The mechanism of MRN accumulation involves direct binding of the Nijmegen breakage syndrome 1 (NBS1) subunit to phosphorylated mediator of the DNA damage checkpoint 1 (MDC1), a large nuclear adaptor protein that interacts directly with phosphorylated H2AX. NBS1 contains an FHA domain and two BRCT domains at its amino terminus. Here, we show that both of these domains participate in the interaction with phosphorylated MDC1. Point mutations in key amino acid residues of either the FHA or the BRCT domains compromise the interaction with MDC1 and lead to defects in MRN accumulation at sites of DNA damage. Surprisingly, only mutation in the FHA domain, but not in the BRCT domains, yields a G2/M checkpoint defect, indicating that MDC1-dependent chromatin accumulation of the MRN complex at sites of DNA breaks is not required for G2/M checkpoint activation.

Keywords: DNA double-strand breaks; chromatin; NBS1; MDC1; G2/M checkpoint

EMBO *reports* advance online publication 12 March 2010; doi:10.1038/embor.2010.30

INTRODUCTION

Nijmegen breakage syndrome (NBS) is a rare autosomal genetic disorder. NBS patients suffer from growth retardation, microcephaly, dismorphal features, immunodeficiency and predisposition to cancer, mainly lymphomas. Cells derived from NBS patients are radiosensitive, show chromosomal instability and cell-cycle checkpoint, as well as apoptotic defects (van der Burgt *et al*, 1996).

The NBS gene codes for a 754-amino-acid protein named NBS1 (p95; nibrin). It exists exclusively in a complex with two enzymes: MRE11, a structure-specific nuclease, and RAD50, an ATPase/adenylate kinase. Together, these three proteins form the MRE11–RAD50–NBS1 (MRN) complex, a conserved and essential DNA-damage response (DDR) factor that functions in many cellular processes involving DNA double-strand breaks (DSBs), including DSB repair, checkpoint signalling, DNA replication, meiotic recombination and induction of apoptosis (Stracker *et al*, 2004; Difilippantonio & Nussenzweig, 2007).

The MRN complex accumulates at sites of DSBs in large microscopically discernible subnuclear structures, usually referred to as DNA-damage foci. The functional implication of this massive accumulation at sites of DSBs is not yet fully understood. We and others showed recently that focus formation by the MRN complex is mediated by a direct interaction between NBS1 and phosphorylated mediator of the DNA damage checkpoint 1 (MDC1), which is a large nuclear adaptor protein that specifically recognises phosphorylated H2AX (γH2AX; Chapman & Jackson, 2008; Melander *et al*, 2008; Spycher *et al*, 2008; Wu *et al*, 2008). The interaction between NBS1 and MDC1 is dependent on the amino-terminal portion of NBS1 that contains the FHA domain and interacts directly with a constitutively phosphorylated acidic repeat region in MDC1, the SDT repeat (Chapman & Jackson, 2008; Melander *et al*, 2008; Spycher *et al*, 2008). The SDT repeat region is characterized by conserved patches of 8–10 amino acids comprising serine and threonine residues typically separated by an aspartate and embedded further in an acidic sequence environment. This SDT region (referred to as the SDTD region in some papers) interacts with the MRN complex in a phosphorylation-dependent manner. In human MDC1, six SDT motifs were identified and deletion of at least five of them leads to complete abrogation of MRN foci formation (Melander *et al*, 2008; Spycher *et al*, 2008). Analysis of NBS1 recruitment to sites of DSBs showed that on expression of an MDC1 version lacking the SDT regions, NBS1 only accumulates in micro-foci and is not found in the broader chromatin compartments usually covered by γH2AX and MDC1 (Chapman & Jackson, 2008). This indicates that the MRN complex is recruited to DSBs in an MDC1-independent manner, but its sustained interaction with the DSB-flanking chromatin requires MDC1.

Interestingly, MDC1 and MRN exist in a complex even in undamaged cells. This interaction is dependent on the activity of the acidophilic casein kinase 2 (CK2), for which the SDT motifs form consensus phosphorylation sites (Spycher *et al*, 2008; Wu *et al*, 2008). Both serine and threonine residues in each SDT motif are phosphorylated by CK2 *in vivo* and only doubly phosphorylated pSDpT motifs are able to mediate the interaction with NBS1 (Melander *et al*, 2008; Spycher *et al*, 2008).

Institute of Veterinary Biochemistry and Molecular Biology, University of Zurich, Winterthurerstrasse 190, Zurich 8057, Switzerland
*These authors contributed equally to this work
+Corresponding author. Tel: +41 44 63 55421; Fax: +41 44 63 56840;
E-mail: m.stucki@vetbio.uzh.ch

Received 22 September 2009; revised 2 February 2010; accepted 4 February 2010; published online 12 March 2010

No structural information of full-length NSB1 is yet available, but recent nuclear magnetic resonance (NMR) structural data suggested that besides the FHA domain, NBS1 might also feature a tandem BRCT domain at its N terminus (Xu *et al*, 2008). Similarly to FHA domains, tandem BRCT domains have been shown to act as phospho-specific protein–protein interaction modules (Glover *et al*, 2004).

Here, we present evidence that both the NBS1 FHA domain and the tandem BRCT domain interact specifically with phosphorylated MDC1. We show that single point mutations in key residues in both the FHA and the tandem BRCT domain of NBS1 disrupt the interaction with MDC1 and abrogate the accumulation and retention of the MRN complex at sites of DSBs. Surprisingly, only a mutation in the FHA domain induces a significant G2/M DNA-damage checkpoint defect, whereas mutation in the tandem BRCT domain does not. Thus, our findings indicate that MDC1-mediated accumulation of the MRN complex at sites of DSBs is not required for G2/M checkpoint activation and strongly suggest that the FHA domain of NBS1 might have additional, as yet unidentified, interaction partners that mediate G2/M checkpoint activation in response to DSBs.

RESULTS AND DISCUSSION

Both FHA and BRCT domains of NBS1 interact with MDC1

Until recently, sequence comparison and structure predication algorithms indicated that the N-terminal region of NBS1 contained an FHA domain and one single BRCT domain (reviewed in D'Amours & Jackson, 2002). Three years ago, a second putative BRCT domain at the N terminus of NBS1 was discovered by means of a refined bioinformatic analysis (Becker *et al*, 2006). The existence of two BRCT domains downstream from the FHA domain at the NBS1 N terminus was partly confirmed by a recently published NMR structure of the second BRCT domain (Xu *et al*, 2008). Interestingly, there seems to be no spacer between the FHA domain and the putative tandem BRCT domain, indicating that these domains might form one single compact globular structure (Fig 1A). Moreover, conservation of key phospho-binding amino-acid residues in the BRCT tandem domain suggests that like the FHA domain, it might act as a phospho-specific protein–protein interaction module.

We and others have shown recently that the FHA domain of NBS1 associates directly with a constitutively phosphorylated region in MDC1, the SDT repeat region (Chapman & Jackson, 2008; Melander *et al*, 2008; Spycher *et al*, 2008). Mammalian MDC1 contains a total of six SDT motifs, and at least three of these are required for efficient MRN accumulation at sites of DSBs (Spycher *et al*, 2008). This might indicate that more than one binding site with affinity to the phosphorylated SDT region might exist in NBS1. Thus, we tested whether the intact NBS1 BRCT tandem domain was required for efficient association of NBS1 with the full-length phosphorylated SDT region. We phosphorylated (or mock-treated) the human glutathione-*S*-transferase (GST)-tagged MDC1 SDT fragment and assessed its ability to interact with *in vitro*-translated full-length NBS1 protein that carried point mutations in key residues in its phospho-binding FHA and BRCT tandem domains, respectively. As shown before, full-length wild-type NBS1 interacted efficiently with the phosphorylated SDT region of MDC1 (Fig 1B; Melander *et al*, 2008; Spycher *et al*, 2008). Interestingly, FHA domain single mutant (R28A) and a BRCT tandem domain single mutant (K160M) also showed residual SDT-binding activity. However, a double phosphopeptide-binding mutant (R28A/K160M) failed to bind to the phosphorylated SDT region (Fig 1B). This indicates that both the FHA domain and the BRCT tandem domain are able to interact with the phosphorylated MDC1 SDT region *in vitro*.

NBS1 does not exist on its own in the nuclei of mammalian cells, as it is always associated with MRE11 and RAD50. Thus, our assay conditions with the *in vitro*-translated NBS1 do not accurately reflect a physiological situation where NBS1 is part of a heterotrimeric complex. Therefore, we co-expressed all three subunits of the MRN complex in insect cells and tested their binding affinity to the phosphorylated SDT region of MDC1. Also in the context of the intact MRN complex, wild-type NBS1 bound efficiently to the phosphorylated SDT region (Fig 1C). Surprisingly, neither the FHA mutant (R28A) nor the BRCT tandem domain mutant (K160M) was able to associate with the phosphorylated SDT region (Fig 1C). This indicates that when NBS1 exists in a heterotrimeric complex with MRE11 and RAD50, both the intact FHA domain and the BRCT tandem domain of NBS1 are essential for efficient association with phosphorylated MDC1. It is not clear why the NBS1 single mutants interacted with the phosphorylated SDT region when translated *in vitro* but did not in the context of the heterotrimeric MRN complex. However, it is possible that when NBS1 is an integral part of the MRN complex, its N-terminal phosphopeptide-binding region might be sterically less accessible so that efficient association with the SDT region is only possible when both the FHA domain and BRCT tandem domain are contributing to the interaction.

As an intact NBS1 FHA domain and a BRCT tandem domain seem to be essential for interaction with the MDC1 SDT region, we next asked if both of these domains were also involved in complex formation with MDC1 in mammalian cell extracts. We co-expressed a Flag-tagged 800-amino-acid N-terminal fragment of MDC1 (containing the SDT region) with Myc-tagged full-length NBS1 wild type and a mutant derivative, respectively, and tested their association by co-immunoprecipitation. Significantly, only wild-type NBS1 interacted with the MDC1 fragment in extracts prepared from the transfected cells, whereas neither the FHA and the BRCT tandem domain single-mutants (R28A; K160M) nor the double mutant (R28A/K160M) showed any significant binding activity towards MDC1 (Fig 1D).

The BRCT domains of NBS1 are required for MRN foci

Next, we investigated whether the K160M mutation in the BRCT tandem domain would also compromise the accumulation of the MRN complex at sites of DSBs, as observed earlier for the FHA domain mutant R28A (Cerosaletti & Concannon, 2003; Lukas *et al*, 2004). We generated NBS-iLB1 fibroblast cell lines stably transduced with wild-type and mutant NBS1 (supplementary Fig S1A online). Then, we assessed nuclear foci formation of NBS1 in these cell lines by immunofluorescence microscopy. In NBS-iLB1 parental fibroblasts, no NBS1 staining was observed (Fig 2A, top row). However, 81% of the cells stably transduced with wild-type NBS1 showed focal accumulation of NBS1 1 h after irradiation at 5 Gy. By contrast, only 20% of cells stably transduced with R28A NBS1 and 13% of cells stably transduced with K160M NBS1, had a focal NBS1 staining pattern (Fig 2A), thus indicating that sustained interaction of

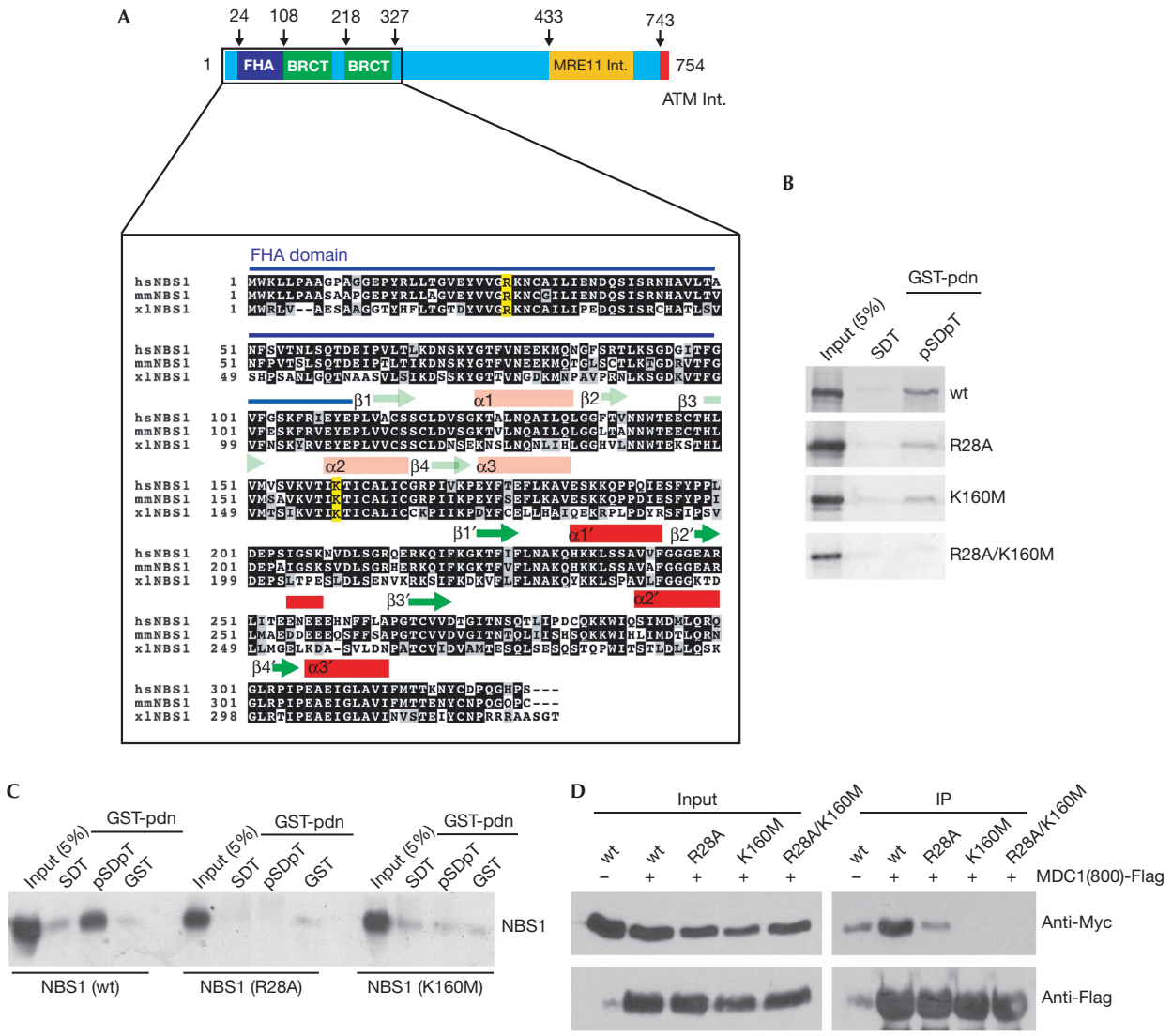

Fig 1 | Both the FHA domain and the tandem BRCT domain of NBS1 are required for the interaction with the phosphorylated SDT region of MDC1 *in vitro*. (**A**) Schematic representation of full-length human NBS1 and its domain composition. The enlarged area shows a sequence alignment of the FHA and BRCT domains of human, mouse and *Xenopus* NBS1. The putative secondary structure of the first (amino-terminal) BRCT domain is indicated by pale colours. The secondary structure of the second (carboxy-terminal) BRCT domain (indicated by bright colours) was derived from Xu *et al* (2008). Phospho-interacting amino acids are highlighted in yellow. (**B**) Purified MDC1 GST-SDT fragment was preincubated with CK2 and ATP. The fragment was then incubated with *in vitro*-translated ^{35}S-labelled NBS1 wild type or mutants for 1 h, washed and resolved by SDS–PAGE and autoradiography. (**C**) Purified MDC1 GST-SDT fragment was preincubated with CK2 and ATP. The fragment was then incubated with purified MRN complex where the NBS1 subunit was either wild type or contained a point mutation in the FHA domain (R28A) or in the BRCT tandem domain (K160M). Bound proteins were separated by SDS–PAGE followed by immunoblotting. The blots were probed with a polyclonal antibody against NBS1. (**D**) Human embryonic kidney 293T cells were transiently transfected with Flag-tagged MDC1(800) fragment and Myc-tagged NBS1 wild type and mutants, as indicated. Flag antibodies were used for co-immunoprecipitation and Myc antibodies for western blot analysis. CK2, casein kinase 2; GST, glutathione-*S*-transferase; IP, immunoprecipitation; MDC1, mediator of the DNA damage checkpoint 1; MRN, MRE11–RAD50–NBS1 complex; NBS1, Nijmegen breakage syndrome 1; SDS–PAGE, sodium dodecyl sulphate–polyacrylamide gel electrophoresis; wt, wild-type.

MRN complex with damaged chromatin requires the phosphopeptide-binding capacity of both the FHA and tandem BRCT domains of NBS1.

To develop these findings further, we used UV-laser microirradiation to induce DSBs in subnuclear volumes (Lukas *et al*, 2004). Under these conditions, wild-type NBS1 accumulated throughout the micro-irradiated nuclear compartments (Fig 2B). However, both the R28A and K160M mutation prevented binding of NBS1 to the γH2AX-coated areas, except for a small fraction of the protein scattered along the irradiated path

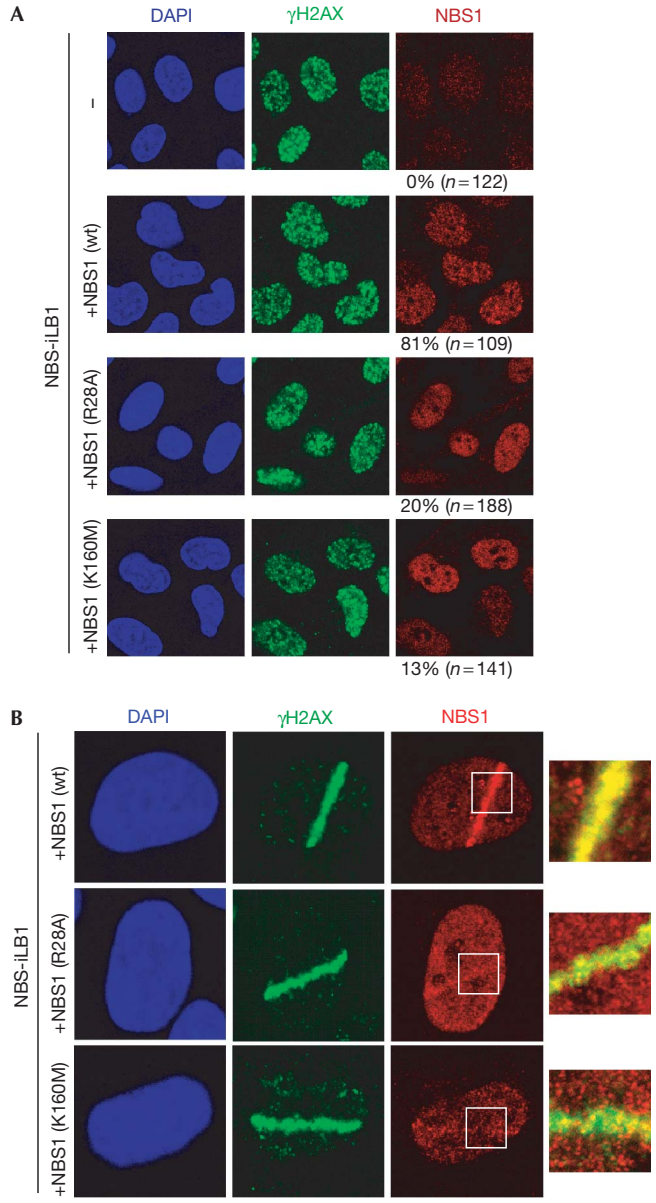

Fig 2 | The BRCT tandem domain of NBS1 is required for focal accumulation of the MRN complex at sites of DSBs *in vivo*. (**A**) NBS-iLB1 fibroblasts and NBS-iLB1 fibroblasts stably transduced with wild-type, R28A or K160M mutant NBS1, respectively, were irradiated at 5 Gy. The irradiated cells were incubated for 1 h, fixed with methanol and probed with the indicated antibodies. Cells were then analysed by confocal microscopy and nuclear foci-positive cells were counted for statistical evaluation. (**B**) NBS-iLB1 fibroblasts stably transduced with wild-type, R28A or K160M mutant NBS1, respectively, were micro-irradiated as described in Methods. The irradiated cells were incubated for 1 h, fixed with methanol and probed with the indicated antibodies. Cells were then analysed by confocal microscopy. DAPI, 4′,6-diamidino-2-phenylindole; MRN, MRE11–RAD50–NBS1 complex; NBS1, Nijmegen breakage syndrome 1.

(Fig 2B, enlarged areas). This indicates that phospho-specific binding of both the NBS1 FHA domain and the BRCT tandem domain to the MDC1 SDT region is essential for efficient accumulation and retention of the MRN complex in damaged nuclear areas.

G2/M checkpoint does not require BRCT domains of NBS1

We proposed previously that MDC1-mediated accumulation of the MRN complex in chromatin regions flanking DSBs was required for efficient activation of the G2/M DNA-damage checkpoint. This was on the basis of the observation that point mutations in the FHA domain that disrupt its phospho-specific binding show partial G2/M checkpoint defects both in human and mouse cells (Difilippantonio *et al*, 2005, 2007; Spycher *et al*, 2008). If this interpretation was correct, we would predict that the K160M mutation in the NBS1 BRCT tandem domain also leads to a G2/M checkpoint defect similar to the R28A FHA mutation, because MDC1-binding and chromatin accumulation are as severely compromised in the K160M mutant as they are in the R28A mutant (see above). Surprisingly, however, we found that several independent clones of NBS fibroblasts stably transduced with K160M NBS1 activated the G2/M checkpoint almost as efficiently as wild-type NBS1 (Fig 3; supplementary Fig S1B online). This indicates that MDC1-binding and MDC1-mediated accumulation of the MRN complex at sites of DSBs are not required for activation of the G2/M checkpoint.

MRN foci formation is not required for the G2/M checkpoint

To verify the aforementioned conclusion, we exploited an earlier observation that overexpression of a C-terminal fragment of MDC1 comprising its γH2AX-binding C-terminal BRCT domains yielded a strong dominant-negative effect on the accumulation and retention of the DDR proteins at sites of DSBs (Stucki *et al*, 2005). We reasoned that if our conclusion was correct, we should not observe a G2/M checkpoint defect on overexpression of the MDC1 BRCT domains. To test this, we used a U2OS cell line carrying a stably integrated, tetracycline-regulated, expression cassette directing the expression of the MDC1 tandem BRCT domain fused to yellow fluorescent protein (YFP). As observed previously (Stucki *et al*, 2005), induction of YFP-BRCT expression by the tetracycline analogue doxocycline (DOX) completely abrogated MRN accumulation at sites of DSBs, as reflected by both NBS1 foci formation (Fig 4A) and UV-laser micro-irradiation (Fig 4B). However, induction of YFP-BRCT expression did not trigger a measurable G2/M checkpoint defect after 1 and 3 Gy of irradiation, respectively (Fig 4C). Significantly, however, down-regulation of endogenous MDC1 in this cell line still yielded a significant G2/M checkpoint defect, irrespective of whether YFP-BRCT expression was induced or not, thus supporting the previous observation that MDC1 is required for G2/M checkpoint activation (Lou *et al*, 2003, 2006; Stewart *et al*, 2003). These data thus support our conclusion that MDC1-mediated accumulation and retention of the MRN complex at sites of DSBs is not required for activation or maintenance of the G2/M checkpoint response.

Speculation

Here, we present a unique divalent FHA/BRCT-binding mechanism that couples the MRN complex to γH2AX-enriched chromatin regions that mark sites of DSBs, and we show for the first time to our knowledge that phospho-binding activities of both the NBS1 FHA domain and the BRCT tandem domain are essential for focal accumulation of the MRN complex at sites of DSBs *in vivo*. It is

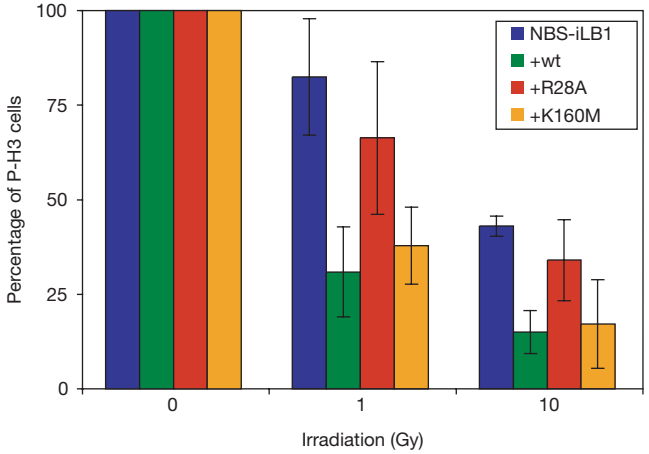

Fig 3 | Mutation in the tandem BRCT domain of NBS1 does not yield a G2/M DNA-damage checkpoint defect. NBS-iLB1 fibroblasts and NBS-iLB1 fibroblasts stably transduced with wild-type, R28A or K160 mutant NBS1, respectively, were left untreated or irradiated at 1 and 10 Gy. Cells were harvested 1 h after irradiation, fixed with methanol and stained with an antibody against phosphorylated H3 (P-H3) and propidium iodide. The percentage of P-H3-positive cells was determined by fluorescence-activated cell sorting analysis. In this graph, three independent experiments (each performed in triplicate) are summarized. The error bars represent the standard deviation. NBS1, Nijmegen breakage syndrome 1.

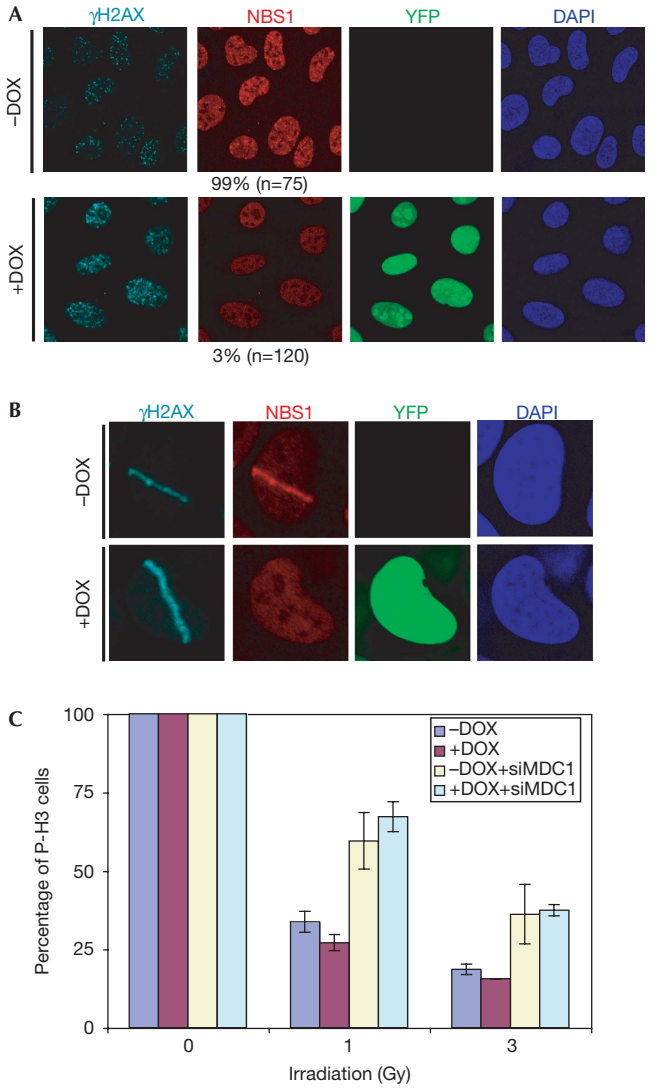

Fig 4 | Experimental uncoupling of the MRN complex from damaged chromatin does not trigger a G2/M checkpoint defect. (**A**) Nuclear foci formation of NBS1 in inducible U2OS YFP-BRCT-overexpressing cells after irradiation at 5 Gy. Non-induced cells (top) and YFP-BRCT-expressing cells (bottom). (**B**) Microlaser-induced DNA-damage recruitment analysis of NBS1 in inducible U2OS YFP-BRCT-overexpressing cells. Non-induced cells (top) and YFP-BRCT-expressing cells (bottom). (**C**) Overexpression of the MDC1 BRCT domains does not trigger a G2/M checkpoint defect. Expression of YFP-BRCT fusion protein was induced 8 h before irradiation (+DOX). Mock-induced cells acted as the control (−DOX). Depletion of endogenous MDC1 by siRNA (siM) partly abrogated the G2/M checkpoint regardless of whether or not MDC1 is proficient for γH2AX binding. The error bars represent the standard deviation. DAPI, 4′,6-diamidino-2-phenylindole; DOX, doxocyclin; MDC1, mediator of the DNA damage checkpoint 1; MRN, MRE11–RAD50–NBS1 complex; NBS1, Nijmegen breakage syndrome 1; siRNA, small interfering RNA; YFP, yellow fluorescent protein.

unknown why such a divalent binding mechanism has evolved, but it is interesting to note that mutation in the NBS1 FHA domain triggers a G2/M checkpoint defect, whereas mutation in the BRCT tandem domain does not. This suggests that besides phosphorylated MDC1, the NBS1 FHA domain might have an additional, as yet unidentified, binding partner that mediates G2/M checkpoint activation in response to DSBs. While this paper was under revision, it was shown that *Schizosaccharomyces pombe* Ctp1, a protein that is involved in the resection of DSBs in the S and G2 phases of the cell cycle, interacts directly with the yeast Nbs1 FHA domain in a mechanism that involves CK2-dependent phosphorylation of SDT-like motifs in Ctp1 (Lloyd *et al*, 2009; Williams *et al*, 2009). Thus, CtIP, the human orthologue of Ctp1, might be a promising candidate for an additional NBS1 interaction partner. CtIP was shown previously to be required for efficient induction of the G2/M DNA-damage checkpoint (Yu & Chen, 2004). Furthermore, human CtIP also contains a region that comprises several conserved CK2 consensus sites; indeed, this region is phosphorylated efficiently by CK2 *in vitro* (F.H. & M.S., unpublished observation). However, whether or not these putative CK2 sites in CtIP interact with human NBS1 to mediate the G2/M DNA-damage checkpoint remains to be established.

METHODS

Cell lines and plasmids. NBS-iLB1 cells stably expressing wild-type and K160M mutant NBS1 were generated by retroviral transduction. The YFP-BRCT-expressing U2OS cell line was described by Stucki *et al* (2005). The human MDC1 GST-SDT construct was described by Spycher *et al* (2008). The MDC1(800) fragment was cloned into a modified pcDNA3.1-Flag mammalian expression vector (Invitrogen, Eugene, OR, USA). Myc-NBS1 was subcloned into a pFastBac transfer vector (Invitrogen) to

generate recombinant NBS1 baculoviruses and into pLPCX (Clontech, Mountain View, CA, USA) to generate retroviral particles, respectively. Point mutations were introduced by using the QuickChange site-directed mutagenesis kit (Stratagene, Cedar Creek, TX, USA).

Single-cell analysis. DSBs in defined nuclear volumes were induced by laser micro-irradiation using an MMI CELLCUT system containing a 355 nm UVA laser (55 Hz; Molecular Machines & Industries, Glattbrugg, Switzerland). Cells were stained with antibodies against human Nbs1 (Novus, Littleton, CO, USA) and γH2AX (Upstate, Temecula, CA, USA). Images were captured by using a Leica SP2 confocal microscope (Leica Microsystems, Wetzlar, Germany) with a 40× (oil immersion, NA 1.25) objective.

Biochemical analysis. GST pulldown assays were performed by mixing 5 μg of GST-fusion proteins with a standard TNT reaction and 5 μg of purified MRN, respectively. For co-immunoprecipitation, human embryonic kidney 293T cells were co-transfected with a Flag-tagged fragment of MDC1 (1–800 amino acids) and Myc-tagged Nbs1 constructs. Anti-Flag(M2)-beads (Sigma-Aldrich, St Louis, MO, USA) were used to immunoprecipitate proteins from total cell extract. All samples were analysed by sodium dodecyl sulphate–polyacrylamide gel electrophoresis and immunoblotting.

G2/M checkpoint analysis. G2/M checkpoint analysis of NBS fibroblasts was performed as described by Spycher *et al* (2008). See the supplementary information online for details.

Supplementary information is available at *EMBO reports* online (http://www.emboreports.org).

ACKNOWLEDGEMENTS

We thank K. Cerosaletti, V. Bohr and S. Jackson for providing valuable reagents. This work was supported by grants from the Swiss National Foundation (Grant number 3100A0-111818), the UBS AG (Im Auftrag eines Kunden) and by the Kanton of Zürich.

CONFLICT OF INTEREST

The authors declare that they have no conflict of interest.

REFERENCES

Becker E, Meyer V, Madaoui H, Guerois R (2006) Detection of a tandem BRCT in Nbs1 and Xrs2 with functional implications in the DNA damage response. *Bioinformatics* **22:** 1289–1292

Cerosaletti KM, Concannon P (2003) Nibrin forkhead-associated domain and breast cancer C-terminal domain are both required for nuclear focus formation and phosphorylation. *J Biol Chem* **278:** 21944–21951

Chapman J, Jackson S (2008) Phospho-dependent interactions between NBS1 and MDC1 mediate chromatin retention of the MRN complex at sites of DNA damage. *EMBO Rep* **9:** 795–801

D'Amours D, Jackson SP (2002) The Mre11 complex: at the crossroads of DNA repair and checkpoint signalling. *Nat Rev Mol Cell Biol* **3:** 317–327

Difilippantonio S, Nussenzweig A (2007) The NBS1-ATM connection revisited. *Cell Cycle* **6:** 2366–2370

Difilippantonio S *et al* (2005) Role of Nbs1 in the activation of the Atm kinase revealed in humanized mouse models. *Nat Cell Biol* **7:** 675–685

Difilippantonio S, Celeste A, Kruhlak MJ, Lee Y, Difilippantonio MJ, Feigenbaum L, Jackson SP, McKinnon PJ, Nussenzweig A (2007) Distinct domains in Nbs1 regulate irradiation-induced checkpoints and apoptosis. *J Exp Med* **204:** 1003–1011

Glover JN, Williams RS, Lee MS (2004) Interactions between BRCT repeats and phosphoproteins: tangled up in two. *Trends Biochem Sci* **29:** 579–585

Lou Z, Chini CCS, Minter-Dykhouse K, Chen J (2003) Mediator of DNA damage checkpoint protein 1 regulates BRCA1 localization and phosphorylation in DNA damage checkpoint control. *J Biol Chem* **278:** 13599–13602

Lou Z *et al* (2006) MDC1 maintains genomic stability by participating in the amplification of ATM-dependent DNA damage signals. *Mol Cell* **21:** 187–200

Lloyd J, Chapman R, Clapperton JA, Haire LF, Hartsuiker E, Li J, Carr AM, Jackson SP, Smerdon SJ (2009) A supramodular FHA/BRCT-repeat architecture mediates Nbs1 adaptor function in response to DNA damage. *Cell* **139:** 100–111

Lukas C, Melander F, Stucki M, Falck J, Bekker-Jensen S, Goldberg M, Lerenthal Y, Jackson SP, Bartek J, Lukas J (2004) Mdc1 couples DNA double-strand break recognition by Nbs1 with its H2AX-dependent chromatin retention. *EMBO J* **23:** 2674–2683

Melander F, Bekker-Jensen S, Falck J, Bartek J, Mailand N, Lukas J (2008) Phosphorylation of SDT repeats in the MDC1 N terminus triggers retention of NBS1 at the DNA damage-modified chromatin. *J Cell Biol* **181:** 213–226

Spycher C, Miller ES, Townsend K, Pavic L, Morrice NA, Janscak P, Stewart GS, Stucki M (2008) Constitutive phosphorylation of MDC1 physically links the MRE11–RAD50–NBS1 complex to damaged chromatin. *J Cell Biol* **181:** 227–240

Stewart GS, Wang B, Bignell CR, Taylor AMR, Elledge SJ (2003) MDC1 is a mediator of the mammalian DNA damage checkpoint. *Nature* **421:** 961–966

Stracker TH, Theunissen JW, Morales M, Petrini JH (2004) The Mre11 complex and the metabolism of chromosome breaks: the importance of communicating and holding things together. *DNA Repair (Amst)* **3:** 845–854

Stucki M, Clapperton JA, Mohammad D, Yaffe MB, Smerdon SJ, Jackson SP (2005) MDC1 directly binds phosphorylated histone H2AX to regulate cellular responses to DNA double-strand breaks. *Cell* **123:** 1213–1226

van der Burgt I, Chrzanowska KH, Smeets D, Weemaes C (1996) Nijmegen breakage syndrome. *J Med Genet* **33:** 153–156

Williams RS *et al* (2009) Nbs1 flexibly tethers Ctp1 and Mre11-Rad50 to coordinate DNA double-strand break processing and repair. *Cell* **139:** 87–99

Wu L, Luo K, Lou Z, Chen J (2008) MDC1 regulates intra-S-phase checkpoint by targeting NBS1 to DNA double-strand breaks. *Proc Natl Acad Sci USA* **105:** 11200–11205

Xu C, Wu L, Cui G, Botuyan MV, Chen J, Mer G (2008) Structure of a second BRCT domain identified in the Nijmegen breakage syndrome protein Nbs1 and its function in an MDC1-dependent localization of Nbs1 to DNA damage sites. *J Mol Biol* **381:** 361–372

Yu X, Chen J (2004) DNA damage-induced cell cycle checkpoint control requires CtIP, a phosphorylation-dependent binding partner of BRCA1 C-terminal domains. *Mol Cell Biol* **24:** 9478–9486

SUPPLEMENTARY MATERIALS

A divalent FHA/BRCT-binding mechanism couples the MRE11/RAD50/NBS1 complex to damaged chromatin

METHODS

Cell extraction and protein purification

Hela nuclear extract was purchased from Cilbiotech (Mons, Belgium). MDC1-GST-SDT fragment was affinity purified on Glutathione-Sepharose (GE Healthcare Biosciences). Recombinant MRN purification from Sf9 cells was described (Spycher et al, 2008). For in vitro-translation of full-length NBS1, the TNT system (Promega) was used.

Microirradiation and single-cell analysis

In order to generate DSBs in defined nuclear volumes laser microirradiation was performed with a MMI CELLCUT system containing a 355 nm UVA laser (55 Hz, Molecular Machines & Industries, Switzerland) coupled to an Olympus IX71 microscope station and focused through an LUCPLFLN 40X objective. The MMICELLTOOLS software with MMIUVCUT plug-in assisted the laser operation using an energy output of 50%. Prior to laser irradiation, cells were grown on coverslips in cell culture dishes in the presence of 10 μM BrdU (Bromodeoxyuridine; Sigma) for 24 h. Coverslips were transferred into LabTek chamber slides (Nunc) and mounted on the microscope stage for irradiation. After irradiation, cells were placed back in the incubator for 30-60 min before fixation.

Biochemical analysis

For GST pull down assays, purified GST-fusion proteins (5 μg) were mixed with 1/5 volume of a standard TNT reaction and 5 μg of purified MRN, respectively. Where indicated, GST fusion proteins were pre-treated with 100 U of CK2 (New England BioLabs). The mixture was incubated at 4°C for 30 min to allow binding. Glutathione sepharose beads were added and the suspension was incubated for further 60 min. The

beads were washed with buffer (50mM Tris pH 7.5, 120 mM NaCl, 1 mM DTT, 0.2% NP-40) and resuspended in SDS loading buffer.
For co-immunoprecipitation, HEK 293T cells were co-transfected with a Flag-tagged fragment of MDC1 (1-800 aa) and Myc-tagged Nbs1 constructs. Cells were lysed in lysis buffer (25 mM Tris pH 7.5, 40 mM NaCl, 2 mM $MgCl_2$, 0.5 % NP-40, protease and phosphatase inhibitors, 25 U/ml benzonase (Novagen)) and incubated for 30 min at 4 °C. The concentration of NaCl was increased to 450 mM and incubated for another 30 min at 4 °C. After centrifugation, extracts were diluted to 100 mM NaCl, added to pre-blocked anti-flag(M2)-beads (Sigma) and incubated for 3 h at 4 °C. The beads were washed with IP-buffer (25 mM Tris pH 7.5, 100 mM NaCl, 10 % glycerol, 2 mM EDTA, 1 mM DTT, 0.5 % NP-40, protease and phosphatase inhibitors) and resuspended in SDS loading buffer. All samples were analyzed by SDS PAGE and immunoblotting.

Checkpoint analysis

Cells were irradiated with a Faxitron X-ray cabinet at the indicated doses during the exponential growth phase. 1h later, cells were harvested, fixed with 70% ethanol/PBS and incubated over night at -20°C. After permeabilization with 0.25% Triton/PBS, cells were stained with anti-phospho-histone H3 (Upstate), followed by secondary anti-FITC (Jackson) or Alexa 700 (Invitrogen) antibodies and propidium iodide. Data were acquired with a Becton Dickinson flow cytometer (NSB fibroblasts) or a Beckham Coulter CyAn ADP 9 Color flow cytometer (U2OS YFP-BRCT cell line).

Supplementary Figure S1

(A) NBS1 expression profile of NBS-iLB1 fibroblasts stably transduced with wild type NBS1, R28A NBS1 and K160M NBS1.

(B) Two independent clones of NBS-iLB1 fibroblasts stably transduced with wild K160M mutant NBS1 were left untreated or irradiated with 1 Gy and 10 Gy. Cells were harvested 1 hour after irradiation, fixed with methanol and stained with an antibody against phosphorylated H3 (P-H3) and propidium iodine. The percentage of P-H3 positive cells was determined by FACS analysis. NBS-iLB1 parental cells and NBS1-iLB1 cells stably transduced with wild type NBS1 served as negative and positive controls, respectively. Error bars represent standard deviation.

A

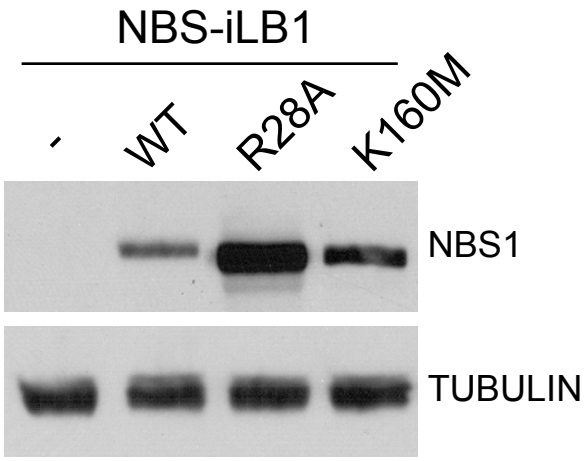
NBS-iLB1
-
WT
R28A
K160M
NBS1
TUBULIN

B

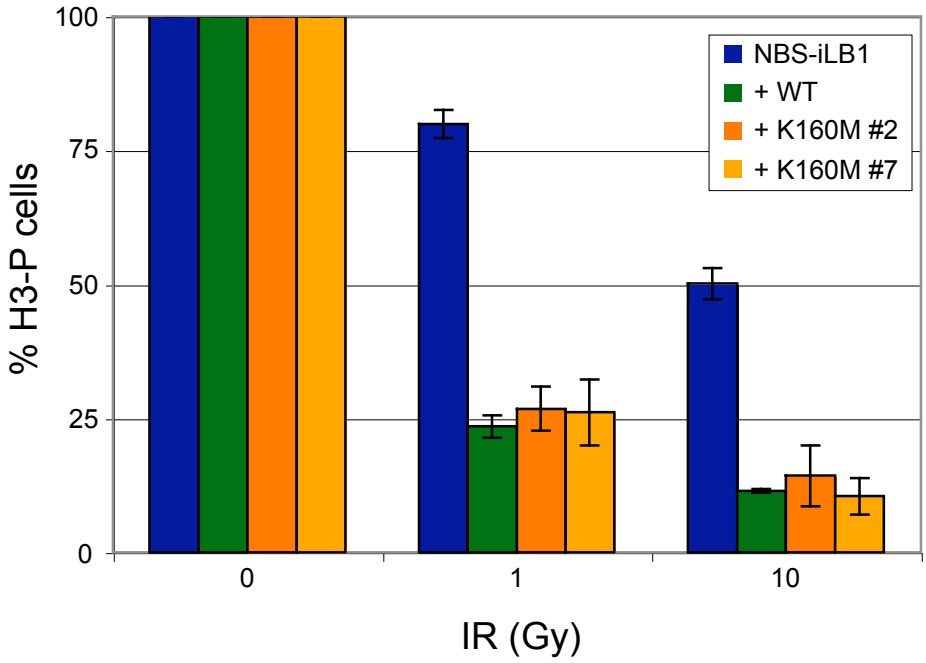
100
75
50
25
0
% H3-P cells
0
1
10
IR (Gy)
NBS-iLB1
+ WT
+ K160M #2
+ K160M #7

5.3 Unpublished data on DNA damage-induced MDC1 dimerization

5.3.1 Extended analysis of MDC1 pT4 phosphorylation and DNA damage-induced dimerization

We previously identified an N-terminal MDC1 fragment (amino acids 1-124) to be phosphorylated *in vitro* by the ATM kinase, and the highly conserved Thr4 as the residue to be modified (Figure 1A and 1B in Jungmichel et al, 2010). Upon this finding, an antibody was generated against a short N-terminal MDC1 phospho-peptide (pThr4). The specificity of this antibody was confirmed *in vitro* using the original peptide in a dot blot assay, where the antibody detected only the phosphorylated but not the unphosphorylated peptide (Figure 5.1A). Moreover, the antibody recognized a recombinant MDC1 protein fragment upon phosphorylation by immunopurified ATM and showed only little cross-reaction with the non-phosphorylated fragment or a fragment containing a T4A mutation (Figure 1B in Jungmichel et al, 2010). We further described *in vivo* phosphorylation of endogenous MDC1 at Thr4 in U2OS cells in a time- and dose-dependent manner in response to IR and in dependency of active ATM since a specific ATM inhibitor strongly reduced the T4-phosphorylation signal of MDC1 (Figure 1C and 1E in Jungmichel et al, 2010 and Figure 5.1B). For further proof of ATM to be acting as the major kinase for MDC1 Thr4 phosphorylation, we set out to analyze cells derived from AT patients that are defective in expressing functionally active ATM. In comparison to U2OS cells treated with 10 Gy of IR, we could not detect a positive signal for phospho-Thr4 in irradiated human AT fibroblasts (Figure 5.1C), indicating that ATM is the responsible kinase for MDC1 Thr4-phosphorylation in response to IR. In addition to IR-induced DNA damage, Thr4 phosphorylation in U2OS cells also occured in response to treatment with 100 J/m^2 of UV radiation, that is known to produce SSBs that might be converted into DSBs during replication (Figure 5.1D).

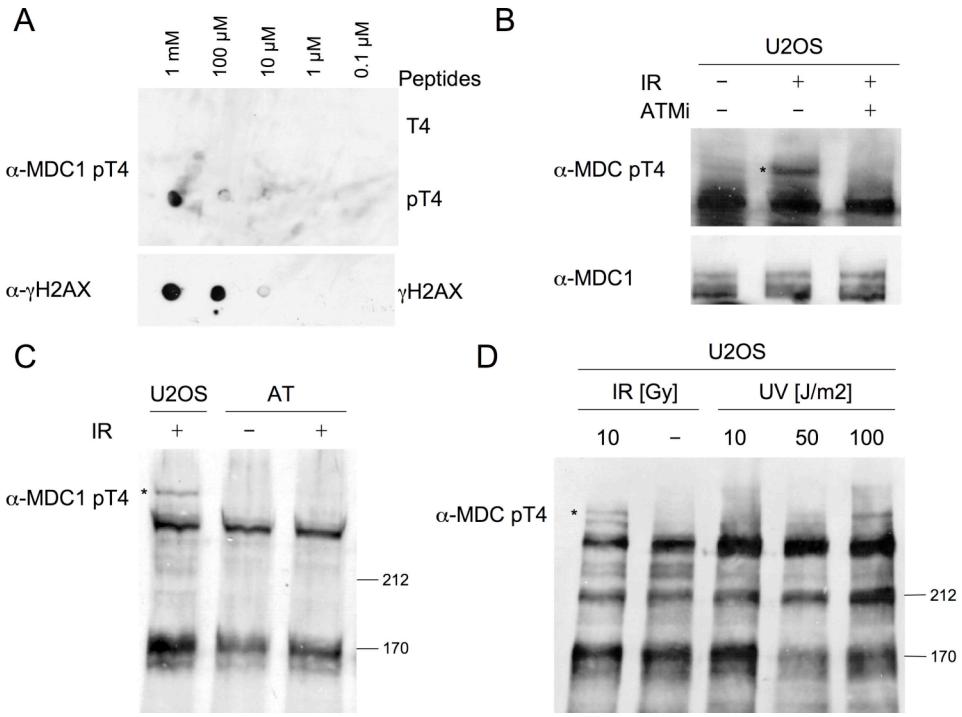

Figure 5.1 MDC1 phosphorylation at Thr4 is dependent on ATM. (A) Unphosphorylated (T4) or phosphorylated (pT4) peptides were dotted in different concentrations on a Nitrocellulose membrane and incubated with α-MDC1 pT4 antibody. γH2AX peptide incubated with α-γH2AX antibody was used as a positive control. (B) U2OS cells were incubated with 10µM ATM inhibitor for 30min and then treated with 10Gy of IR. Cell extracts were prepared 30min after IR and analyzed with α-MDC1 pT4 and α-MDC1 (889) antibodies. (C, D) U2OS cells or human AT fibroblasts were treated with 10Gy of IR or UV radiation and cell extracts were analyzed with α-MDC1 pT4 antibody. (* indicates pT4-phosphorylated MDC1)

Previously, an oriented phosphopeptide library screen identified the optimal sequence for binding to certain classes of FHA domains (Durocher et al, 2000). Interestingly, phosphopeptide sequences with high similarity to the phosphorylated N-terminus of MDC1 (M-E-D-pT-Q-A-I) selectively bound to the FHA domain of MDC1. These data showed a strong preference for isoleucine at the +3 position following the phosphorylated threonine. Based on this information, we performed a series of interaction studies that would support the emerging idea of an interaction between the Thr4-phosphorylated MDC1 N-terminus with the MDC1 FHA domain. Indeed, peptide pulldowns revealed an interaction of the T4-phosphopeptide but not its unphosphorylated form with the purified recombinant MDC1 FHA domain as well as with endogenous MDC1. In addition, several known interactions partners of MDC1 were retrieved from HeLa nuclear extract, namely NBS1, MRE11 and RAD50, (Figure 2B in Jungmichel et al, 2010). In order to demonstrate a DNA damage-

dependent interaction between two different MDC1 molecules *in vivo*, we transiently expressed differently tagged MDC1 fragments (amino acids 1-800) in 293T cells that had either been treated with IR or left untreated and subsequently performed co-immunoprecipitation experiments. C-terminally truncated fragments of MDC1 lacking the BRCT domain were used since it has generally been difficult to strip full-length MDC1 from chromatin. As expected, wild-type sequences of Myc-tagged and FLAG-tagged MDC1 were immunoprecipitated in irradiated cell extracts with the aid of an anti-FLAG affinity gel, whereas a Myc-tagged mutant fragment (T4A) showed almost no interaction (Figure 5A in Jungmichel et al, 2010). In another experiment, the immunoprecipitated samples were blotted with the MDC1 pT4 antibody to test its reactivity against ectopically expressed wild-type or T4A mutant MDC1 protein in a DNA damage-dependent manner, this time using CPT as DSB-causing agent (Figure 5.2A). The antibody specifically detected the enriched wild-type MDC1 fragments in the immunoprecipitate, but not the T4A mutant proteins. Thr4 phosphorylation seemed to occur in cells that had not been exposed to DNA damage. We suspect that the phosphorylation may arise as a consequence of the calcium phosphate transfection procedure, which has been described to elicit a stress response possibly leading to activation of DNA damage signaling (Rodriguez and Flemington, 1999; Nickoloff, 1998). We therefore analyzed U2OS cells that stably express the wild-type FHA domain or a T4A mutant (amino acids 1-154) upon induction with Doxocycline so that potential activation of the DNA damage response during calcium phosphate transfection can be avoided (Figure 5.2B). Thus, it appeared that the antibody recognized the pT4 of the wild-type FHA domain in a damage-dependent manner, although the antibody showed some unspecific reactivity against unphosphorylated FHA domains (as already observed in Figure 1B in Jungmichel et al, 2010), which could be circumvented by lower exposures of the blot. The phosphorylation of MDC1 in response to transfection strain might also account for the observed interaction between differently tagged MDC1 fragments in non-irradiated cell extracts (Figure 5A in Jungmichel et al, 2010 and Figure 5.2A). Former attempts to immunoprecipitate MDC1 fragments with a FLAG antibody subsequently coupled to G-sepharose beads, mostly failed to retrieve sufficient protein from the extract to be detected in Western blot. However, in some cases, the amount of protein loaded was adequate to detect a clear increase in interaction between Myc- and FLAG-tagged MDC1 in irradiated as compared to non-irradiated cell extracts (Figure 5.2C). In conclusion, the above

experiments strongly support the interpretation that phosphorylation of MDC1 at Thr4 occurs *in vivo* in response to exogenous DNA damage and that this leads to a multimerisation of the protein.

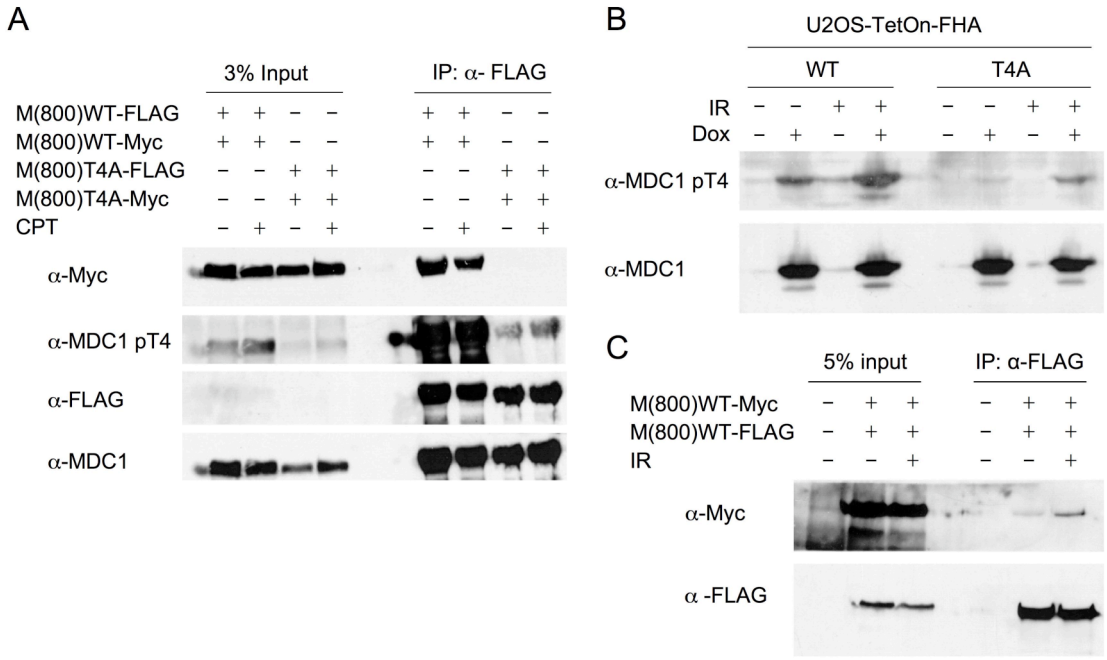

Figure 5.2 DNA damage-dependent Thr4 phosphorylation and dimerization of MDC1 (A) 293T cells were transfected with plasmids expressing wild-type or T4A mutant MDC1 (amino acids 1-800) carrying a C-terminal FLAG or Myc tag. After 48h, cells were treated with 10 µM Camptothecin for 1h, washed and replaced with fresh medium for further incubation of 2.5h. Protein complexes were immunoprecipitated with monoclonal α-FLAG agarose and immunoblotted with α-Myc, α-MDC1 pT4, α-FLAG and α-MDC1 (889) antibodies. (B) U2OS TetOn-FHA cells (wild-type and T4A mutant) were induced with 1µg/ml Doxocyclin for 12h and treated with 10Gy of IR. Cell extracts were analyzed with α-MDC1 pT4 and α-MDC1 (3835) antibodies. (C) 293T cells were transfected with plasmids expressing wild-type MDC1 (amino acids 1-800) carrying a C-terminal FLAG or Myc tag. After 48h, cells were treated with 10Gy of IR. After 30 min protein complexes were immunoprecipitated with monoclonal α-FLAG antibody and immunoblotted with α-Myc and α-FLAG antibodies.

5.3.2 Functional characterization of the MDC1 FHA domain in an overexpression system

In order to understand the role of the MDC1 FHA domain in the context of the proposed MDC1 dimerization mechanism during the DNA damage response we sought to analyze the effects of overexpression of an N-terminal MDC1 fragment containing the FHA domain in human cells. We applied a system that allows tight control of mammalian gene expression via tetracycline-responsive promoters and offers the additional advantage of using isogenic cell lines in assays evaluating responses to DNA damage: U2OS cells stably expressing the tetracycline repressor were transfected with plasmids encoding a fusion protein of EYFP and the wild-type or mutant MDC1 FHA domain (amino acids 1-154) and selected with G418 for stable integrants. Clones of comparable expression were isolated after induction with the tetracycline-analogue Doxocycline. As depicted in Figure 5.3A, the increase of protein levels for the wild-type FHA domain and the T4A mutant reached a maximum 8 h after induction with 1 µg/ml Doxocycline and was maintained for at least 24 h.

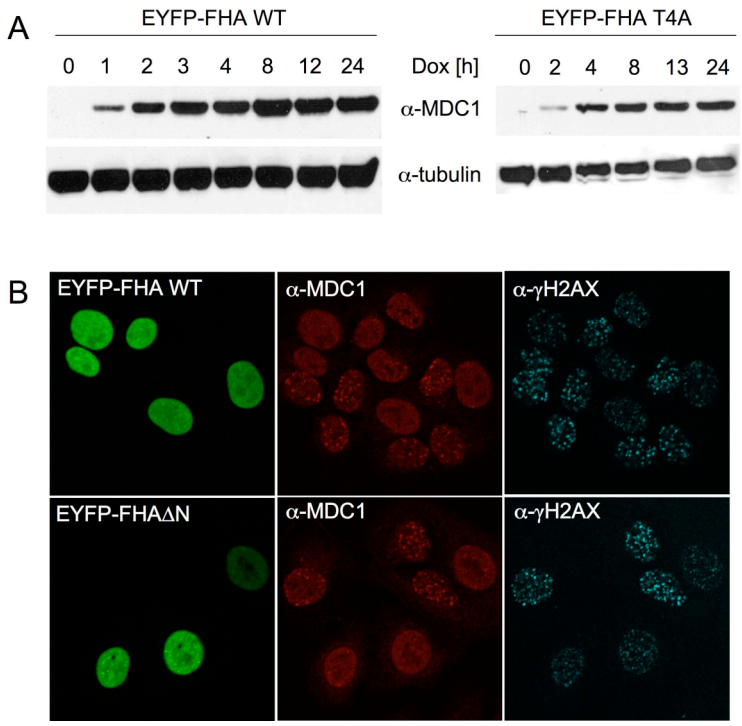

Figure 5.3 Overexpression of the FHA domain abrogates MDC1 foci formation. (A) U2OS TetOn cells stably expressing a tetracycline-inducible EYFP-FHA(WT or T4A) fusion protein were induced with 1µg/ml Doxocyclin for the indicated times. Protein expression was analyzed with α-MDC1 (3835) and α-tubulin antibodies. (B) U2OS TetOn EYFP-FHA(WT) or -FHAΔN cells were induced with 1µg/ml Doxocyclin for 12h, subjected to 10Gy of IR, 1h later fixed in PFA and immunostained for MDC1 (3838) and γH2AX.

Previous studies demonstrated that overexpression of the FHA domain exerts a dominant-negative effect on MDC1 and MRN foci formation, similar to what has been observed for the overexpressed BRCT domain (Goldberg et al, 2003; Stucki et al, 2005). Hence, in some of the following experiments BRCT overexpressing U2OS cells were used as a control. We could confirm that the induced overexpression of the wild-type FHA domain impaired endogenous MDC1 foci formation, but not γH2AX foci (Figure 5.3B). Overexpression of the FHA domain lacking the Thr4-containing N-terminus had a similar effect on MDC1 and γH2AX foci as the wild-type.

To further substantiate the dominant negative effect of the FHA domain on MDC1 chromatin retention we examined release of endogenous MDC1 from chromatin in a biochemical fractionation assay. In non-irradiated cells MDC1 was mainly found in the nuclear chromatin pellet and only salt concentrations of higher than 210 mM NaCl led to a substantial release of MDC1 into the nuclear soluble fraction (Figure 5.4A). However, a small fraction of MDC1 was already released at 125 mM NaCl, which was not observed upon treatment with 3 Gy of IR, indicating that induction of DNA damage causes a stronger retention of MDC1 at chromatin. As expected, overexpression of the FHA domain promoted release of endogenous MDC1 from chromatin already at 125 mM after irradiation, an effect that could similarly be observed for the overexpressed BRCT domain (Figure 5.4A). Concomitantly, the nuclear chromatin pellet showed a slightly decreased MDC1 protein level in case of the FHA domain, though this effect seems to be even enhanced for the BRCT domain. These data corroborate the dominant negative effect of the MDC1 FHA domain overexpression on chromatin retention of MDC1 and presumably other DDR factors.

With regards to the above-mentioned cellular effects of the overexpressed FHA domain, we wondered whether an excess of the purified recombinant FHA domain would also displace HNE-derived MDC1 from binding to a γH2AX-peptide *in vitro* and whether the T4A mutation would reverse this effect (Figure 5.4B). It has been shown before that an excess of the MDC1 BRCT domain competed for binding to the γH2AX-peptide and led to an almost complete release of endogenous MDC1 (Stucki et al, 2005). However, we did not observe a change in binding of MDC1 to the γH2AX-peptide (lane 5 and 7) in the presence of an excess of purified FHA domain. This may be caused by the fact that we used cell extract from undamaged cells, and FHA domain purified from bacteria, thus lacking posttranslational modification.

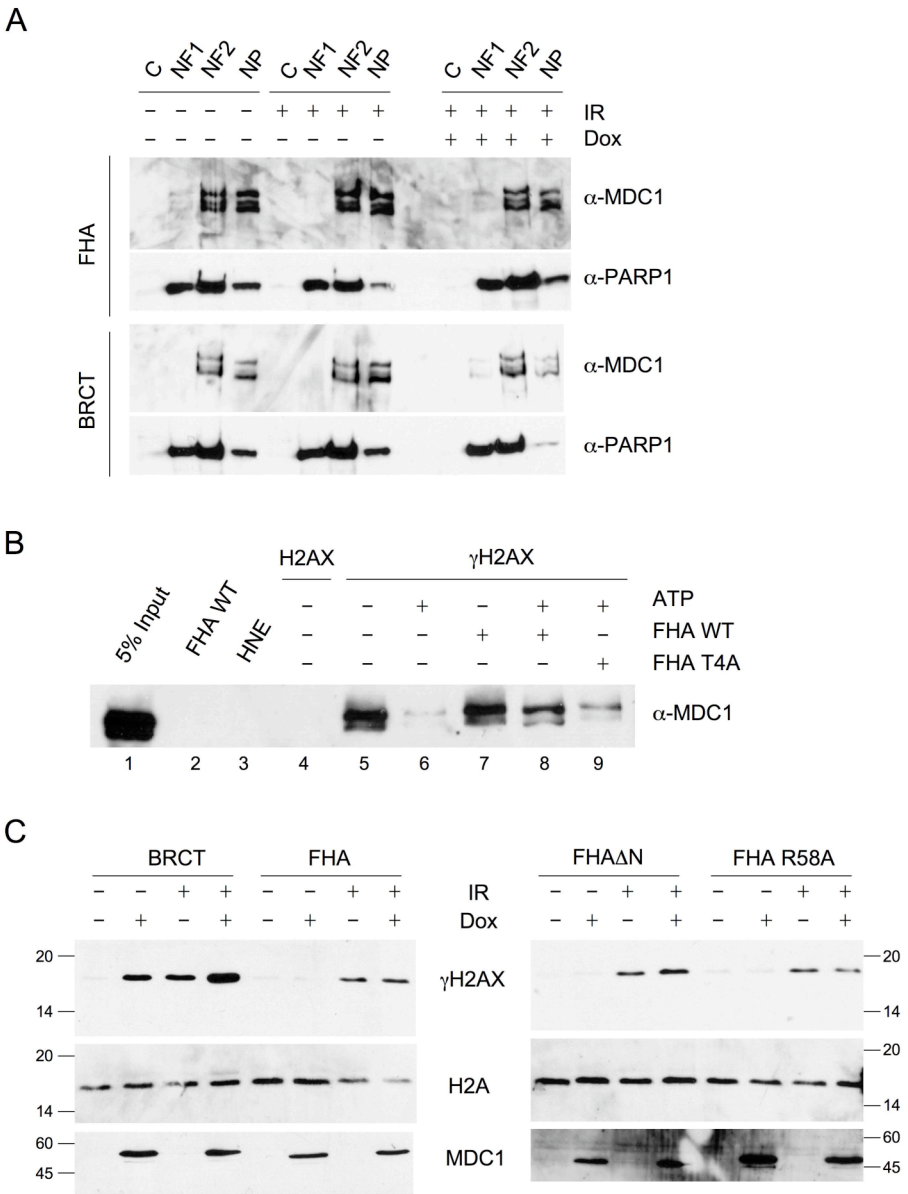

Figure 5.4 Effects of the overexpressed FHA domain on MDC1 chromatin retention and H2AX phosphorylation (A) U2OS TetOn EYFP-FHA(WT) or EYFP-BRCT cells were induced with 1µg/ml Doxocycline for 12h or mock-treated. Cells were irradiated with 3Gy of IR and 1h later subjected to chromatin fractionation (C = cytosol, NF1 = soluble nuclear fraction with 125 mM, NF2 = soluble nuclear fraction with 210 mM NaCl, NP = nuclear pellet). Different fractions were analyzed for presence of endogenous MDC1 with α-MDC1 (889) antibody. Fractionation was controlled with α-PARP1 antibody. (B) γH2AX pulldown. HeLa nuclear extract was supplemented with ATP for *in vitro* kinase activation and purified recombinant FHA domains (WT or T4A) and subjected to a pulldown with H2AX or γH2AX peptides. Protein analysis was performed with α-MDC1 (889) antibody. (C) U2OS TetOn cells expressing EYFP fused to BRCT, FHA WT, FHAΔN or FHA-R58A domains were induced with 1µg/ml Doxocycline for 24h. Cell extracts were prepared 1 h after treatment with 10 Gy of IR and proteins analyzed with α-MDC1 (3835), α-MDC1 (3838), α-γH2AX and α-H2A antibodies.

Therefore, we supplemented HeLa nuclear extract with ATP and specific buffer reagents that are required for activation of ATM *in vitro* (Kozlov et al, 2003). We expected that this would facilitate phosphorylation of pT4 in the MDC1 FHA domain and promote an interaction with full length MDC1. Surprisingly, the presence of ATP alone in the extracts led to almost complete dissociation of MDC1 from the γH2AX-peptide (lane 5 and 6), which rendered the further interpretation of effects of the purified FHA domain impossible.

Consistent with earlier observations (Stucki et al, 2005) overexpression of the BRCT domain led to H2AX phosphorylation even in non-irradiated cells, whereas simple overexpression of the FHA domain or of either of its mutants did not change the γH2AX phosphorylation status (Figure 5.3B and Figure 5.4C). In response to ionizing radiation, γH2AX was hyperphosphorylated upon induction of the BRCT domain as compared to non-induced cells that showed a similar γH2AX level as non-irradiated BRCT overexpressing cells. However, overexpression of the FHA domain did not seem to change γH2AX levels upon treatment with IR. In summary, we conclude that overexpression of the FHA domain does not influence the phosphorylation status of γH2AX.

Previously, Goldberg et al. (2003) reported an RDS phenotype in transiently transfected HeLa cells overexpressing MDC1 FHA-GFP and to a lesser extent for an R58A mutant. The Arg58 has been suggested to be an essential residue in the phosphopeptide-binding site of the MDC1 FHA domain. Unfortunately, we could not reproduce these results using our inducible U2OS-TetOn system, since no difference in the reduction of ^{3}H-Thymidine incorporation could be observed between non-induced or induced cells. This was the case for FHA wild-type, T4A or L120E/L127E mutants upon 15 Gy of IR (Figure 5.5A). We therefore suspected that overexpression of the FHA domain might induce a defect in G2/M checkpoint activation. Unexpectedly, we could also not detect a pronounced G2/M checkpoint defect in FHA-overexpressing cells treated with different doses of IR. As a positive control cells were analysed with siRNA-mediated downregulation of endogenous MDC1, which have been described to be defective in G2/M checkpoint activation (Figure 5.5C and Stewart, 2003). An extended analysis of cells overexpressing either wild-type or R58A mutant FHA domain at different doses of irradiation did not reveal any disturbance of G2/M checkpoint activation (Figure 5.5B). Interestingly, overexpression of the BRCT domain did neither exhibit a G2/M checkpoint defect

(Figure 4C in Hari et al, 2010) nor an intra-S-phase checkpoint defect, whereas a strong defect in random plasmid integration was observed (Stucki et al, 2005), indicating that MDC1 accumulation and retention at sites of DNA damage is not required for the G2/M checkpoint response but might rather be involved in DSB repair.

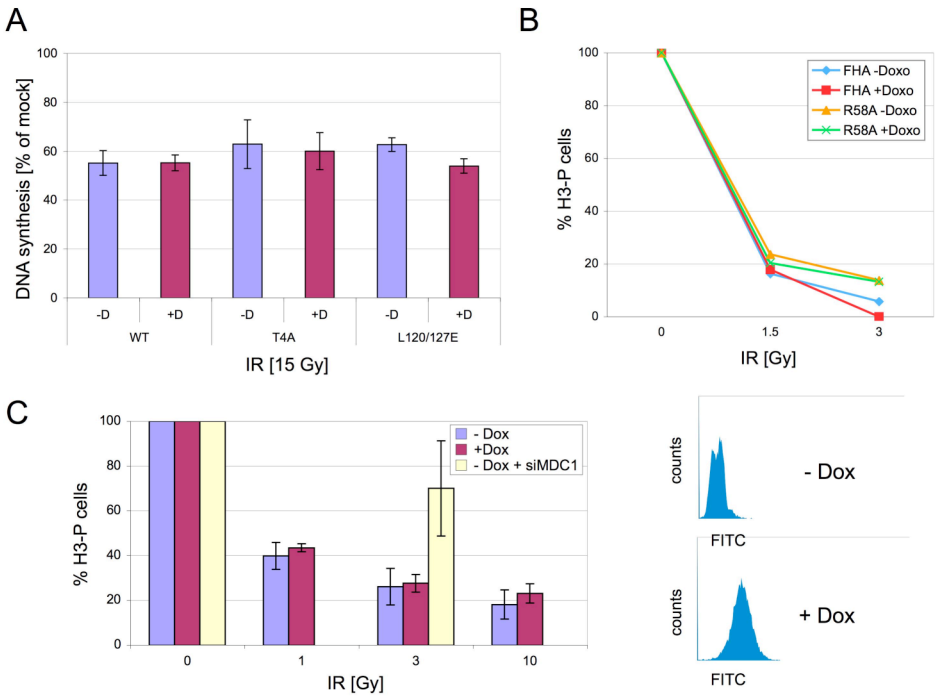

Figure 5.5 Overexpression of the MDC1 FHA domain does not elicit defects in activation of intra-S-phase and G2/M checkpoints. (A) RDS assay. U2OS TetOn EYFP-FHA WT, T4A or L120/127E were induced with 1µg/ml Doxocycline for 12h and subsequently treated with 15Gy of IR. Inhibition DNA synthesis was analyzed by measuring [^{3}H]-thymidine incorporation standardized to [^{14}C]-thymidine incorporation. (B) G2/M checkpoint assay. U2OS TetOn EYFP-FHA WT or R58A were induced with 1µg/ml Doxocycline for 12h. 1h after treatment with the indicated doses of IR, cells were fixed and stained with α-pH3 antibody and propidium iodide and analyzed by flow cytometry. (C) *Left panel:* G2/M checkpoint assay. U2OS TetOn EYFP-FHA WT were induced with 1µg/ml Doxocycline for 24h or treated with siRNA against endogenous MDC1 (siM_R). 1h after treatment with the indicated doses of IR cells were fixed and stained with α-pH3 antibody and propidium iodide and analyzed by flow cytometry. *Right panels:* FACS profiles of cells used for the checkpoint assay induced or not for expression of the EYFP-FHA fusion protein. The EYFP signal was detected in the FITC channel.

5.3.3 Towards the generation of a human MDC1 complementation system

The previous data support the idea that MDC1 dimerizes in response to DNA damage in a mechanism that is mediated through DNA-damage induced pT4 phosphorylation and the binding of pT4 to the FHA domain of MDC1. In order to analyze the functional implications of this dimerization e.g. in the regulation of DNA damage signaling and repair pathways, the establishment of an MDC1 complementation system is required. In a first approach, we stably expressed full-length MDC1 fused to GFP at the N-terminus and carrying an siRNA-resistant cassette at the C-terminus and transiently downregulated endogenous MDC1 with specific siRNAs in U2OS cells. Isolation of single clones, which had been selected with G418 for two weeks, yielded about 50% GFP-MDC1_WT and 20% GFP-MDC1_T4A expressing cells with relatively equal protein expression levels as detected by immunofluorescence (data not shown). Enrichment of GFP-positive cells by FACS sorting did, however, not result in a constant increase of the cell population expressing GFP-MDC1. Rather, expression of recombinant MDC1 seemed to rapidly decrease over time in cells kept in culture, so that early passages had to be used for cellular analysis. Initial screens of different stable clones using siRNA (siM_C) against endogenous MDC1 proved siRNA-resistance of GFP-MDC1, since the GFP signal was not affected by siM_C (Figure 5.6A). As a control, a siRNA (siM_R) targeting a sequence in the MDC1 repeat region, efficiently downregulated both endogenous MDC1 and recombinant GFP-MDC1. Figure 5.6B further illustrates efficient knockdown of MDC1 in U2OS cells through siM_C, as IRIF formation was fully abrogated for MDC1 and strongly suppressed for its downstream effector 53BP1.

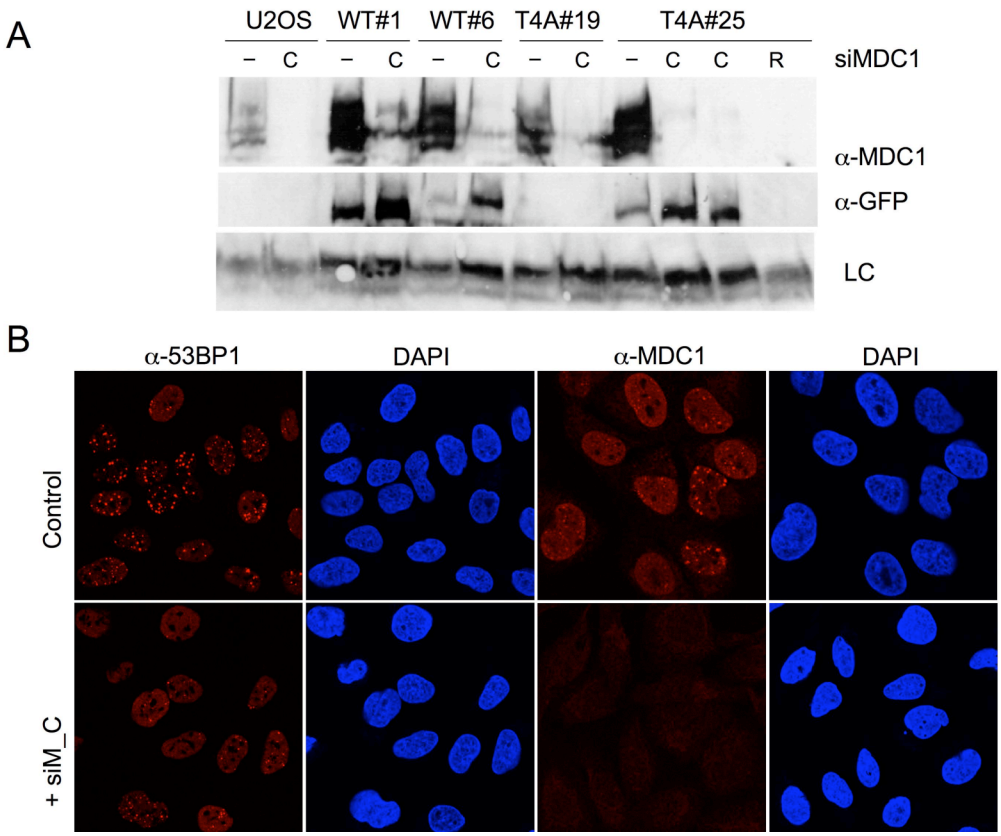

Figure 5.6 Efficient knockdown of MDC1 by siRNAs. (A) Different clones of U2OS cells stably expressing siM_C-resistant GFP-MDC1 WT or T4A were treated with siRNA against the MDC1 C-terminus (C = siM_C) or the repeat region (R = siM_R). Cell extracts were analyzed with α-MDC1 (889) and α-GFP antibodies. (LC = loading control, unspecific bands of GFP antibody) (B) U2OS cells were treated with siRNA against MDC (siM_C). After 72h, cells were subjected to 4Gy of IR, fixed after 4h or 1h and immunostained with α-53BP1 and α-MDC1 (3835) antibodies, respectively.

Immunofluorescence studies confirmed the capability of GFP-MDC1_WT to form nuclear foci upon treatment with IR or laser microirradiation (Figure 5.7 and Figure 5.8). Mutation of Thr4 did not measurably affect foci formation of GFP-MDC1. Since MDC1 is known to be required for efficient accumulation and retention of 53BP1 at DSBs (Stewart et al, 2003), we tested whether GFP-MDC1_WT expressing cells would be proficient for 53BP1 foci formation in the absence of endogenous MDC1. Surprisingly, expression of GFP-MDC1_WT appeared to exert a dominant-negative effect on 53BP1 foci formation in the presence of endogenous MDC1 after 4 Gy of IR (Figure 5.7). Moreover, GFP-MDC1_WT could also not rescue 53BP1 foci formation after siRNA-mediated depletion of endogenous MDC1, even though some 53BP1 foci could still be detected in MDC1-depleted cells without a GFP-signal (Figure 5.7). The same effect was observed for GFP-MDC1-T4A expressing cells. Only cells with a very low expression level did not show abrogated

53BP1 foci, but the barely detectable GFP-signal complicated a reliable analysis of immunofluorescence samples. The dominant-negative effect exerted by GFP-MDC1 on 53BP1 retention and the corresponding sensitivity to small changes in expression levels became even more apparent by means of laser microirradiation (Figure 5.8A). Interestingly, NBS1 localization in laser tracks of GFP-MDC1 expressing cells was not affected (Figure 5.8B).

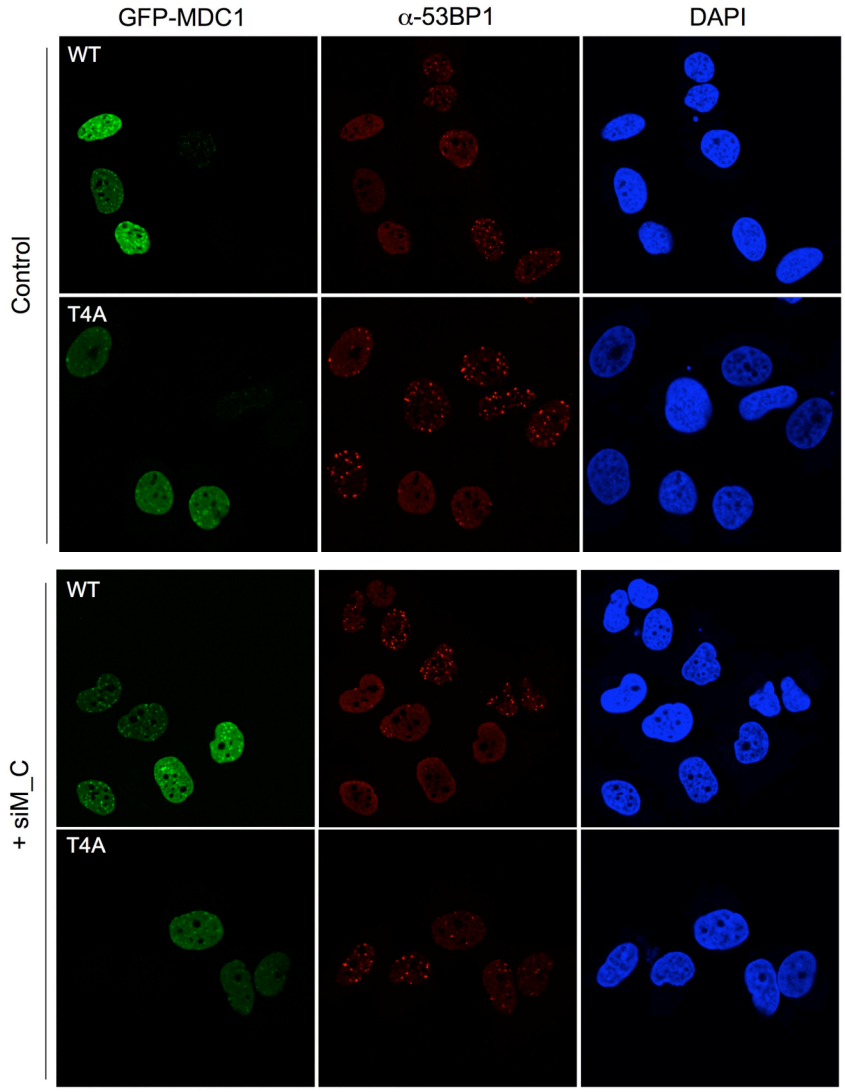

Figure 5.7 Mutation of Thr4 does not affect accumulation of GFP-MDC1 in IRIF but GFP-MDC1 expression, in general, exerts a dominant negative effect on 53BP1 foci formation. U2OS cells stably expressing siM_C-resistant GFP-MDC1 WT or T4A were mock-treated or treated with siRNA (siM_C) against endogenous MDC1. Cells were fixed 4h after 4Gy of IR and immunostained with α-53BP1 antibody.

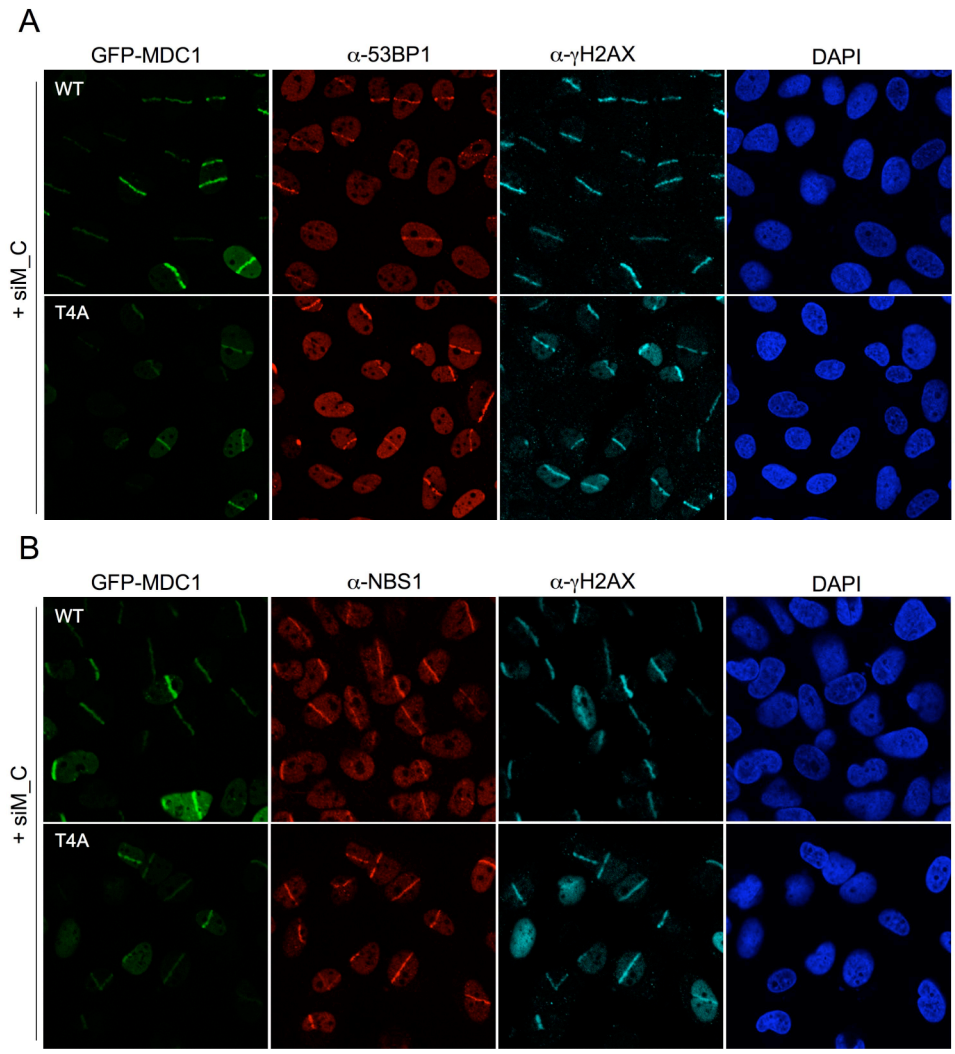

Figure 5.8 Stable expression of GFP-MDC1 causes dominant negative effect on relocalization of 53BP1 to sites of DNA damage but not of NBS1. U2OS cells stably expressing siM_C-resistant GFP-MDC1 WT or T4A were treated with siRNA (siM_C) against endogenous MDC1. Cells were fixed 1h after laser microirradiation and immunostained with (A) α-53BP1 and (B) α-NBS1 antibodies.

Even though this apparent dominant-negative effect of GFP-MDC1 expression constitutes a major drawback for in vivo structure/function analysis, we nevertheless tested whether the GFP-MDC1_WT expressing cells would complement the G2/M checkpoint defect of MDC1-depleted cells (Stewart et al, 2003). Knockdown of the entire MDC1 pool in U2OS control and GFP-MDC1_WT expressing cells through siM_R as well as pre-treatment with an ATM inhibitor caused a rather mild checkpoint defect at 3 Gy detected as an increase in the mitotic index (pH3-positive cells) (Figure 5.9A). The same degree of checkpoint deficiency was reached in GFP-MDC1_WT cells treated with siM_C to deplete endogenous MDC1. Hence, rescue of G2/M checkpoint activation could not be accomplished with our GFP-MDC1_WT

complemented cell lines. The results retrieved from this study led us to the conclusion that a complementation system employing human U2OS cells is not suitable to study the functional implications of MDC1 dimerization.

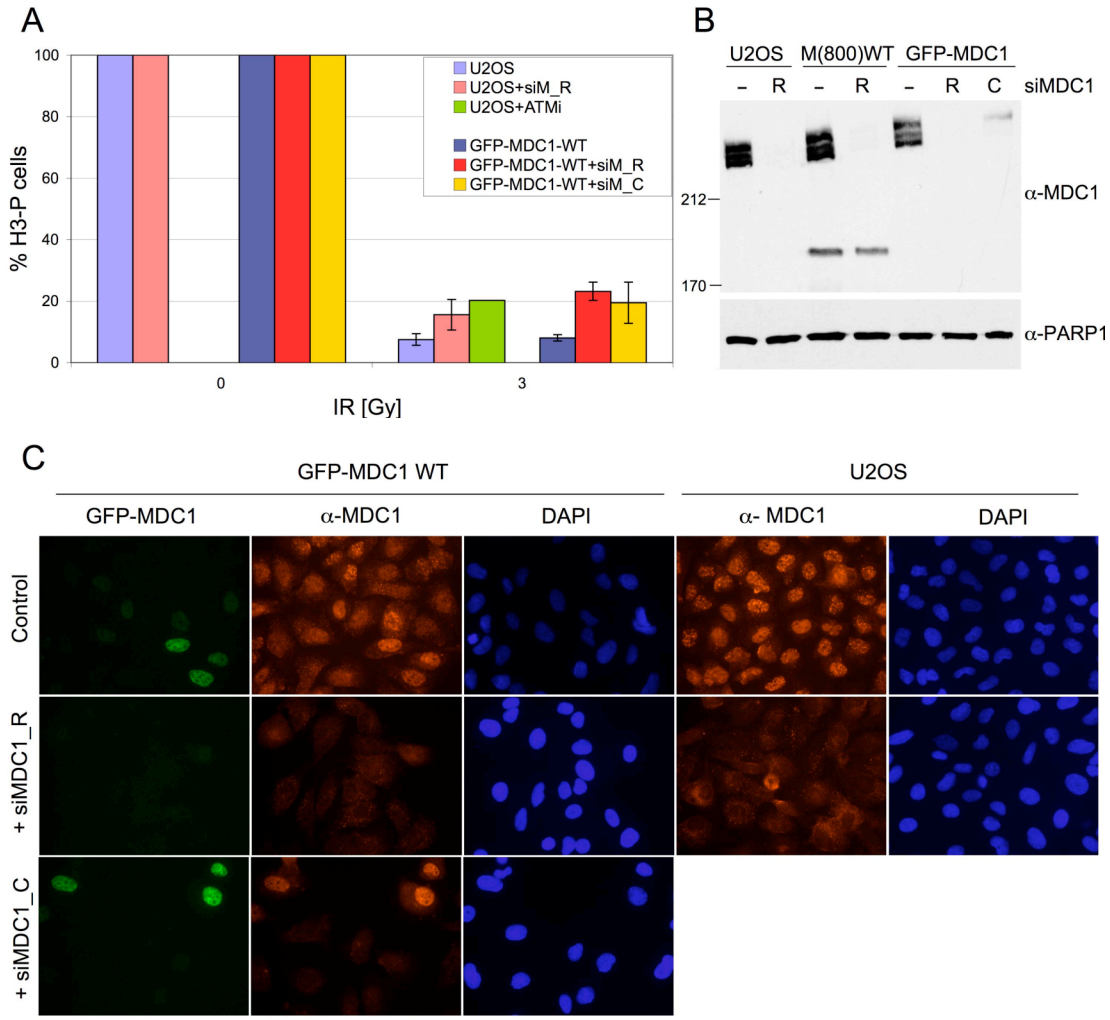

Figure 5.9 Stable expression of GFP-MDC1 did not rescue the defect in G2/M checkpoint activation in the absence of endogenous MDC1. (A) G2/M checkpoint assay. U2OS cells or stable siM_C resistant GFP-MDC1 expressing cells were treated with siRNAs (siM_C or siM_R) 72h prior to IR or with ATM inhibitor 30 min prior to IR, as indicated. Cells were fixed 1h after 3 Gy of IR, stained with α-pH3 antibody and propidium iodide and analyzed by flow cytometry. (B, C) Control of siRNA-mediated downregulation of MDC1 with α-MDC1 (889) antibody for cells used in (A) and cells expressing fragment M(800)WT.

5.3.4 Towards the generation of a mouse MDC1 complementation system

Since the human MDC1 complementation system failed to yield the required data, we aimed in a second approach at complementing transformed MEFs derived from MDC1$^{-/-}$ mice (untransformed MDC1$^{-/-}$ MEFs grow poorly in culture) (Lou et al, 2006). When we received the MDC1$^{-/-}$ cells from the Chen/Scully/Peggo laboratories, we noticed a significant contamination of the cell population with cells apparently expressing normal levels of MDC1. This contamination was apparent in all the cell lines we received. Thus, we first had to isolate single cell clones to assure a clean MDC1$^{-/-}$ population (Figure 5.10A). Testing these cells in an initial G2/M checkpoint assay, we could confirm the previously described defect of MDC1$^{-/-}$ cells in G2/M checkpoint activation, particularly at low doses of irradiation (Figure 5.11)(Lou et al, 2006).

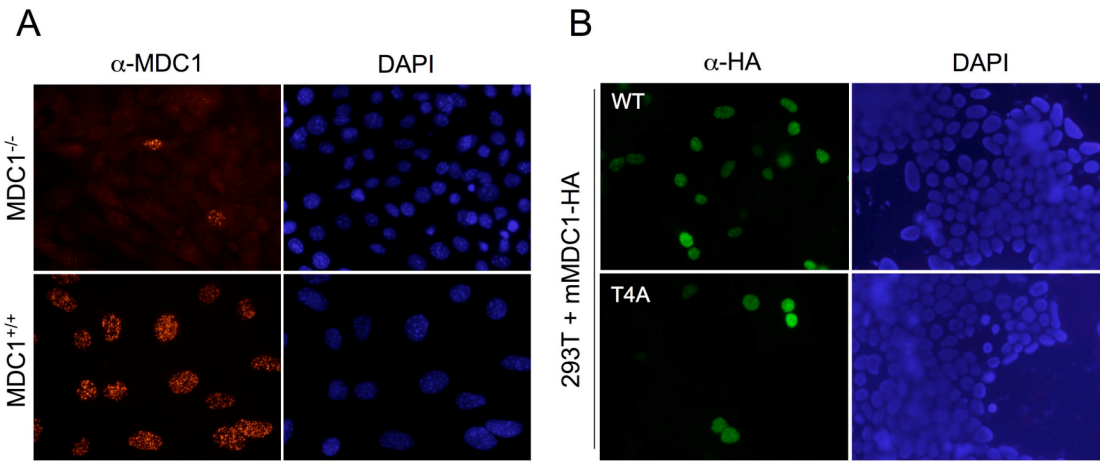

Figure 5.10 Expression of mMDC1-HA in MDC1$^{-/-}$ MEFs. (A) Irradiation of MDC1$^{-/-}$ and MDC1$^{+/+}$ mouse embryonic fibroblasts with 4 Gy of IR and staining with polyclonal rabbit α-mMDC1 antibody reveals contamination of MDC1$^{-/-}$ MEFs with MDC1-expressing cells, which subsequently required isolation of MDC1$^{-/-}$ single cell clones. (B) Transient transfection of 293T cells with wild-type or T4A mutant mMDC1-HA in MSIPuro retroviral expression vectors. Expression was analyzed with α-HA antibody.

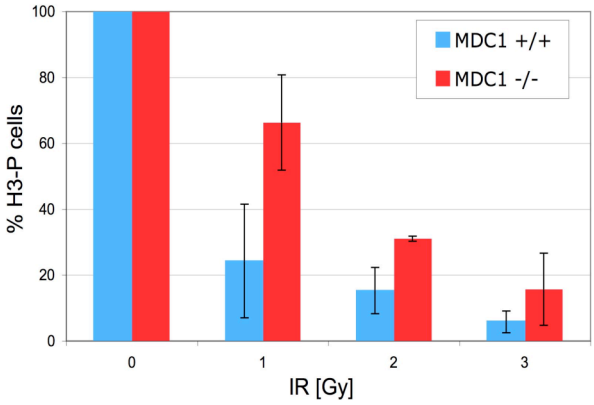

Figure 5.11 Loss of MDC1 causes a defect in G2/M checkpoint activation. Transformed MDC1$^{-/-}$ and MDC1$^{+/+}$ mouse embryonic fibroblasts were irradiated at the indicated doses, fixed and stained with α-phospho Histone H3 antibody to identify cells in mitosis. Cells were analyzed by flow cytometry.

In the course of various attempts to stably express mouse MDC1 (mMDC1) in MDC1$^{-/-}$ cells we encountered several difficulties. MDC1$^{-/-}$ cells showed very low transfection efficiency (~ 1%) when transfected with HA-tagged mMDC1 inserted into the pcDNA3.1 or pLPCX expression vector. Moreover, after selection with puromycin we could not isolate stable clones that positively stained for mMDC1-HA. In order to increase the chance to isolate positive clones, we subcloned mMDC1-HA in pIRESpuro vector containing an internal ribosomal entry site for expression of the puromycin resistance gene on the same mRNA as the transgene. However, again no stable clone expressing full-length mMDC1-HA could be isolated. Therefore, we sought to isolate stable transfectants by retroviral transduction employing pCL-Eco or pCL-Ampho vectors for retroviral packaging. Following co-transfection of 293T cells with mMDC1-HA in pLPCX retroviral expression vectors and transduction of MDC1$^{-/-}$ MEFs, puromycin resistant clones were isolated. However, immuno-fluorescent screenings revealed no expression of mMDC1-HA. The use of an alternative mMDC1-HA retroviral expression vector that additionally contained an internal ribosomal entry site for expression of the puromycin resistance gene on the same mRNA as the transgene (MSIPuro) yielded similar results despite efficient transfection in 293T cells (Figure 5.10B). We suspect that the lack of stable integration of mMDC1 in MDC1$^{-/-}$ MEFs might be attributed to inefficient packaging of the mMDC1 mRNA (5.1 kb) in retrovirus particles and further, to defects of MDC1-deficient cells in random plasmid integration and HR (Lou et al, 2004; Xie et al, 2007).

6 DISCUSSION

The main body of this thesis describes the molecular mechanism of DNA damage-induced MDC1 dimerization. We showed that the N-terminally located and highly conserved Thr4 residue of MDC1 is phosphorylated by ATM *in vitro* and *in vivo* upon induction of DSBs. The phosphorylated Thr4 engages in a highly specific and phosphorylation-dependent interaction with the FHA domain of MDC1. X-ray structure analysis revealed that this interaction occurs in trans, i.e. the pThr4 of one MDC1 molecule interacts with the FHA domain of another MDC1 molecule. Binding of pThr4 to the FHA domain leads to an enhanced interaction between weakly associated MDC1 FHA domains, resulting in the formation of a tight dimer. The pThr4-dependent self-association of MDC1 molecules was confirmed to occur *in vivo*. Finally, *in vivo* dimerization mediates the accumulation of the FHA domain at sites of DNA damage in dependency of the phosphorylated Thr4 residue and the presence of endogenous MDC1.

What could be the possible physiological roles of MDC1 dimerization? Unlike the mediator proteins 53BP1 and Crb2, whose oligomerization seems not to be regulated by post-translational modifications, dimer formation of MDC1 is dependent on DNA damage-induced phosphorylation as has been observed for Rad9p, suggesting a regulatory role of this mechanism in the DNA damage response. Yet in contrast to Rad9p and Crb2, disruption of oligomerization seems not to affect chromatin retention of MDC1 in IRIF (Figure 5.7). However, abolished oligomerization of Rad9p and Crb2 additionally leads to a defect in checkpoint-dependent cell cycle arrest (Kilkenny et al, 2008; Usui et al, 2009). Interestingly, deletion of the MDC1 FHA domain was shown to also cause a defect in G2/M checkpoint activation indicating that MDC1 dimerization might be involved checkpoint activation (Lou et al, 2006). In line of this interpretation, overexpression of the FHA domain has also been reported to elicit an intra-S-phase checkpoint defect upon transient transfection of HeLa cells with FHA expressing plasmids (Goldberg et al, 2003). However, in this work, we could not observe any effect of the overexpressed MDC1 FHA domain on the activation of the intra-S-phase or G2/M checkpoint (Figure 5.5). This may be attributed to the expression level of the stably integrated FHA domain, which may not be sufficient to cause a pronounced

checkpoint defect, or to the EYFP tag being at the N-terminus instead of the C-terminus of the FHA domain expression construct, which may interfere with dimerization. Another indication for a possible involvement of FHA domain-mediated dimerization in checkpoint activation arises from the fact that only a very mild G2/M checkpoint defect at very low doses of irradiation has been reported for H2AX deficient cells in contrast to a more pronounced intra-S-phase and G2/M checkpoint defects of MDC1-depleted cells (Celeste et al, 2002; Fernandez-Capetillo et al, 2002; Goldberg et al, 2003; Lou et al, 2006; Stewart et al, 2003). Even more specifically, the interaction between the MDC1 BRCT domain and γH2AX was not required for intra-S-phase and G2/M checkpoint activation, indicating that another region in MDC1, possibly the FHA domain, could participate in these functions (Stucki et al, 2005). Alternatively, MDC1 dimerization may not be involved in checkpoint activation but rather in its maintenance. This appears to be the case for yeast proteins Rad9p and Crb2 (Kilkenny et al, 2008; Usui et al, 2009).

On the molecular level, MDC1 dimerization might regulate the interaction of the FHA domain with other proteins, from which three different possibilities emerge. First of all, pThr4-mediated dimer formation could preclude the availability of the FHA phospho-binding surface for another protein with a suitable pThr-containing motif. This might be a feasible mechanism for the regulation of the checkpoint kinase CHK2. It was shown that CHK2 dimerizes upon ATM-dependent phosphorylation of Thr68 in a manner similar to MDC1. Dimerization is mediated by intermolecular binding of the FHA domain to phosphorylated Thr68 and is required to bring the kinase domains in close proximity for efficient trans-autophosphorylation. Following complete activation, CHK2 dissociates into active monomers (Ahn et al, 2002; Ahn et al, 2000; Li et al, 2008). Previously, pThr68 of CHK2 was demonstrated to directly bind the FHA domain of MDC1 *in vitro* and an enhanced interaction between these proteins was observed *in vivo* after treatment with IR (Lou et al, 2003). However, activated CHK2 is not retained at DSBs and its localization remains rather diffuse after induction of DNA damage. Still though, CHK2 requires the relocalization to sites of DNA damage in order to become efficiently activated (Lukas et al, 2003). MDC1 might therefore act as an adaptor to initially couple CHK2 to the DSB to facilitate its complete activation via ATM-dependent phosphorylation, but it might also regulate its subsequent release from the chromatin via MDC1 self-association in order to spread the CHK2-dependent DNA damage checkpoint signal throughout the

nucleus. A second possibility for how MDC1 dimerization modulates protein interactions would be that the MDC1 FHA domain provides a phospho-independent interaction surface for another protein, which is occluded upon DNA-damage induced dimerization, thus resulting in the release of the former interaction partner. Such a scenario has been previously described for the FHA domain-containing protein Rv1827 from Mycobacterium tuberculosis (Nott et al, 2009). In a third option, dimerization would create a new phospho-independent interaction surface spanning both FHA domains.

To date, several interaction partners have been suggested for the MDC1 FHA domain. Besides CHK2, the ATM kinase was proposed to directly bind the MDC1 FHA domain, although it remains unclear if this interaction is DNA damage-dependent (Lou et al, 2006). Moreover, the MDC1 FHA domain was recently shown to interact with RAD51 in a phosphorylation- and DNA damage-independent manner (Zhang et al, 2005). Unfortunately, these publications lack the description of the sequences of their FHA constructs used for the interaction studies with CHK2, ATM and RAD51 (Lou et al, 2006; Lou et al, 2003; Zhang et al, 2005). It is thus unclear whether the sequences of the FHA domain comprised the N-terminal Thr4, whose DNA damage-dependent phosphorylation may be important to modulate the interaction with other proteins and substantially influence the regulation of the DDR. However, the proposed interactions with ATM and/or RAD51 support the notion that MDC1 dimerization might be involved in DNA repair processes. In fact, MDC1 mutants lacking the FHA domain were shown to be defective in efficient DSB repair through HR (Xie et al, 2007; Zhang et al, 2005).

The analysis of the biological function of MDC1 dimerization mutants in a MDC1 null background requires the establishment of an efficient complementation system in order to perform bulk cellular assays such as checkpoint activation or maintenance, DSB repair and cell survival assays. Stable integration of siRNA-resistant GFP-tagged recombinant MDC1 into human U2OS cells with the aim to downregulate endogenous MDC1 via siRNA transfection was not successful, as recombinant MDC1 expression appeared to disturb downstream effects of MDC1 signaling (e.g. defective in 53BP1 foci formation). This indicates that the cell might need to carefully balance the protein levels of MDC1 and 53BP1 in order to adequately respond to DNA damage. In support of this notion, overexpression of the MDC1 FHA domain triggers a dominant-negative effect upon 53BP1 accumulation in

dysfunctional telomere-induced foci in normal human fibroblasts (Dimitrova & de Lange, 2006). In a different complementation attempt, we did not succeed to isolate stable clones efficiently expressing the MDC1 gene in transformed MDC1$^{-/-}$ mouse embryonic fibroblasts after transfection or viral transduction. This might be attributed to the low transfection efficiency of transformed MDC1$^{-/-}$ MEFs and the random plasmid integration defect observed in MDC1-depleted cells (Lou et al, 2004).

An elegant approach for the identification of specific interaction partners for the MDC1 FHA domain involving phosphorylation of Thr4 would be SILAC (Stable Isotope Labeling by Amino acids in Cell culture). This is a mass spectrometry-based technique, which analyzes cell populations that have metabolically incorporated the light or heavy nitrogen isotope form of an amino acid (usually Arg and Lys). Subsequent analysis by quantitative MS can distinguish between the different stable isotopes, and comparison of the peak intensities allows the quantification of the relative abundance of the proteins. Thus, this method allows the efficient detection of differences in cell signaling, protein expression or protein-protein interactions. In order to analyze dimerization-dependent protein-protein interactions, cells would be grown in medium supplemented with differentially labeled amino acids and simultaneously be transfected with the wild-type or T4A mutant MDC1-FHA domain fused to a suitable tag for protein purification. After treatment (e.g. IR) cell populations would be combined to equal amounts and the subsequently prepared cell extract subjected to affinity purification or immunoprecipitation. Proteins would then be analyzed by MS. In this way, specific binding partners of non-phosphorylated and Thr4-phosphorylated FHA domains could be identified in non-irradiated and irradiated cell extracts, respectively. Moreover, protein interactions could be analyzed at different time points after induction of DNA damage. Hence, the application of this method has a great potential to unravel specific *in vivo* interaction partners that may be regulated through MDC1 dimerization.

Dimerization/oligomerization seems to be a common theme for mediator proteins participating in the DDR. Homo-dimerization has recently been described for the mediators PALB2, TopBP1 and MCPH1 (Liu et al, 2006; Sy et al, 2009; Yang et al, 2008) and has been extensively studied for the yeast proteins Rad9p in *S. cerevisae* and Crb2 in *S. pombe,* and for the metazoan protein 53BP1 (Kilkenny et al, 2008; Soulier & Lowndes, 1999; Zgheib et al, 2009).

Even though there does not seem to exist a clear MDC1 or 53BP1 orthologue in yeast, similar domain organizations and functions in DNA damage signaling and repair have been reported for oligomerizing mediator proteins. Rad9p, Crb2 and 53BP1 comprise a tandem Tudor domain, which has been suggested to mediate chromatin binding at sites of DSBs, although the mode of chromatin recognition slightly differs between the proteins. Their Tudor domains were shown to bind methylated histones H3 and/or H4, but in case of Rad9p and 53BP1, they have also been implicated in the direct sensing of DNA breaks (Botuyan et al, 2006; Grenon et al, 2007; Huyen et al, 2004; Lancelot et al, 2007; Sanders et al, 2004). Moreover, all four proteins, Rad9p, Crb2, 53BP1 and MDC1, do share a tandem BRCT domain at their C-terminus. This tandem BRCT fold mediates the common function of binding to γH2AX for MDC1, and γH2A for Rad9p and Crb2, respectively, whereas for 53BP, it mediates binding to p53 in a phosphorylation-independent manner. (Derbyshire et al, 2002; Hammet et al, 2007; Javaheri et al, 2006; Joo et al, 2002; Stucki et al, 2005). However, there are clearly differences in the mechanism of dimerization and also how the individual domains, in particular the dimerization motifs, contribute to the physiological function of these proteins.

In the case of Crb2, the tandem BRCT domain is responsible for both phosphopeptide binding and dimerization, which was shown to be essential for a proper checkpoint function (Du et al, 2004). The crystal structure of the BRCT domains of Crb2 revealed that residues in the inter-BRCT linker segment (C663, S666) form the interface for the head-to-tail dimer, whereas the γH2A peptide is bound in a cleft at the junction of the two BRCT domains (R616, K617, K619) (Kilkenny et al, 2008). Interestingly, mutations that disrupt dimerization of the BRCT domains do not affect phosphopeptide binding and vice versa. Consequently, mutations that distinguish between these two functions lead to different physiological outcomes. Dimerization-defective Crb2 (S666R) is not recruited to IRIF, and cells harboring this mutant are compromised in Chk1 phosphorylation, which causes a defect in cell cycle checkpoint arrest, but it had only little effect on activation of DNA repair. On the other hand, the K619E mutation, which disrupts binding to γH2A, did not affect IR-induced Crb2 foci formation or checkpoint responses, but reduced DNA repair kinetics, subsequently leading to the extension of the DNA damage checkpoint (Kilkenny et al, 2008). However, the precise mechanism of the Crb2 dimer formation,

especially whether or not the interaction occurs constitutively or is regulated by DNA damage remains unclear.

DNA damage-induced dimerization was also shown to be essential for the biological function of Rad9p (Soulier & Lowndes, 1999; Usui et al, 2009). The earlier of these studies demonstrated that purified Rad9p BRCT domains interacted with each other *in vitro*. The authors further showed that the Rad9p BRCT domain preferentially interacts with hyperphosphorylated Rad9p from UV-irradiated cell extracts and that BRCT mutations disrupting the homodimerization of Rad9p molecules also affect DNA damage checkpoint activation and cell survival (Soulier & Lowndes, 1999). The more recent study refined the model for the molecular mechanism of Rad9p oligomerization by showing that, instead of the Rad9p BRCT domain itself, the phosphorylated SQ/TQ cluster domain (SCD) of Rad9p forms the binding substrate for the Rad9p BRCT domain with the phosphorylated T427 as the main residue contributing to this interaction (Usui et al, 2009). The SCD-BRCT mediated Rad9p oligomerization appears to be dispensable for initial Rad53 activation and for relocalization of Rad9p to sites of DNA damage. However, Rad9p oligomerization is required for the maintenance of Rad53 activation and checkpoint-dependent cell cycle arrest. Interestingly, Rad53-dependent phosphorylation of the Rad9p BRCT domain seems to attenuate the SCD-BRCT mediated Rad9p oligomerization, thereby providing a feedback loop of Rad53 activation (Usui et al, 2009).

Furthermore, homo-oligomerization of 53BP1 was found to occur in a DNA damage-independent and BRCT-independent manner (Adams et al, 2005; Ward et al, 2006). The Tudor domain, which is essential for accumulation of 53BP1 in IRIF (Huyen et al, 2004), is also not required for 53BP1 oligomerization. However, a region upstream of the Tudor domain was identified to be responsible for 53BP1 oligomerization (Adams et al, 2005). In addition to the Tudor domain, this independently folding oligomerization domain and a C-terminal extension of the Tudor domain were recently shown to be required for efficient 53BP1 focus formation (Zgheib et al, 2009). However, the exact role of oligomerization in 53BP1 foci formation is not yet understood. Interestingly, there seems to exist two independent mechanisms that regulate the relocalization of 53BP1 to IRIF. Initial 53BP1 recruitment rapidly occurs in an H2AX-independent manner but accumulation and maintenance of 53BP1 at sites of DNA damage requires phosphorylation of

H2AX (Celeste et al, 2003). This process is regulated by phosphorylation of MDC1, which binds to γH2AX and in turn recruits the E3 ligase RNF8, thus leading to ubiquitination of histones H2A and H2AX, which facilitates the efficient assembly of 53BP in IRIF (Huen et al, 2007; Kolas et al, 2007; Mailand et al, 2007). It remains to be established to what extent 53BP1 oligomerization is involved in these processes. Importantly, an oligomerization-defective mutant caused residual γH2AX foci 27h after IR, suggesting a role of this mechanism in DSB repair (Ward et al, 2006). In contrast to Rad9p and Crb2, 53BP1 has only limited checkpoint functions. Depletion of 53BP1 causes a modest G2/M checkpoint defect at only low doses of IR and a partial intra-S-phase checkpoint defect in mammalian cells (Wang et al, 2002), which is also true for depletion of MDC1.

While one mediator protein (Rad9p or Crb2) has been implicated in the PIKK-mediated phosphorylation of effector kinases in yeast, the much more complex signaling network in metazoans might explain the need of several mediator proteins such as 53BP1, MDC1 and BRCA1. It had been suggested that 53BP1, MDC1 and BRCA1 may function redundantly. However, the phenotype of 53BP1/MDC1 double knockout mice does not significantly add to the DDR defects observed in the single knockouts, which indicates that both proteins act in same pathway, e.g., MDC1 acting as the upstream regulator of 53BP1 (Minter-Dykhouse et al, 2008). Nevertheless, 53BP1 plays a prominent role during NHEJ, V(D)J recombination and CSR, whereas MDC1 seems to be primarily involved in HR, although it may also participate in NHEJ of dysfunctional telomeres and in CSR by controlling 53BP1 retention at sites of DSBs (Difilippantonio et al, 2008; Dimitrova & de Lange, 2006; Lou et al, 2006; Manis et al, 2004; Ward et al, 2004; Xie et al, 2007).

Additional DDR mediators were recently described to homo-oligomerize and this mechanism was also proven to be important for cellular responses to DNA damage. The scaffold protein PALB2 has been suggested to be responsible for the relocalization the BRCA2•RAD51 complex to DSBs in order to facilitate DNA repair through HR (Xia et al, 2006). Recently, oligomerization of PALB2 was shown to be induced upon treatment with IR (Sy et al, 2009). It was further demonstrated that an N-terminal coiled-coil domain mediates homo-oligomerization and is required for accumulation of PALB2 in nuclear foci. Deletion of this domain impedes the function of PALB2 in HR (Sy et al, 2009). However, the precise mechanism of PALB2

recruitment to DNA lesions remains to be elucidated. In another example, Akt-mediated phosphorylation of TopBP1 (topoisomerase II-binding protein 1) was shown to induce oligomerization through its seventh and eighth BRCT domain. This leads to an increased interaction with the transcriptional regulator E2F1, thereby inhibiting E2F1-mediated apoptosis. Thus, TopBP1 oligomerization likely influences transcriptional regulation under normal physiological conditions. However, whether oligomerization of TopBP1 also plays a role in the DDR remains to be determined (Liu et al, 2006). A similar BRCT-dependent oligomerization mechanism seems to exist for MCPH1, which also induces binding to E2F1 and subsequently influences the transcriptional regulation of genes involved in DNA repair, DNA damage checkpoints and apoptosis (Yang et al, 2008). This raises the idea that oligomerization of DDR mediator proteins in general might regulate the transcription of target genes involved in DNA damage checkpoint, DNA repair and apoptosis.

In conclusion, dimerization/oligomerization as a common theme for DDR mediator proteins strongly implies that DNA-damage induced MDC1 dimerization may similarly contribute to the regulation of some aspect of the DDR in higher eukaryotes. Future analysis of the physiological implication of MDC1 dimerization will shed more light on its specific role in the DDR.

7 MATERIALS AND METHODS

Cell lines and transfections

293T, U2OS, MDC1$^{-/-}$ MEFs, MDC1$^{+/+}$ MEFs and human AT cells were cultured in Dulbecco's modiefied Eagle's Medium (Invitrogen) supplemented with 10% fetal calf serum (Gibco) and penicillin/streptomycin (100 U/ml, Gibco). MDC1$^{-/-}$ cells were retrieved from Junjie Chen and Ralph Scully, the according MDC1$^{+/+}$ from Penny Jeggo. U2OS-TetOn cells stably expressing the EYF-BRCT fusion protein were generated as described (Stucki et al, 2005). Transfection of plasmids was performed either with calcium phosphate, FuGene 6 (Roche) or Lipofectamine 2000 (Invitrogen) according to the manufacturer's protocol. SiRNA duplexes were purchased from Dharmacon. The coding strand for siRNA against the MDC1 C-terminus (siMDC1-C) was 5'-GUCUCCCAGAAGACAGUGAdTdT-3' and for siRNA against the MDC1 repeat region (siMDC1-R) was 5'-ACAGUUGUCCCCACAGCCCdTdT-3'. SiRNA transfections were performed with RNAiMAX (Invitrogen). For this, 4 µl of RNAiMAX and 4 µl of 10 µM siRNA duplexes were separately added to 250 µl OptiMEM (Gibco). Both solutions were mixed by carefully pipetting up and down. After 20 min incubation at room temperature, the transfection mix was added to the cells (50% confluency) on ∅6cm dishes containing 2 ml medium. Cellular analysis was performed 72 h after transfection. For retroviral transduction, 293T cells were transfected with pCL-Ampho vector and the according retroviral vectors expressing mMDC1-HA using the calcium phosphate method. Alternatively, 293T Phoenix-Eco cells stably expressing the genes of the pCL-Eco packaging vector were used directly for transfection of the retroviral expression vectors. Fresh medium was added 24 h after transfection. Another 24 h later, the supernatant containing the virus particles was either transferred directly to MDC1$^{-/-}$ cells in ∅6cm dishes or concentrated with the Lenti-X Concentrator (Clontech, #631231) prior to that. For efficient infection, 6µg/ml Polybrene was added to the medium. After 48-72 h, the transduced cells were splitted to ∅10cm dishes and selected with Puromycin for at least one week. Stable clones were analyzed for expression of the gene of interest by immunofluorescence.

Plasmids

The pcDNA3.1 expression plasmid for wild-type GFP-MDC1 was kindly provided by Ross Chapman. The construct carries a siMDC1-C-resistant sequence containing 6 silent wobble base mutations (5'-GTCTCGCAAAAAACGGTCATC-3'). The T4A mutation was inserted with primers using standard cloning procedures. The retroviral expression construct for MSIPuro-Myc-mMDC1 and the empty vector control were obtained from Ralph Scully. The Myc-mMDC1 sequence was cut out and replaced with either wild-type or T4A mutant mMDC1 carrying a C-terminal HA-tag in a two-step cloning procedure. The pIRESpur2 vector for insertion of mMDC1-HA was kindly provided by Dennis Castor.

Antibodies

The rabbit polyclonal PARP1 antibody was provided by Michael O. Hottiger. The mouse monoclonal β-tubulin antibody was purchased from Sigma, polyclonal rabbit H2A antibody from Upstate, polyclonal rabbit NBS1 antibody from Novus and polyclonal rabbit 53BP1 antibody from Santa Cruz (sc-22760).

Chromatin fractionation

U2OS cells were trypsinized, washed with PBS and resuspended in buffer A (10 mM HEPES, pH 7.9, 10 mM KCl, 1.5 mM $MgCl_2$, 0.34 M sucrose, 10 % glycerol, 1 mM DTT, 1 mM PMSF (Sigma), 1 µg/ml Leupeptin/ Bestatin/ Pepstatin A). Triton X-100 (0.1 %) was added to the solution and incubated for 5 min on ice. Following centrifugation (4 min at 1300g, 4°C), the supernatant containing the cytosolic fraction was collected (S) and the pellet containing the nuclear fraction was washed once in buffer A and then lysed in buffer B (3 mM EDTA, 0.2 mM EGTA, 1 mM DTT, 1 mM PMSF, 1 µg/ml Leupeptin/ Bestatin/ Pepstatin) containing 125 mM NaCl. After centrifugation (4 min at 1700g, 4°C), the supernatant containing the soluble nuclear fraction was collected and the remaining pellet again dissolved in buffer B under more stringent conditions (210 mM NaCl) to remove stronger adhering proteins from the chromatin. Centrifugation was repeated, the supernatant collected and the resulting insoluble chromatin pellet resuspended in Laemmli buffer and sonicated for 15 s. Protein concentration was determined with the Lowry Method and the samples analyzed by SDS-PAGE and Western Blot.

G2/M checkpoint assay

U2OS cells grown in ∅6cm dishes were irradiated with a Faxitron X-ray cabinet at the indicated doses in the exponential growth phase (50% confluency). Following an incubation at 37°C for 30-45 min, cells were carefully washed in PBS, trypsinized, resuspended in growth medium and subsequently transferred from the cell culture dish into 5 ml tubes suitable for flow cytometry analysis. Cells were centrifuged (1500g at 4°C for 5 min), washed once in 5 ml PBS, resuspended in 600 µl PBS and fixed by dropwise adding 1.4 ml of 100% icecold ethanol (to achieve a final concentration of 70% ethanol) while vortexing gently. After incubation at – 20°C for at least 1 h or overnight, the ethanol-fixed cells were again centrifuged (1500g at 4°C for 5 min), washed twice with PBS and permeabilized with 1 ml of 0.25% Triton X-100/PBS for 10 min on ice. After centrifugation at 1800g for 5 min, the supernatant was aspirated and 100 µl of rabbit anti-pH3 antibody (Millipore) in 1% BSA/PBS added to a final concentration of 7.5 µg/ml and incubated with the cells at room temperature for 3 h. Thereafter, cells were washed with 4 ml 1% BSA/PBS (2500g for 5 min) and stained with 50 µl of either anti-FITC (Jackson ImmunoResearch) 1:30 or Alexa700 (Invitrogen) 1:30 in 1% BSA/PBS at room temperature for 30 min. Following two additional wash steps with PBS, cells were finally resuspended in 500 µl PBS containing 0.25 µg/ml of Propidium Iodide (Sigma) and 0.1 mg/ml RNase A (Roche). Analysis was performed with a flow cytometer (Becton Dickinson FC500 or Beckham Coulter CyAn ADP 9 Color).

RDS assay

U2OS cells grown on 6-well plates were pre-labeled with 20 nCi/ml [14C]-thymidine (Amersham, CFA219) for 24 h, which was then replaced with fresh medium. After another 24 h, cells were irradiated and incubated for 45 min, before 2.5 µCi/ml [3H]-thymidine (Amersham, TRK120) was added for 15 min. Subsequently, cells were washed in PBS, trypsinized and resuspended in warm growth medium. Following two additional washes in 5 ml of cold 1% FCS/PBS, cells were resuspended in 280 µl PBS and fixed by adding 720 µl icecold methanol dropwise while vortexing gently. For proper fixation, cells were kept at least 30 min at 4°C. The cell suspension was then filtered through GF/C filters (WhatmanA, 25 mm circles), washed twice with 70% methanol and once with 95% methanol. Dried filters were put in scintillation tubes

and 2.5 ml Emulsifier-Safe (PerkinElmer) was added. Inhibition of DNA synthesis was measured with a MicroBeta TriLux 1450 liquid scintillation counter.

Additional information on Materials and Methods is provided in Jungmichel et al, 2010.

8 REFERENCES

Adams MM, Wang B, Xia Z, Morales JC, Lu X, Donehower LA, Bochar DA, Elledge SJ, Carpenter PB (2005) 53BP1 oligomerization is independent of its methylation by PRMT1. *Cell Cycle* **4**(12)**:** 1854-1861

Ahn JY, Li X, Davis HL, Canman CE (2002) Phosphorylation of threonine 68 promotes oligomerization and autophosphorylation of the Chk2 protein kinase via the forkhead-associated domain. *J Biol Chem* **277**(22)**:** 19389-19395

Ahn JY, Schwarz JK, Piwnica-Worms H, Canman CE (2000) Threonine 68 phosphorylation by ataxia telangiectasia mutated is required for efficient activation of Chk2 in response to ionizing radiation. *Cancer Res* **60**(21)**:** 5934-5936

Ahnesorg P, Smith P, Jackson SP (2006) XLF interacts with the XRCC4-DNA ligase IV complex to promote DNA nonhomologous end-joining. *Cell* **124**(2)**:** 301-313

Bakkenist CJ, Kastan MB (2003) DNA damage activates ATM through intermolecular autophosphorylation and dimer dissociation. *Nature* **421**(6922)**:** 499-506

Bartek J, Falck J, Lukas J (2001) CHK2 kinase--a busy messenger. *Nat Rev Mol Cell Biol* **2**(12)**:** 877-886

Bartkova J, Horejsi Z, Koed K, Kramer A, Tort F, Zieger K, Guldberg P, Sehested M, Nesland JM, Lukas C, Orntoft T, Lukas J, Bartek J (2005) DNA damage response as a candidate anti-cancer barrier in early human tumorigenesis. *Nature* **434**(7035)**:** 864-870

Bartkova J, Rezaei N, Liontos M, Karakaidos P, Kletsas D, Issaeva N, Vassiliou LV, Kolettas E, Niforou K, Zoumpourlis VC, Takaoka M, Nakagawa H, Tort F, Fugger K, Johansson F, Sehested M, Andersen CL, Dyrskjot L, Orntoft T, Lukas J, Kittas C, Helleday T, Halazonetis TD, Bartek J, Gorgoulis VG (2006) Oncogene-induced senescence is part of the tumorigenesis barrier imposed by DNA damage checkpoints. *Nature* **444**(7119)**:** 633-637

Beckman RA, Loeb LA (2006) Efficiency of carcinogenesis with and without a mutator mutation. *Proc Natl Acad Sci U S A* **103**(38)**:** 14140-14145

Bernstein NK, Williams RS, Rakovszky ML, Cui D, Green R, Karimi-Busheri F, Mani RS, Galicia S, Koch CA, Cass CE, Durocher D, Weinfeld M, Glover JN (2005) The molecular architecture of the mammalian DNA repair enzyme, polynucleotide kinase. *Mol Cell* **17**(5)**:** 657-670

Bohr VA (2008) Rising from the RecQ-age: the role of human RecQ helicases in genome maintenance. *Trends Biochem Sci* **33**(12)**:** 609-620

Bork P, Hofmann K, Bucher P, Neuwald AF, Altschul SF, Koonin EV (1997) A superfamily of conserved domains in DNA damage-responsive cell cycle checkpoint proteins. *FASEB J* **11**(1)**:** 68-76

Botuyan MV, Lee J, Ward IM, Kim JE, Thompson JR, Chen J, Mer G (2006) Structural basis for the methylation state-specific recognition of histone H4-K20 by 53BP1 and Crb2 in DNA repair. *Cell* **127**(7)**:** 1361-1373

Byeon IJ, Li H, Song H, Gronenborn AM, Tsai MD (2005) Sequential phosphorylation and multisite interactions characterize specific target recognition by the FHA domain of Ki67. *Nat Struct Mol Biol* **12**(11)**:** 987-993

Cahill DP, Lengauer C, Yu J, Riggins GJ, Willson JK, Markowitz SD, Kinzler KW, Vogelstein B (1998) Mutations of mitotic checkpoint genes in human cancers. *Nature* **392**(6673)**:** 300-303

Cai Z, Chehab NH, Pavletich NP (2009) Structure and activation mechanism of the CHK2 DNA damage checkpoint kinase. *Mol Cell* **35**(6)**:** 818-829

Celeste A, Fernandez-Capetillo O, Kruhlak MJ, Pilch DR, Staudt DW, Lee A, Bonner RF, Bonner WM, Nussenzweig A (2003) Histone H2AX phosphorylation is dispensable for the initial recognition of DNA breaks. *Nat Cell Biol* **5**(7)**:** 675-679

Celeste A, Petersen S, Romanienko PJ, Fernandez-Capetillo O, Chen HT, Sedelnikova OA, Reina-San-Martin B, Coppola V, Meffre E, Difilippantonio MJ, Redon C, Pilch DR, Olaru A, Eckhaus M, Camerini-Otero RD, Tessarollo L, Livak F, Manova K, Bonner WM, Nussenzweig MC, Nussenzweig A (2002) Genomic instability in mice lacking histone H2AX. *Science* **296**(5569)**:** 922-927

Chappell C, Hanakahi LA, Karimi-Busheri F, Weinfeld M, West SC (2002) Involvement of human polynucleotide kinase in double-strand break repair by non-homologous end joining. *EMBO J* **21**(11)**:** 2827-2832

Chen XB, Melchionna R, Denis CM, Gaillard PH, Blasina A, Van de Weyer I, Boddy MN, Russell P, Vialard J, McGowan CH (2001) Human Mus81-associated endonuclease cleaves Holliday junctions in vitro. *Mol Cell* **8**(5)**:** 1117-1127

Clapperton JA, Manke IA, Lowery DM, Ho T, Haire LF, Yaffe MB, Smerdon SJ (2004) Structure and mechanism of BRCA1 BRCT domain recognition of phosphorylated BACH1 with implications for cancer. *Nat Struct Mol Biol* **11**(6)**:** 512-518

Derbyshire DJ, Basu BP, Serpell LC, Joo WS, Date T, Iwabuchi K, Doherty AJ (2002) Crystal structure of human 53BP1 BRCT domains bound to p53 tumour suppressor. *EMBO J* **21**(14)**:** 3863-3872

Di Micco R, Fumagalli M, Cicalese A, Piccinin S, Gasparini P, Luise C, Schurra C, Garre M, Nuciforo PG, Bensimon A, Maestro R, Pelicci PG, d'Adda di Fagagna F (2006) Oncogene-induced senescence is a DNA damage response triggered by DNA hyper-replication. *Nature* **444**(7119)**:** 638-642

Difilippantonio S, Gapud E, Wong N, Huang CY, Mahowald G, Chen HT, Kruhlak MJ, Callen E, Livak F, Nussenzweig MC, Sleckman BP, Nussenzweig A (2008) 53BP1 facilitates long-range DNA end-joining during V(D)J recombination. *Nature* **456**(7221)**:** 529-533

Dimitrova N, de Lange T (2006) MDC1 accelerates nonhomologous end-joining of dysfunctional telomeres. *Genes Dev* **20**(23)**:** 3238-3243

Du LL, Moser BA, Russell P (2004) Homo-oligomerization is the essential function of the tandem BRCT domains in the checkpoint protein Crb2. *J Biol Chem* **279**(37)**:** 38409-38414

Durocher D, Taylor IA, Sarbassova D, Haire LF, Westcott SL, Jackson SP, Smerdon SJ, Yaffe MB (2000) The molecular basis of FHA domain:phosphopeptide binding specificity and implications for phospho-dependent signaling mechanisms. *Mol Cell* **6**(5)**:** 1169-1182

Falck J, Coates J, Jackson SP (2005) Conserved modes of recruitment of ATM, ATR and DNA-PKcs to sites of DNA damage. *Nature* **434**(7033)**:** 605-611

Feldser DM, Hackett JA, Greider CW (2003) Telomere dysfunction and the initiation of genome instability. *Nat Rev Cancer* **3**(8)**:** 623-627

Fernandez-Capetillo O, Chen HT, Celeste A, Ward I, Romanienko PJ, Morales JC, Naka K, Xia Z, Camerini-Otero RD, Motoyama N, Carpenter PB, Bonner WM, Chen J, Nussenzweig A (2002) DNA damage-induced G2-M checkpoint activation by histone H2AX and 53BP1. *Nat Cell Biol* **4**(12)**:** 993-997

Goldberg M, Stucki M, Falck J, D'Amours D, Rahman D, Pappin D, Bartek J, Jackson SP (2003) MDC1 is required for the intra-S-phase DNA damage checkpoint. *Nature* **421**(6926)**:** 952-956

Gorgoulis VG, Vassiliou LV, Karakaidos P, Zacharatos P, Kotsinas A, Liloglou T, Venere M, Ditullio RA, Jr., Kastrinakis NG, Levy B, Kletsas D, Yoneta A, Herlyn M, Kittas C, Halazonetis TD (2005) Activation of the DNA damage checkpoint and genomic instability in human precancerous lesions. *Nature* **434**(7035)**:** 907-913

Gottlieb TM, Jackson SP (1993) The DNA-dependent protein kinase: requirement for DNA ends and association with Ku antigen. *Cell* **72**(1)**:** 131-142

Grawunder U, Wilm M, Wu X, Kulesza P, Wilson TE, Mann M, Lieber MR (1997) Activity of DNA ligase IV stimulated by complex formation with XRCC4 protein in mammalian cells. *Nature* **388**(6641)**:** 492-495

Greenman C, Stephens P, Smith R, Dalgliesh GL, Hunter C, Bignell G, Davies H, Teague J, Butler A, Stevens C, Edkins S, O'Meara S, Vastrik I, Schmidt EE, Avis T, Barthorpe S, Bhamra G, Buck G, Choudhury B, Clements J, Cole J, Dicks E, Forbes S, Gray K, Halliday K, Harrison R, Hills K, Hinton J, Jenkinson A, Jones D, Menzies A, Mironenko T, Perry J, Raine K, Richardson D, Shepherd R, Small A, Tofts C, Varian J, Webb T, West S, Widaa S, Yates A, Cahill DP, Louis DN, Goldstraw P, Nicholson AG, Brasseur F, Looijenga L, Weber BL, Chiew YE, DeFazio A, Greaves MF, Green AR, Campbell P, Birney E, Easton DF, Chenevix-Trench G, Tan MH, Khoo SK, Teh BT, Yuen ST, Leung SY, Wooster R, Futreal PA, Stratton MR (2007) Patterns of somatic mutation in human cancer genomes. *Nature* **446**(7132)**:** 153-158

Grenon M, Costelloe T, Jimeno S, O'Shaughnessy A, Fitzgerald J, Zgheib O, Degerth L, Lowndes NF (2007) Docking onto chromatin via the Saccharomyces cerevisiae Rad9 Tudor domain. *Yeast* **24**(2)**:** 105-119

Gurley KE, Kemp CJ (2001) Synthetic lethality between mutation in Atm and DNA-PK(cs) during murine embryogenesis. *Curr Biol* **11**(3)**:** 191-194

Halazonetis TD, Gorgoulis VG, Bartek J (2008) An oncogene-induced DNA damage model for cancer development. *Science* **319**(5868)**:** 1352-1355

Hammet A, Magill C, Heierhorst J, Jackson SP (2007) Rad9 BRCT domain interaction with phosphorylated H2AX regulates the G1 checkpoint in budding yeast. *EMBO Rep* **8**(9)**:** 851-857

Harper JW, Elledge SJ (2007) The DNA damage response: ten years after. *Mol Cell* **28**(5)**:** 739-745

Hartlerode AJ, Scully R (2009) Mechanisms of double-strand break repair in somatic mammalian cells. *Biochem J* **423**(2)**:** 157-168

Hofmann K, Bucher P (1995) The FHA domain: a putative nuclear signalling domain found in protein kinases and transcription factors. *Trends Biochem Sci* **20**(9)**:** 347-349

Huen MS, Grant R, Manke I, Minn K, Yu X, Yaffe MB, Chen J (2007) RNF8 transduces the DNA-damage signal via histone ubiquitylation and checkpoint protein assembly. *Cell* **131**(5)**:** 901-914

Huertas P DNA resection in eukaryotes: deciding how to fix the break. *Nat Struct Mol Biol* **17**(1)**:** 11-16

Huyen Y, Zgheib O, Ditullio RA, Jr., Gorgoulis VG, Zacharatos P, Petty TJ, Sheston EA, Mellert HS, Stavridi ES, Halazonetis TD (2004) Methylated lysine 79 of histone H3 targets 53BP1 to DNA double-strand breaks. *Nature* **432**(7015)**:** 406-411

Ip SC, Rass U, Blanco MG, Flynn HR, Skehel JM, West SC (2008) Identification of Holliday junction resolvases from humans and yeast. *Nature* **456**(7220)**:** 357-361

Javaheri A, Wysocki R, Jobin-Robitaille O, Altaf M, Cote J, Kron SJ (2006) Yeast G1 DNA damage checkpoint regulation by H2A phosphorylation is independent of chromatin remodeling. *Proc Natl Acad Sci U S A* **103**(37)**:** 13771-13776

Jazayeri A, Falck J, Lukas C, Bartek J, Smith GC, Lukas J, Jackson SP (2006) ATM- and cell cycle-dependent regulation of ATR in response to DNA double-strand breaks. *Nat Cell Biol* **8**(1)**:** 37-45

Joo WS, Jeffrey PD, Cantor SB, Finnin MS, Livingston DM, Pavletich NP (2002) Structure of the 53BP1 BRCT region bound to p53 and its comparison to the Brca1 BRCT structure. *Genes Dev* **16**(5)**:** 583-593

Kerzendorfer C, O'Driscoll M (2009) Human DNA damage response and repair deficiency syndromes: linking genomic instability and cell cycle checkpoint proficiency. *DNA Repair (Amst)* **8**(9)**:** 1139-1152

Kilkenny ML, Dore AS, Roe SM, Nestoras K, Ho JC, Watts FZ, Pearl LH (2008) Structural and functional analysis of the Crb2-BRCT2 domain reveals distinct roles in checkpoint signaling and DNA damage repair. *Genes Dev* **22**(15)**:** 2034-2047

Kolas NK, Chapman JR, Nakada S, Ylanko J, Chahwan R, Sweeney FD, Panier S, Mendez M, Wildenhain J, Thomson TM, Pelletier L, Jackson SP, Durocher D (2007) Orchestration of the DNA-damage response by the RNF8 ubiquitin ligase. *Science* **318**(5856)**:** 1637-1640

Kozlov S, Gueven N, Keating K, Ramsay J, Lavin MF (2003) ATP activates ataxia-telangiectasia mutated (ATM) in vitro. Importance of autophosphorylation. *J Biol Chem* **278**(11)**:** 9309-9317

Lancelot N, Charier G, Couprie J, Duband-Goulet I, Alpha-Bazin B, Quemeneur E, Ma E, Marsolier-Kergoat MC, Ropars V, Charbonnier JB, Miron S, Craescu CT, Callebaut I, Gilquin B, Zinn-Justin S (2007) The checkpoint Saccharomyces cerevisiae Rad9 protein contains a tandem tudor domain that recognizes DNA. *Nucleic Acids Res* **35**(17)**:** 5898-5912

Lee H, Yuan C, Hammet A, Mahajan A, Chen ES, Wu MR, Su MI, Heierhorst J, Tsai MD (2008) Diphosphothreonine-specific interaction between an SQ/TQ cluster and an FHA domain in the Rad53-Dun1 kinase cascade. *Mol Cell* **30**(6)**:** 767-778

Lee JH, Paull TT (2007) Activation and regulation of ATM kinase activity in response to DNA double-strand breaks. *Oncogene* **26**(56)**:** 7741-7748

Li H, Byeon IJ, Ju Y, Tsai MD (2004) Structure of human Ki67 FHA domain and its binding to a phosphoprotein fragment from hNIFK reveal unique recognition sites and new views to the structural basis of FHA domain functions. *J Mol Biol* **335**(1)**:** 371-381

Li J, Taylor IA, Lloyd J, Clapperton JA, Howell S, MacMillan D, Smerdon SJ (2008) Chk2 oligomerization studied by phosphopeptide ligation: implications for regulation and phosphodependent interactions. *J Biol Chem* **283**(51)**:** 36019-36030

Liu K, Paik JC, Wang B, Lin FT, Lin WC (2006) Regulation of TopBP1 oligomerization by Akt/PKB for cell survival. *EMBO J* **25**(20)**:** 4795-4807

Lou Z, Chen BP, Asaithamby A, Minter-Dykhouse K, Chen DJ, Chen J (2004) MDC1 regulates DNA-PK autophosphorylation in response to DNA damage. *J Biol Chem* **279**(45)**:** 46359-46362

Lou Z, Minter-Dykhouse K, Franco S, Gostissa M, Rivera MA, Celeste A, Manis JP, van Deursen J, Nussenzweig A, Paull TT, Alt FW, Chen J (2006) MDC1 maintains genomic stability by participating in the amplification of ATM-dependent DNA damage signals. *Mol Cell* **21**(2)**:** 187-200

Lou Z, Minter-Dykhouse K, Wu X, Chen J (2003) MDC1 is coupled to activated CHK2 in mammalian DNA damage response pathways. *Nature* **421**(6926)**:** 957-961

Lukas C, Falck J, Bartkova J, Bartek J, Lukas J (2003) Distinct spatiotemporal dynamics of mammalian checkpoint regulators induced by DNA damage. *Nat Cell Biol* **5**(3)**:** 255-260

Ma Y, Pannicke U, Schwarz K, Lieber MR (2002) Hairpin opening and overhang processing by an Artemis/DNA-dependent protein kinase complex in nonhomologous end joining and V(D)J recombination. *Cell* **108**(6)**:** 781-794

Mahajan A, Yuan C, Lee H, Chen ES, Wu PY, Tsai MD (2008) Structure and function of the phosphothreonine-specific FHA domain. *Sci Signal* **1**(51)**:** re12

Mailand N, Bekker-Jensen S, Faustrup H, Melander F, Bartek J, Lukas C, Lukas J (2007) RNF8 ubiquitylates histones at DNA double-strand breaks and promotes assembly of repair proteins. *Cell* **131**(5)**:** 887-900

Manis JP, Morales JC, Xia Z, Kutok JL, Alt FW, Carpenter PB (2004) 53BP1 links DNA damage-response pathways to immunoglobulin heavy chain class-switch recombination. *Nat Immunol* **5**(5)**:** 481-487

Manke IA, Lowery DM, Nguyen A, Yaffe MB (2003) BRCT repeats as phosphopeptide-binding modules involved in protein targeting. *Science* **302**(5645)**:** 636-639

Matsuoka S, Ballif BA, Smogorzewska A, McDonald ER, 3rd, Hurov KE, Luo J, Bakalarski CE, Zhao Z, Solimini N, Lerenthal Y, Shiloh Y, Gygi SP, Elledge SJ (2007) ATM and ATR substrate analysis reveals extensive protein networks responsive to DNA damage. *Science* **316**(5828)**:** 1160-1166

Minter-Dykhouse K, Ward I, Huen MS, Chen J, Lou Z (2008) Distinct versus overlapping functions of MDC1 and 53BP1 in DNA damage response and tumorigenesis. *J Cell Biol* **181**(5)**:** 727-735

Mohammad DH, Yaffe MB (2009) 14-3-3 proteins, FHA domains and BRCT domains in the DNA damage response. *DNA Repair (Amst)* **8**(9)**:** 1009-1017

Moshous D, Callebaut I, de Chasseval R, Corneo B, Cavazzana-Calvo M, Le Deist F, Tezcan I, Sanal O, Bertrand Y, Philippe N, Fischer A, de Villartay JP (2001) Artemis, a novel DNA double-strand break repair/V(D)J recombination protein, is mutated in human severe combined immune deficiency. *Cell* **105**(2)**:** 177-186

Myers JS, Cortez D (2006) Rapid activation of ATR by ionizing radiation requires ATM and Mre11. *J Biol Chem* **281**(14)**:** 9346-9350

Nick McElhinny SA, Ramsden DA (2004) Sibling rivalry: competition between Pol X family members in V(D)J recombination and general double strand break repair. *Immunol Rev* **200:** 156-164

Nott TJ, Kelly G, Stach L, Li J, Westcott S, Patel D, Hunt DM, Howell S, Buxton RS, O'Hare HM, Smerdon SJ (2009) An intramolecular switch regulates phosphoindependent FHA domain interactions in Mycobacterium tuberculosis. *Sci Signal* **2**(63)**:** ra12

Nyberg KA, Michelson RJ, Putnam CW, Weinert TA (2002) Toward maintaining the genome: DNA damage and replication checkpoints. *Annu Rev Genet* **36:** 617-656

Pardo B, Gomez-Gonzalez B, Aguilera A (2009) DNA repair in mammalian cells: DNA double-strand break repair: how to fix a broken relationship. *Cell Mol Life Sci* **66**(6)**:** 1039-1056

Rogakou EP, Pilch DR, Orr AH, Ivanova VS, Bonner WM (1998) DNA double-stranded breaks induce histone H2AX phosphorylation on serine 139. *J Biol Chem* **273**(10)**:** 5858-5868

Sancar A, Lindsey-Boltz LA, Unsal-Kacmaz K, Linn S (2004) Molecular mechanisms of mammalian DNA repair and the DNA damage checkpoints. *Annu Rev Biochem* **73:** 39-85

Sanders SL, Portoso M, Mata J, Bahler J, Allshire RC, Kouzarides T (2004) Methylation of histone H4 lysine 20 controls recruitment of Crb2 to sites of DNA damage. *Cell* **119**(5)**:** 603-614

Sartori AA, Lukas C, Coates J, Mistrik M, Fu S, Bartek J, Baer R, Lukas J, Jackson SP (2007) Human CtIP promotes DNA end resection. *Nature* **450**(7169)**:** 509-514

Schwartz MF, Duong JK, Sun Z, Morrow JS, Pradhan D, Stern DF (2002) Rad9 phosphorylation sites couple Rad53 to the Saccharomyces cerevisiae DNA damage checkpoint. *Mol Cell* **9**(5)**:** 1055-1065

Shiotani B, Zou L (2009) Single-stranded DNA orchestrates an ATM-to-ATR switch at DNA breaks. *Mol Cell* **33**(5)**:** 547-558

Shiozaki EN, Gu L, Yan N, Shi Y (2004) Structure of the BRCT repeats of BRCA1 bound to a BACH1 phosphopeptide: implications for signaling. *Mol Cell* **14**(3)**:** 405-412

Sibanda BL, Critchlow SE, Begun J, Pei XY, Jackson SP, Blundell TL, Pellegrini L (2001) Crystal structure of an Xrcc4-DNA ligase IV complex. *Nat Struct Biol* **8**(12)**:** 1015-1019

Sjoblom T, Jones S, Wood LD, Parsons DW, Lin J, Barber TD, Mandelker D, Leary RJ, Ptak J, Silliman N, Szabo S, Buckhaults P, Farrell C, Meeh P, Markowitz SD, Willis J, Dawson D, Willson JK, Gazdar AF, Hartigan J, Wu L, Liu C, Parmigiani G, Park BH, Bachman KE, Papadopoulos N, Vogelstein B, Kinzler KW, Velculescu VE (2006) The consensus coding sequences of human breast and colorectal cancers. *Science* **314**(5797)**:** 268-274

Soulier J, Lowndes NF (1999) The BRCT domain of the S. cerevisiae checkpoint protein Rad9 mediates a Rad9-Rad9 interaction after DNA damage. *Curr Biol* **9**(10)**:** 551-554

Stewart GS, Wang B, Bignell CR, Taylor AM, Elledge SJ (2003) MDC1 is a mediator of the mammalian DNA damage checkpoint. *Nature* **421**(6926)**:** 961-966

Stiff T, O'Driscoll M, Rief N, Iwabuchi K, Lobrich M, Jeggo PA (2004) ATM and DNA-PK function redundantly to phosphorylate H2AX after exposure to ionizing radiation. *Cancer Res* **64**(7)**:** 2390-2396

Stucki M, Clapperton JA, Mohammad D, Yaffe MB, Smerdon SJ, Jackson SP (2005) MDC1 directly binds phosphorylated histone H2AX to regulate cellular responses to DNA double-strand breaks. *Cell* **123**(7)**:** 1213-1226

Sy SM, Huen MS, Zhu Y, Chen J (2009) PALB2 regulates recombinational repair through chromatin association and oligomerization. *J Biol Chem* **284**(27)**:** 18302-18310

Usui T, Foster SS, Petrini JH (2009) Maintenance of the DNA-damage checkpoint requires DNA-damage-induced mediator protein oligomerization. *Mol Cell* **33**(2)**:** 147-159

Walker JR, Corpina RA, Goldberg J (2001) Structure of the Ku heterodimer bound to DNA and its implications for double-strand break repair. *Nature* **412**(6847)**:** 607-614

Wang B, Matsuoka S, Carpenter PB, Elledge SJ (2002) 53BP1, a mediator of the DNA damage checkpoint. *Science* **298**(5597)**:** 1435-1438

Wang Z, Cummins JM, Shen D, Cahill DP, Jallepalli PV, Wang TL, Parsons DW, Traverso G, Awad M, Silliman N, Ptak J, Szabo S, Willson JK, Markowitz SD, Goldberg ML, Karess R, Kinzler KW, Vogelstein B, Velculescu VE, Lengauer C (2004) Three classes of genes mutated in colorectal cancers with chromosomal instability. *Cancer Res* **64**(9)**:** 2998-3001

Ward I, Kim JE, Minn K, Chini CC, Mer G, Chen J (2006) The tandem BRCT domain of 53BP1 is not required for its repair function. *J Biol Chem* **281**(50)**:** 38472-38477

Ward IM, Reina-San-Martin B, Olaru A, Minn K, Tamada K, Lau JS, Cascalho M, Chen L, Nussenzweig A, Livak F, Nussenzweig MC, Chen J (2004) 53BP1 is required for class switch recombination. *J Cell Biol* **165**(4)**:** 459-464

Weterings E, Verkaik NS, Bruggenwirth HT, Hoeijmakers JH, van Gent DC (2003) The role of DNA dependent protein kinase in synapsis of DNA ends. *Nucleic Acids Res* **31**(24)**:** 7238-7246

Williams RS, Chasman DI, Hau DD, Hui B, Lau AY, Glover JN (2003) Detection of protein folding defects caused by BRCA1-BRCT truncation and missense mutations. *J Biol Chem* **278**(52)**:** 53007-53016

Wood LD, Parsons DW, Jones S, Lin J, Sjoblom T, Leary RJ, Shen D, Boca SM, Barber T, Ptak J, Silliman N, Szabo S, Dezso Z, Ustyanksky V, Nikolskaya T, Nikolsky Y, Karchin R, Wilson PA, Kaminker JS, Zhang Z, Croshaw R, Willis J, Dawson D, Shipitsin M, Willson JK, Sukumar S, Polyak K, Park BH, Pethiyagoda CL, Pant PV, Ballinger DG, Sparks AB, Hartigan J, Smith DR, Suh E, Papadopoulos N, Buckhaults P, Markowitz SD, Parmigiani G, Kinzler KW, Velculescu VE, Vogelstein B (2007) The genomic landscapes of human breast and colorectal cancers. *Science* **318**(5853)**:** 1108-1113

Wu L, Hickson ID (2003) The Bloom's syndrome helicase suppresses crossing over during homologous recombination. *Nature* **426**(6968)**:** 870-874

Xia B, Sheng Q, Nakanishi K, Ohashi A, Wu J, Christ N, Liu X, Jasin M, Couch FJ, Livingston DM (2006) Control of BRCA2 cellular and clinical functions by a nuclear partner, PALB2. *Mol Cell* **22**(6)**:** 719-729

Xie A, Hartlerode A, Stucki M, Odate S, Puget N, Kwok A, Nagaraju G, Yan C, Alt FW, Chen J, Jackson SP, Scully R (2007) Distinct roles of chromatin-associated proteins MDC1 and 53BP1 in mammalian double-strand break repair. *Mol Cell* **28**(6)**:** 1045-1057

Xu X, Tsvetkov LM, Stern DF (2002) Chk2 activation and phosphorylation-dependent oligomerization. *Mol Cell Biol* **22**(12)**:** 4419-4432

Yaffe MB, Smerdon SJ (2004) The use of in vitro peptide-library screens in the analysis of phosphoserine/threonine-binding domain structure and function. *Annu Rev Biophys Biomol Struct* **33:** 225-244

Yaneva M, Kowalewski T, Lieber MR (1997) Interaction of DNA-dependent protein kinase with DNA and with Ku: biochemical and atomic-force microscopy studies. *EMBO J* **16**(16)**:** 5098-5112

Yang SZ, Lin FT, Lin WC (2008) MCPH1/BRIT1 cooperates with E2F1 in the activation of checkpoint, DNA repair and apoptosis. *EMBO Rep* **9**(9)**:** 907-915

Yu X, Chini CC, He M, Mer G, Chen J (2003) The BRCT domain is a phospho-protein binding domain. *Science* **302**(5645)**:** 639-642

Yuan C, Yongkiettrakul S, Byeon IJ, Zhou S, Tsai MD (2001) Solution structures of two FHA1-phosphothreonine peptide complexes provide insight into the structural basis of the ligand specificity of FHA1 from yeast Rad53. *J Mol Biol* **314**(3)**:** 563-575

Yun MH, Hiom K (2009) CtIP-BRCA1 modulates the choice of DNA double-strand-break repair pathway throughout the cell cycle. *Nature* **459**(7245)**:** 460-463

Zgheib O, Pataky K, Brugger J, Halazonetis TD (2009) An oligomerized 53BP1 tudor domain suffices for recognition of DNA double-strand breaks. *Mol Cell Biol* **29**(4)**:** 1050-1058

Zhang J, Ma Z, Treszezamsky A, Powell SN (2005) MDC1 interacts with Rad51 and facilitates homologous recombination. *Nat Struct Mol Biol* **12**(10)**:** 902-909

Zhou BB, Elledge SJ (2000) The DNA damage response: putting checkpoints in perspective. *Nature* **408**(6811)**:** 433-439

9 ACKNOWLEDGEMENTS

I would like to especially thank PD Dr. Manuel Stucki for giving me the opportunity to join his group and for the supervision of my PhD thesis, for all the stimulating discussions, his constant encouragement, for sharing his knowledge and experience, and for providing an excellent scientific environment to perform successful research.

I am grateful for the invaluable support from Flurina, Lucijana, Christoph and Mario during all the ups and downs in the everyday lab life, and for sharing so many laughs. I thank all institute members for their company, their help and support and for creating such a great working atmosphere.

I would like to express my gratitude to Dr. Stephen J. Smerdon and his colleagues for the fruitful collaborations that have been essential for this work, to Prof. Dr. Jiri Lukas and Dr. Claudia Lukas for their efforts, ideas, critical discussions and for giving me the opportunity to collect valuable data in their laboratory, and further to my thesis committee members Prof. Dr. Josef Jiricny and Prof. Dr. Ulrich Hübscher for their helpful suggestions and the evaluation of my thesis.

Special thanks to Dani, my companion of fortune and misfortune, and to Kai for endlessly providing chocolate and sharing every kind of mood.

Very special thanks to Matthias for always being there and his support on a personal as well as scientific level, and to my family and friends for their continuous encouragement in every phase of my life. Thanks for always having trusted in me.

10 CURRICULUM VITAE

Surname, First Name	Jungmichel, Stephanie
E-Mail	jung@vetbio.uzh.ch
Date of Birth	4th May 1981
Place of Birth	Zittau, Germany
Nationality	German
Marital Status	Single

Education

04/2006 – present	**PhD in Biochemistry and Molecular Biology** Institute of Veterinary Biochemistry and Molecular Biology, University of Zurich, Switzerland ***Thesis:*** *Mechanism of DNA Damage-Induced MDC1 Dimerization*
10/2003 – 10/2005	**Diploma in Biochemistry** University of Leipzig, Germany ***Thesis:*** *Comparative Transport of Drugs in Tumor Cells Using Peptides as Carriers*
10/2002 – 06/2003	**Bachelor of Science** University of Glasgow, UK *Main Course: Biochemistry*
10/2000 – 09/2002	**Pre-Diploma in Biochemistry** University of Leipzig, Germany
09/1992 – 06/1999	**A-levels (Abitur)** Gymnasium Seifhennersdorf, Germany

Scientific Work Experience

10/2008 – 11/2009	**Lecture Assistant** for "Swiss Cancer League" Writer of scientific summaries for publication on the Krebsliga Zurich homepage
07/2004 – 09/2004	**Research Assistant** Institute of Biochemistry, University of Leipzig
07/2004 – 09/2004	**Research Internship** Neuro-oncological Laboratory, Martin-Luther University Halle-Wittenberg, Germany
07/2004 – 09/2004	**Research Assistant** Environmental Research Center (Ufz) Leipzig Halle GmbH, Germany